**REPUBLIC OF TURKEY**
**MUĞLA SITKI KOÇMAN UNIVERSITY**
**GRADUATE SCHOOL OF**
**NATURAL AND APPLIED SCIENCES**

**DEPARTMENT OF CIVIL ENGINEERING**

# PREDICTING PERMANENT DISPLACEMENT OF CONCRETE FACED ROCKFILL DAMS SUBJECTED TO EARTHQUAKE LOADING

**MASTER OF SCIENCE**

**SELDA DURMAZ**

**DECEMBER 2016**
**MUĞLA**

**MUĞLA SITKI KOÇMAN UNIVERSITY**

**Graduate School of Natural and Applied Sciences**

## APPROVAL OF THE THESIS

The thesis entitled **PREDICTING PERMANENT DISPLACEMENT OF CONCRETE FACED ROCKFILL DAMS SUBJECTED TO EARTHQUAKE LOADING** is submitted by **SELDA DURMAZ** in partial fulfillment of the requirements for degree of Master of Science in Civil Engineering Department by,

---

**EXAMINING COMMITTEE MEMBERS**

Assist. Prof. Dr. Selman SAĞLAM **(Head of Committee)**

Department Of Civil Engineering,
Adnan Menderes University, Aydın

Assist. Prof. Dr. Deniz ÜLGEN **(Supervisor)**

Department Of Civil Engineering,
Muğla Sıtkı Koçman University, Muğla

Assist. Prof. Dr. Altuğ SAYGILI **(Member)**

Department Of Civil Engineering,
Muğla Sıtkı Koçman University, Muğla

---

**APPROVAL OF HEAD OF THE DEPARTMENT**

Assoc. Prof. Dr. Recep BİRGÜL

Head, Civil Engineering Department,
Muğla Sıtkı Koçman University, Muğla

Assist. Prof. Dr. Deniz ÜLGEN

Supervisor, Civil Engineering Department,
Muğla Sıtkı Koçman University, Muğla

Date: 09/12/2016

---

I hereby declare that all information in this document has been obtained and presented in accordance with academic rules and ethical conduct. I also declare that, as required by these rules and conduct, I have fully cited and referenced all material and results that are not original to this work.

Selda DURMAZ

09/12/2016

## ABSTRACT

## PREDICTING PERMANENT DISPLACEMENT OF CONCRETE FACED ROCKFILL DAMS SUBJECTED TO EARTHQUAKE LOADING

Selda DURMAZ

Master of Science (M.Sc.)

Graduate School of Natural and Applied Sciences

Department of Civil Engineering

Supervisor: Assist. Prof. Dr. Deniz ÜLGEN

December 2016, 99 pages

Concrete faced rockfill dams (CFRD) are widely known with their safeness and high performance against the seismic loadings. Correspondingly, a rapid progress is made in construction of rockfill dams especially at highly seismic hazardous regions. However, earthquake exposures and dam failures show the inadequacy of information. Available studies concentrate on earth and cored type composite dams that is less specification is made merely for rockfill dams. This study aims to investigate the dynamic behavior of concrete faced rockfill dams subjected to earthquake loading. In accordance with this purpose, a series of dynamic analyses are conducted with various parameters. Dam models prepared with different geometries and material properties. These numerical models are subjected to various seismic excitations provided from real earthquake records. Finite element method based QUAKE/W is used for dynamic analyses and equivalent linear approach process is applied under 2D plain strain conditions to scrutinize the seismic response of CFRDs. Limit equilibrium and pseudo-static approach based calculations are carried out for factor of safety, yield acceleration and seismic coefficient evaluations. Earthquake induced permanent displacements are calculated with Newmark method. Consequently, it is aimed to give recommendations for engineers in the preliminary design stage of CFRDs. Based on the analyses results, preliminary design charts are suggested for the prediction of earthquake induced deformations and acceleration responses.



**Keywords**: Concrete Faced Rockfill Dams, Permanent Displacement, Finite Element, Acceleration Response, Dynamic Analysis, Newmark Method.

# ÖZET

## ÖN YÜZÜ BETON KAPLI KAYA DOLGU BARAJLARIN DEPREM YÜKLERİ ALTINDAKİ KALICI DEFORMASYONLARININ TAHMİN EDİLMESİ

Selda DURMAZ

Yüksek Lisans Tezi

Fen Bilimleri Enstitüsü

İnşaat Mühendisliği Anabilim Dalı

Danışman: Yrd. Doç. Dr. Deniz ÜLGEN

Aralık 2016, 99 sayfa

Ön yüzü beton kaplı kaya dolgu barajlar (ÖYBKKDB) genellikle sismik yükler altında yüksek performans sergilemeleri ve depreme karşı güvenli oluşları ile bilinirler. Buna bağlı olarak da, özellikle sismik aktivitenin yüksek olduğu bölgelerde kaya dolgu baraj inşasında hızlı bir ilerleme kaydedilmiştir. Ancak depreme maruz kalan barajlarda oluşan deformasyonlar bu konudaki bilginin yetersiz olduğunu göstermiştir. Mevcut çalışmalar toprak dolgu ve diğer kompozit barajlar üzerinde yoğunlaştığından kaya dolgu barajlara özgü çalışma oldukça azdır. Bu çalışma, ön yüzü beton kaplı kaya dolgu barajların deprem yükleri altındaki dinamik davranışlarını incelemeyi amaçlamaktadır. Bu amaçla, değişen parametreler altında bir dizi dinamik analiz yapılmıştır. Farklı geometri ve malzeme parametrelerine sahip modeller oluşturulmuştur. Hazırlanan sayısal modeller için gerçek deprem kayıtları kullanılarak farklı sismik yüklemeler oluşturulmuştur. Sonlu elemanlar yöntemiyle hesap yapan QUAKE/W programı kullanılarak gerçekleştirilen dinamik analizler iki boyutta düzlem birim şekil değiştirme koşulları altında eşdeğer doğrusal hesap yöntemini temel alınarak yapılmıştır. Limit denge ve yarı statik hesap yöntemleri kullanılarak güvenlik katsayısı, kayma ivmesi ve sismik katsayı hesaplamaları yapılmıştır. Depreme bağlı kalıcı deformasyonların hesaplanmasında Newmark yöntemi kullanılmıştır. Çalışmanın sonucunda, ön yüzü beton kaplı kaya dolgu barajların ön tasarımı aşamasına yönelik tavsiyelerde bulunulması amaçlanmıştır. Kaya dolgu barajların kalıcı deformasyonunun ve ivme tepkilerinin tahmini için analiz sonuçları doğrultusunda hazırlanan çizelgeler önerilmiştir.

**Anahtar Kelimeler:** Beton Kaplı Kaya Dolgu Barajlar, Kalıcı Deformasyon, Sonlu Elemanlar, İvme Tepkileri, Dinamik Analiz, Newmark Metodu.

To my beloved mother and father…

## ACKNOWLEDGEMENT

I would like to express my sincere gratitude to my supervisor Assist. Prof. Dr. Deniz ÜLGEN for his consistent support, wise guidance and immense understanding. I also owe a debt of gratitude to him for his contributions to my personality and knowledge.

My sincere thanks also goes to my teachers, Assist. Prof. Dr. M. Rifat KAHYAOĞLU, Assoc. Prof. Dr. Recep BİRGÜL and Assist. Prof. Dr. Altuğ SAYGILI.

I would like to thank to Assist. Prof. Dr. Selman SAĞLAM for his precious contributions to this study.

I also would like to thank to Erdem TÜRK and Ali ALUÇ for their supports computer based troubles and my special thanks also goes to Erdem TÜRK for programming helps in Matlab.

I would like to express my deepest appreciation to my colleagues, my dearest friends Aysu GÖÇÜGENCİ, Uğur Can ÖZÖĞÜT, Gaye GÖKALP YILMAZ, Gökhan YILMAZ, Pınar DOĞAN and Gülhan ÇAKMAK for being by myside every time.

I would like to thank to my dearest friend Burçin KARATAŞ for her presence in my life.

Finally, my deepest gratitude goes to my mother and my father for their understanding and supporting me spiritually throughout writing this thesis and my life in general. It is difficult to explain my gratitude with words but I wish to dedicate this thesis to them with love from their daughter.

This study is supported and funded by Muğla Sıtkı Koçman University Scientific Research Project (BAP) Office with project number 15-131.

## TABLE OF CONTENTS

## LIST OF TABLES

## LIST OF FIGURES

## LIST OF SYMBOLS / ABBREVIATIONS

| | |
|---|---|
| $\sigma_1^{'}$ | Vertical effective stress |
| $\sigma_2^{'}$ | Horizontal effective stress |
| $\sigma_3^{'}$ | Horizontal effective stress |
| $\sigma_m$ | Mean principle effective stress |
| $\lambda$ | Wave length |
| $\lambda$ | Scale factor of Morgenstern-Price method |
| $\omega_n$ | Natural frequency |
| $c'$ | Cohesion |
| c | Apparent (total) cohesion |
| $\sigma'$ | Effective stress |
| $\varphi'$ | Internal friction angle |
| $\varphi$ | Internal friction angle |
| $\tau$ | Shear stress |
| $\alpha$ | Angle of inclined plane |
| $\rho$ | Mass density |
| $\xi$ | Damping |
| $\gamma$ | Strain |
| $\gamma$ | Unit weight |
| $\upsilon$ | Poisson's ratio |
| $\beta$ | Slope inclination angle |
| a | Acceleration |
| $a$ | Fitting parameter |
| $a_{bottom}$ | Acceleration at bottom of dam |
| $a_{crest}$ | Acceleration at crest of dam |
| $a_{max}$ | Maximum acceleration |
| $a_h$ | Horizontal pseudo-static accelerations |
| $a_v$ | Vertical pseudo-static accelerations |

| | |
|---|---|
| $A_{loop}$ | Area of loop |
| $A_n$ | Coefficient of Bessel function |
| $A_1$ | Fitting parameter |
| $A_2$ | Fitting parameter |
| $b$ | Fitting parameter |
| $B_n$ | Coefficient of Bessel function |
| D | Permanent displacement |
| D | Damping |
| e | Void ratio |
| E | Elastic modulus |
| E | Interslice normal force |
| F | Force |
| $F_v$ | Vertical pseudo-static force |
| $F_h$ | Horizontal pseudo-static force |
| g | Gravitational acceleration |
| G | Shear modulus |
| $G_{max}$ | Maximum shear modulus |
| h | Dam height |
| h | Average height of a slice from the slip surface |
| $J_0$ | Bessel function of first kind and order zero |
| $k_y$ | Yield coefficient |
| $k_v$ | Vertical pseudo-static coefficients |
| $k_h$ | Horizontal pseudo-static coefficients |
| K | Constant |
| $K_0$ | Coefficient of lateral earth pressure at rest |
| L | Slip surface length |
| $m$ | Fitting parameter |
| M | Moment |
| $M_L$ | Local magnitude |
| $M_B$ | Body wave magnitude |

| | |
|---|---|
| $M_S$ | Surface wave magnitude |
| $M_W$ | Moment magnitude |
| $n$ | Fitting parameter |
| N | Normal force |
| R | Radius |
| s | Shear strength |
| $S_u$ | Undrained shear strength |
| t | Time |
| T | Interslice shear force |
| $T_1$ | Period of first mode shape |
| $T_2$ | Period of second mode shape |
| $T_3$ | Period of third mode shape |
| U | Horizontal displacement |
| $V_s$ | Shear wave velocity |
| $W_D$ | Dissipated energy |
| $W_S$ | Maximum strain energy |
| W | Weight of sliding mass |
| X | Moment arm |
| $x_0$ | Fitting parameter |
| Z | Depth |
| 1D | One dimensional |
| 2D | Two dimensional |
| 3D | Three dimensional |
| CFRD | Concrete faced rockfill dam |
| FEM | Finite element method |
| FS | Factor of safety |
| LE | Limit Equilibrium |
| OCR | Over consolidation ratio |
| PEER | Pacific Earthquake Engineering Research Center |
| PHA | Peak horizontal acceleration |
| PI | Plasticity index |

# 1. INTRODUCTION

## 1.1. General

Development of strategies for conservation and effective usage of natural resources become significant when the heavy increase of population in world, effects of global warming, environmental pollution due to industrialization and overpopulation are considered. Water resource management has the primary importance for continuation of life. In respect thereof, dams are the most efficient options for the essential necessities as drinking water supply, irrigation, energy generation and flood control.

According to the indefinite records, it is known that history of dams date back to about 5000 years and the current dam cross section is shaped with Anantha dam around 1213 (Anonymous, 2015). When it comes to 1931, dumped fill dams increase until it is replaced with earth-core rockfill dams in 1940s and concrete faced rockfill dams in 1960s (Anonymous, 1989). Convenience of higher construction and being applicable with steeper slopes which means less embankment, being lowest-cost, less settlement and leakage potential make the CFRDs suitable from all engineering standpoints (Sherard, 1987). Meanwhile, occurrence of substantial failures at Lower San Fernando Dam in 1971 affected the attitude of researchers to the seismic reliability of earth dams (Seed, 1981). Therefore engineers started to concentrate upon the seismic behavior and design criteria of fill dams. Improving technologies enable the back analyses of damaged dams to see the possible cause of failures, redesign of case histories with computer programs and the instrumentation and monitoring of dams.

Completed studies and surveys of earthquake subjected dams, form a frame for the reasons of likely failure. Understanding of dam behavior help the development of basic considerations for earthquake resistant designs. Starting from early studies, accumulated data are mostly adequate to accept the slope stability, overtopping, seepage, piping, bearing capacity loss of foundation, settlement and sliding for failure reasons. In addition to this general acceptance, after searching Northridge, Chi-Chi,

Kocaeli and Kobe earthquakes, following failure mechanisms are stated by Pinto (2001).

- Sliding or shear distortion of embankment or foundation or both,
- Transverse cracks,
- Longitudinal cracks,
- Loss of freeboard due to compaction of embankment or foundation,
- Rupture of underground conduits,
- Overtopping due to seiches in reservoir,
- Overtopping due to slides or rock falls into reservoir,
- Disruption of dam by major fault movement in foundation,
- Differential tectonic ground movements,
- Failure of spillway or outlet works,
- Piping failure through cracks induced by ground motions,
- Liquefaction of embankment or foundation,

Previous studies, until 1960s, generally based on factor of safety calculations of possible sliding masses and these calculations do not satisfy the requirements of seismic risk assessment. Newmark's (1965) proposal for calculation of permanent displacement of earth fill dams leads the deformation based studies. Associated with the development of dynamic procedures, permanent displacement analyses of fill dams are conducted by using finite element or discrete element based software (Kramer and Smith, 1997). Usage of permanent displacement instead of factor of safety is thought as more realistic and Lin and Whitman (1986), Ambraseys and Menu (1988), Jibson (1993), Bray et.al (1995), Kramer and Smith (1997), focus on the Newmark's (1965) method. Assumptions of Newmark's original method were modified by the researchers. In addition to the deterministic methods, Jibson (2007), Bray and Travasarou (2007), Saygılı and Rathje (2009) made probabilistic studies to consider the unpredictable nature of seismic excitations.

Bayraktar and Kartal (2010) simulated Torul Dam to investigate the linear and nonlinear dynamic response of concrete face slab during earthquake and deformations were majorly observed in face slab around the crest of dam.

Meehan and Vahedifard (2013) compared the present simplified displacement based sliding block models. 122 case studies including earth dams and embankments were reevaluated by using fifteen different approaches. Comparisons indicated that observed deformations were greater than calculated ones. Liu et al. (2014) conducted a large scale shaking table test on a CFRD prototype. Analyses results revealed that crest settlement is greater in comparison with the other parts. Thus, using geogrid or cemented rockfill in the top 1/5 zone were introduced to improve the stability. Despite the 100 cm displacement suggestion of Hyness-Griffin and Franklin (1984), available probabilistic and deterministic works still specify no well-defined limit for permanent displacement which can threat the overall stability of dam.

## 1.2. Scope of the Study

Even the evaluations on dynamic response of CFRDs gain importance due to increasing application, especially at seismically active regions, still there are some uncertainties need to be clarified. Rarity of only rockfill based researches is the main motivation for this thesis. Present study covers a series of numerical analyses to investigate the behavior of CFRDs under earthquake excitation. In the light of this purpose, examined parameters can be listed as below:

- Effects of dam height
- Effects of crest width
- Effects of slip surface depth
- Effects of horizontal seismic coefficient
- Effects of maximum ground acceleration
- Effects of upstream and downstream slope inclination

According to the conducted analyses, contributions of listed parameters on the response of rockfill dams are observed. Some relations are established between the most efficient parameters and earthquake induced permanent displacements. Besides, less effective factors on the variation of acceleration are determined.

All these findings are provided as a useful means for preliminary design stages of concrete faced rockfill dams. Prior to the comprehensive analyses, the level of

deformations and the acceleration deviations induced by the selected combinations of parameters can be predicted by using the illustrated findings.

### 1.3. Outline of the Study

This study is divided into five parts as follows:

- Chapter 1 includes an introductory explanation on CFRDs and organization of thesis. Also, aim and scope of the study are mentioned in this chapter.
- Chapter 2 summarizes the literature and the previous studies on the dynamic behavior of embankment dams in terms of methodologies to be followed and available tools to be utilized for designing and analyzing.
- Chapter 3 gives the geometric details of numerical models, material properties and other parameters to be used. Additionally the stages of static and dynamic analyses, procedure of permanent displacement calculations are described here. This chapter also includes a numerical simulation with QUAKE/W for permanent displacement evaluation of Sürgü Dam. Suitability of the software in dynamic analyses of concrete faced rockfill dams has been examined.
- Chapter 4 represents the results of analyses in terms of permanent displacement, factor of safety and acceleration response.
- Chapter 5 involves interpretations of the results and conclusion of the study.

# 2. STATIC AND DYNAMIC ANALYSES OF EMBANKMENT DAMS

## 2.1. Static Analyses

Stabilizing the slopes during the construction issues like excavation or embankment have a wide coverage in geotechnical engineering applications. Starting with Swedish/Ordinary Method of Fellenius (1936), many slope stability analyses have been developed in time. Suggested methods generally based on defining a slip surface and dividing the soil above the slip surface into slices. Then, writing force or moment equilibrium equations in terms of normal and shear forces for which shear strength of soil is calculated according to Mohr-Coulomb failure theory (Equation 2.1 and Equation 2.2). Consequently, the driving forces (shear stresses applied to soil) and resisting forces (shear strength of soil) are divided into each other to have an index value called factor of safety (FS) (Equation 2.3). This conventional procedure is known as Limit Equilibrium (LE) method.

Myriad of limit equilibrium based slope stability approaches are recommended up to now. Bishop (1955), Janbu (1954a), Morgenstern-Price (1965), Spencer (1967), Sarma (1973) and Chugh (1986) are well-known researchers with their contributions to slope stability and limit equilibrium subjects. Even the analogy of proposed methods is same, they differ from each other with shape of assumed slip surface, consideration of internal normal and shear forces between the slices, the way of evaluations of these forces and application to slices. While the method of slices, Fellenius' method and Bishop's method are amenable for circular failure surfaces, Janbu's method, infinite slope method and stability charts can be used for non-circular failure surfaces.

A brief explanation of limit equilibrium is made by Abramson, et al. (2002) as shown in Figure 2.1.

$$\text{Available shear strength} : s = c' + \sigma' \tan\varphi' \tag{2.1}$$

$$\text{Mobilized shear stress: } \tau = \frac{s}{FS} = \frac{c' + \sigma' \tan\varphi'}{FS} \tag{2.2}$$

$$FS = \frac{\text{resisting force}}{\text{driving force}} = \frac{\text{shear strength (s)}}{\text{shear stress}(\tau)} \tag{2.3}$$

Where $c'$ is cohesion and $\varphi'$ is internal friction angle.

Limit equilibrium:

$$\text{Total stress: } FS = \frac{s}{\tau} \tag{2.4}$$

$$\text{Effective stress : } FS = \frac{c' + \sigma' \tan\varphi'}{\tau} \tag{2.5}$$

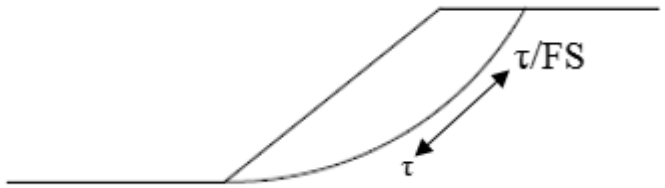


**(a)**

Force equilibrium:

$$FS = \frac{\Sigma \text{ resisting forces}}{\Sigma \text{ driving forces}} \tag{2.6}$$

$$FS = \frac{s}{W\sin\alpha} = \frac{cL + N\tan\alpha}{W\sin\alpha} \tag{2.7}$$

L is total length of sliding mass

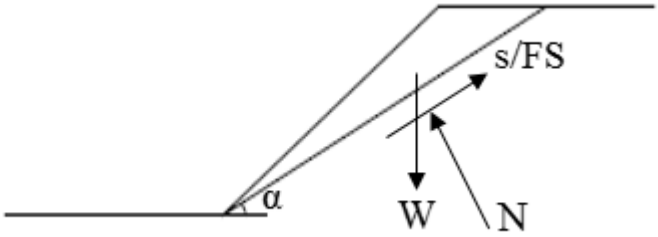


**(b)**

Moment equilibrium:

$$FS = \frac{\Sigma \text{ resisting moments}}{\Sigma \text{ driving moments}} \tag{2.8}$$

$$FS = \frac{R\int_{0}^{L} S_u dl}{W.x} \tag{2.9}$$

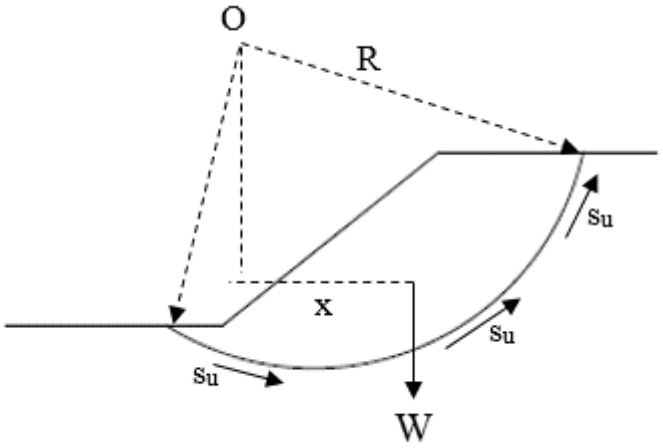


**(c)**

**Figure 2.1. Various definitions of factor of safety (FS) (a) limit equilibrium (b) force equilibrium (c) moment equilibrium (Abramson et al., 2002)**

Although LE method is the most common approach, it has some shortages. LE method is applicable for only Mohr-Coulomb soil model and needs a user defined critical slip surface. Since the only output is FS, this method cannot compute displacement of pertinent sliding block. Unity is accepted as criteria for slope stability. For the

situations that FS is equal or more than unity, the slope is assumed as safe. In order to overcome these limitations, limit equilibrium based finite element method is used for slope stability analyses. A brief summary of LE methods is given in Table 2.1.

**Table 2.1. Summary of LE methods (Aryal, 2006)**

| Methods | Circular | Non-cir. | ΣM = 0 | ΣF = 0 | Assumptions for T and E |
|---|---|---|---|---|---|
| Ordinary | x | - | x | - | Neglects both E and T |
| Bishop simplified | x | (*) | x | (**) | Considers E, but neglects T |
| Janbu simplified | (*) | x | - | x | Considers E, but neglects T |
| Janbu GPS | x | x | (***) | x | Considers both E and T, act at LoT |
| Lowe-Karafiath | - | x | - | x | Resultant inclines at, $\theta = ½(\alpha + \beta)$ |
| Corps of Engineers | - | x | - | x | Resultant inclines at, $\theta = ½(\alpha_1 + \alpha_2)$ |
| Sarma | x | x | x | x | Interslice shear, $T = ch + E \tan\varphi$ |
| Spencer | x | (*) | x | x | Constant inclination, $T = \tan\theta\ E$ |
| Morgenst.-Price | x | x | x | x | Defined by f(x), $T = f(x).\lambda.E$ |
| (*) Can be used for both circular and non-circular failure surfaces,<br>(**) satisfies vertical force equilibrium for base normal force, and<br>(***) satisfies moment equilibrium for intermediate thin slices (Janbu 1957, Grande 1997) | | | | | |

## 2.2. Dynamic Analyses

### 2.2.1. Seismic slope stability

Seismic slope stability evaluation is a compelling topic in geotechnical earthquake engineering. In general manner, either internal instabilities under static loading or earthquake induced weakening cause landslide activities. Geological parameters (planes of weakness, discontinuities etc.), hydraulic effects (seepage, precipitation, swelling, pore pressure increment), construction activities (excavation, external loading), cyclic loading (earthquake, blasting) can be listed as the possible reasons for instability of the slopes.

Terzaghi (1950) can be said to be pioneer of the reconnaissance on seismic slope stability analysis with adjusting pseudo-static theory to seismic slope stability subject. Until that moment, the compelling issue was the application of earthquake forces to the earthen structures. Pseudo-static theory is used to render the seismic loads as a horizontal static load by multiplying with a coefficient called pseudo-static coefficient or seismic coefficient or yield coefficient ($k_h$ or $k_v$). This method aims to achieve the minimum seismic load that can cause instability in the slope. Although, a factor of safety can be obtained with this method, it is not adequate for a comprehensive hazard assessment. A more realistic and reliable method is required.

Newmark (1965), tried to clarify the hesitations about factor of safety with a new limit equilibrium based sliding block method. This method proposed a procedure to calculate the earthquake induced deformations. Permanent displacement calculation is widely accepted to be more accurate treatment against the factor of safety based approaches. Initially the sliding mass is assumed as a sliding rigid block and then a yield acceleration is determined. This yield acceleration can be defined as the acceleration that makes factor of safety 1.0 during dynamic loading. Second step is to evaluate the earthquake induced accelerations in the embankment. For the accelerations exceeding the yield acceleration, a cumulative integration is applied. Finally, double integration of exceeding accelerations results in permanent displacement.

Pseudo-static analysis and Newmark's sliding block theory are combined with finite element method by Chopra in 1966 (Jibson, 2011). In finite element method, continuum mass is divided in to small discrete elements. Static and dynamic calculations are made on the basis of finite elements.

### 2.2.2. Pseudo-static analysis method

Pseudo-static approach dates back to 1920s and is one of the widely used method for the seismic stability assessment of earth structures. Whereas, this method was firstly recommended for retaining structures by Mononobe and Okabe in 1924 (Pathmanathan, 2007), adjustment to slope stability is made by Terzaghi (1950).

Pseudo-static method contains limit equilibrium based force or moment calculations, in addition to static conditions, the dynamic force caused by earthquake is treated as a static force. Despite the earthquake forces always change direction and magnitude, horizontal force caused by earthquake is assumed as a constant force just in one way. The earthquake forces acting on structure are expressed in terms of gravitational force and a seismic coefficient called pseudo-static coefficient (k) (Equation 2.10 and Equation 2.11). In order to represent the seismic loads as a horizontal force, the gravitational force is multiplied with the horizontal pseudo-static coefficient. The vertical component of earthquake force is commonly neglected by the engineers, because of being relatively small. This method involves the evaluation of minimum factor of safety against the earthquake induced sliding forces along a critical potential failure surface. The aim of the pseudo-static analysis is to determine the value of pseudo-static coefficient required for the evaluation of minimum factor of safety. Since, for the slope stability problems, unity is accepted as a limit of safety. The slices of sliding mass, having factor of safety less than "1", are assumed as an unsafe situation. However, in some cases, during the excitation, despite the factor of safety sometimes drops below 1, no deformation may be observed. Illustrations of pseudo-static forces are given below in Figure 2.2.

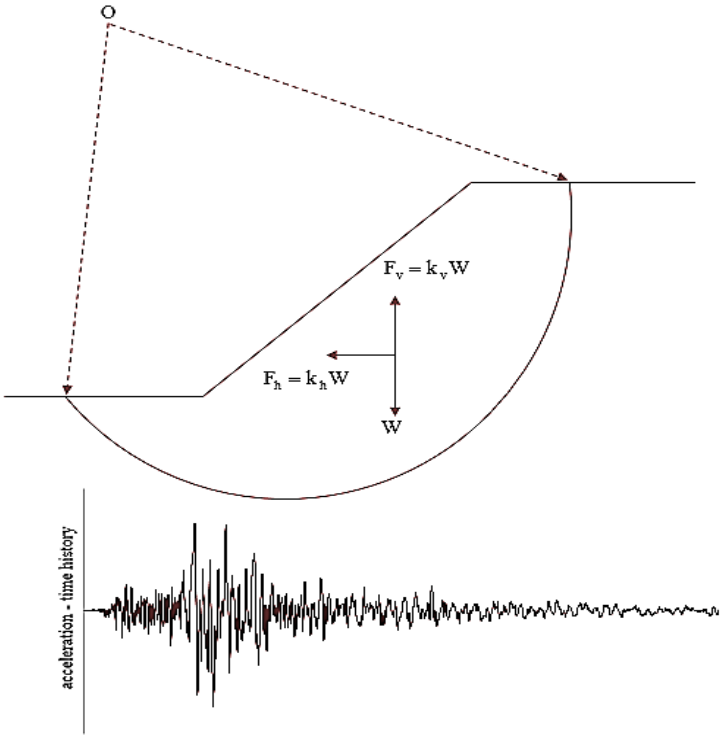


**Figure 2.2. Pseudo-static forces acting on a slip surface**

$$F_h = \frac{a_h W}{g} = k_h W \tag{2.10}$$

$$F_v = \frac{a_v W}{g} = k_v W \tag{2.11}$$

$a_v, a_h$ : Vertical and horizontal pseudo-static accelerations, respectively

$k_v, k_h$ : Vertical and horizontal pseudo-static coefficients, respectively

W : Weight of sliding mass

g : Gravitational acceleration

The most formidable part of this approach is the selection of convenient and representative pseudo-static coefficient which affects whole analyses and results. According to the assumptions, slopes are rigid and are subjected to the peak horizontal acceleration of earthquake throughout the duration of motion, however, in fact exactly the opposite situation is valid, that is, slopes are not rigid and the peak horizontal acceleration of earthquake is applied for a short time. Kramer (1996) suggested that

the seismic coefficient should be related with the inertial forces generated in the slope due to the dynamic forces caused by earthquake excitation and put together available recommendations for design as in Table 2.2.

**Table 2.2. Recommended horizontal seismic coefficients (Kramer, 1996)**

| Horizontal seismic coefficient $k_h$ | Description | |
|---|---|---|
| 0.05 - 015 | In the United States | |
| 0.12 – 0.25 | In Japan | |
| 0.1 | Severe earthquakes | Terzaghi |
| 0.2 | Violent, destructive earthquakes | |
| 0.5 | Catastrophic earthquakes | |
| 0.1 - 0.2 | Seed , FS $\geq$ 1.15 | |
| 0.10 | Major Earthquake, FS > 1.0 | Crops of Engineers |
| 0.15 | Great Earthquake, FS > 1.0 | |
| 1/2 to 1/3 of PHA | Marcuson, FS >1.0 | |
| 1/2 of PHA | Hynes-Griffin FS > 1.0 | |
| FS = Factor of Safety. PHA = Peak Horizontal Acceleration, in g's. | | |

Melo and Sharma (2004) studied on the selection of seismic coefficient for pseudo-static analysis and the influencing factors. According to this parametric research:

- Steeper slopes generate higher seismic coefficients than flatter ones
- The seismic coefficients appear to be directly proportional to the embankment height
- The seismic coefficients also appear to be directly proportional to the PHA of the input ground motion
- The analyses in which the embankment had a higher shear wave velocity (stiffer) than the foundation yielded the highest seismic coefficients, while the reverse was true for the analyses in which the embankment had a lower shear wave velocity (less stiff) than the foundation.

In addition to these numerical assessments, Bray and Travasarou (2009) focused on the rational basis studies for seismic coefficient prediction. This proposed study necessitate to specify the permissible dynamic displacement of the structure to be analyzed and then the dynamic behavior of sliding mass can be expressed in terms of its fundamental period. Considering the earthquake magnitude, spectral acceleration, fundamental period of sliding mass and predefined displacement, they suggested probabilistic procedures to calculate the seismic coefficient.

### 2.2.3. Shear beam method

Shear beam method is the earliest theory for the dynamic response analysis of fill dams (Mononobe, 1936). This theory is based on many assumptions as listed below:

- The triangular dam body is an assemblage of horizontal thin planes with interconnection of slices are provided by elastic springs and viscous damping devices.
- The dam model is infinitely long and formed homogeneously.
- The dam section is symmetric.
- Material properties as elastic modulus (E), shear modulus (G) and mass density ($\rho$) are constant.
- Earthquake generated motion and dam motion are in only horizontal direction.
- Calculations capture only the shear forces and the dynamic normal forces, deformations are excluded.
- The shear stress is distributed uniformly over the planes.
- The effect of stored water in reservoir is omitted.

According to assumptions, the dam can be drawn as in Figure 2.3.

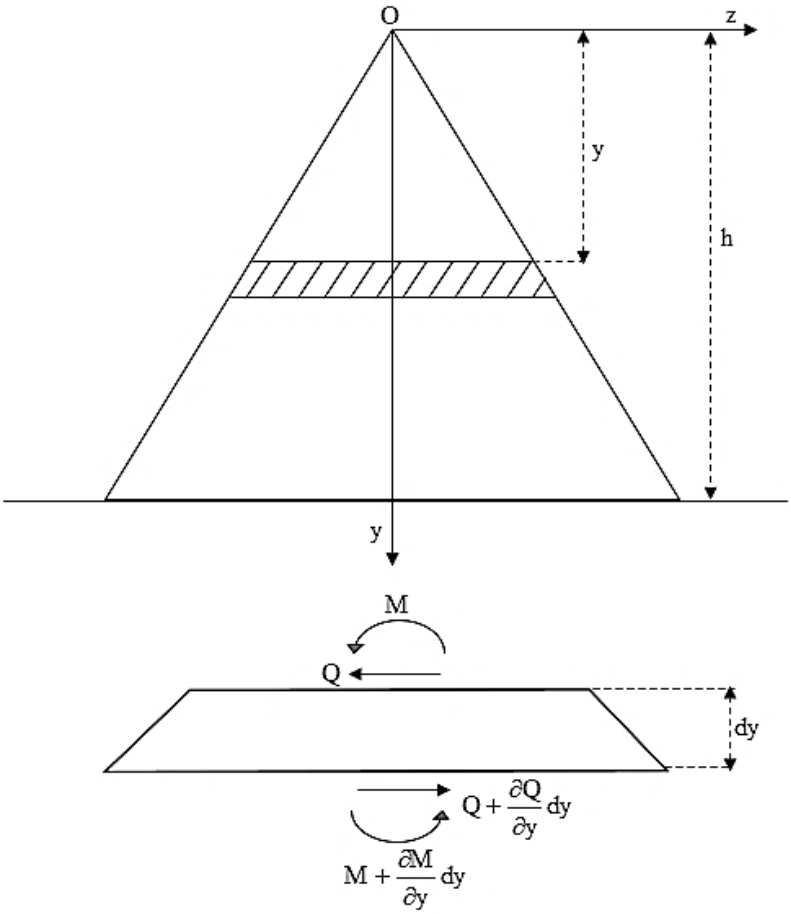


**Figure 2.3. Shear beam method**

The dynamic equilibrium is obtained utilizing following differential equation, u is horizontal displacement at depth z, t is time and G is shear modulus and $\rho$ is mass density of filling material.

$$\frac{\partial^2 u}{\partial t^2} = \frac{G}{\rho}\left(\frac{\partial^2 \mathrm{u}}{\partial \mathrm{z}^2} + \frac{1}{\mathrm{z}}\frac{\partial \mathrm{u}}{\partial \mathrm{z}}\right) \tag{2.12}$$

Solution of this differential equation using Bessel function considering dam height h, constants $A_n$ and $B_n$, $J_0$ is the Bessel function of first kind and order zero.

$$\mathrm{U(z,t)} = \sum_{\mathrm{n=1}}^{\infty}\left[\mathrm{A_n sinw_n t + B_n cosw_n t}\right]\mathrm{J_0}\left(\beta_n \frac{\mathrm{y}}{\mathrm{h}}\right) \tag{2.13}$$

Natural frequency is expressed as;

$$\omega_n = \frac{\beta_n}{h}\frac{G}{\rho} = \frac{\beta_n}{h}V_s \quad , \quad \text{n=1, 2, 3...} \tag{2.14}$$

Likewise, natural periods are calculated as;

$$T_1 = 2.613\frac{h}{V_s} \tag{2.15}$$

$$T_2 = 2.14\frac{h}{V_s} \tag{2.16}$$

$$T_3 = 0.73\frac{h}{V_s} \tag{2.17}$$

The factor $J_0\left(\beta_n \frac{y}{h}\right)$ in the equation is used to evaluate the modal shapes. Figure 2.4. shows the first three mode shapes.

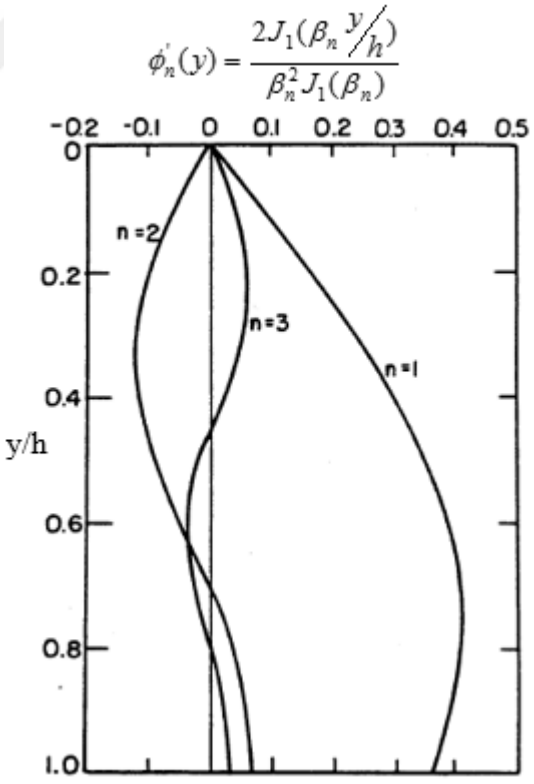


**Figure 2.4. Variation of shear strain mode participation factors with depth-shear slice method (Makdisi and Seed, 1978)**

### 2.2.4. Finite element method

The finite element expression is firstly used by Clough in 1960 to evaluate the stress-deformation analysis of homogeneous embankments statically. Since then, many researchers contributed this method like Idriss and Seed (1970),Idriss and Lee (1975) to use in geotechnical issues both static and dynamic cases.

Finite element theory is based on discretization of sliding mass into triangular or quadrilateral small sized elements and then reconnecting them from the boundary of each element named “node”. Different finite element models in 1D, 2D and 3D are given in Figure 2.5. Additionally, mesh generation and nodes are shown in Figure 2.6. Since the response is related with the finite element model a definition is stated for division of continuum model. The dimension of finite elements are associated with wave length. One-eighth to one-fifth of shortest wavelength is determined as an upper limit for dimension of any element (Kuhlemeyer and Lysmer, 1973). Initially, equation of motion is written for every element considering the nodal boundary conditions of itself and then all the equations are combined to achieve global equation of motion.

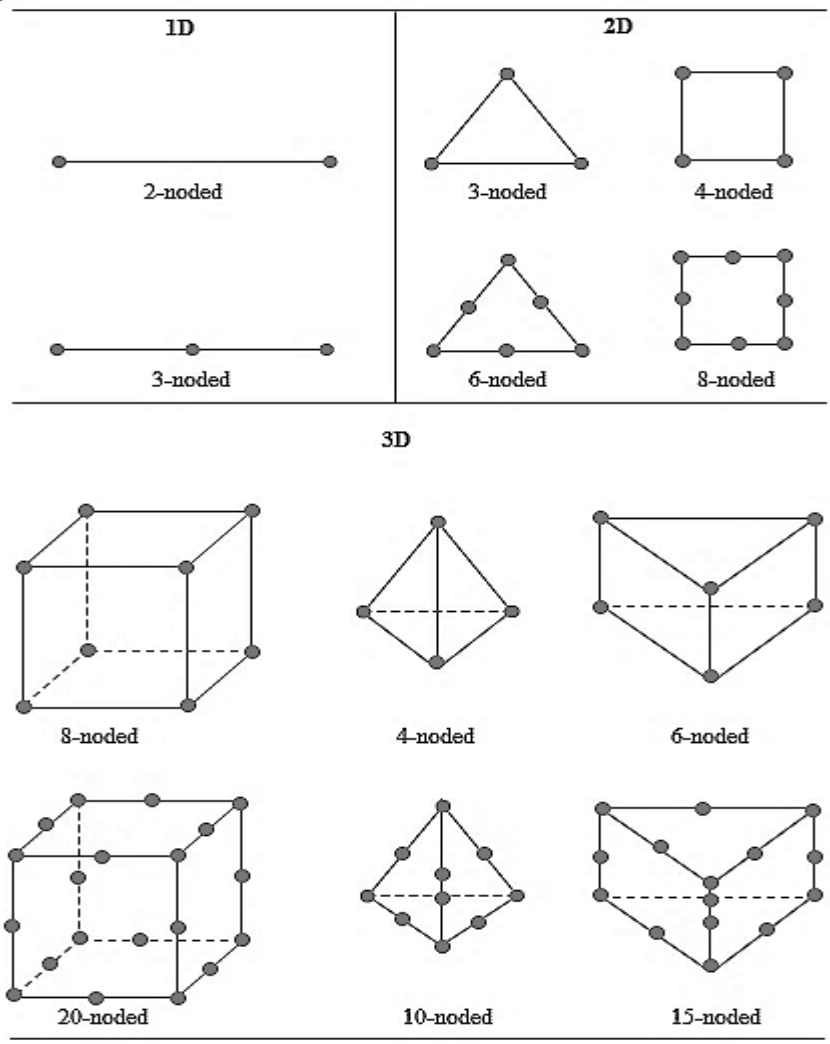


**Figure 2.5. Finite elements in 1D, 2D and 3D**

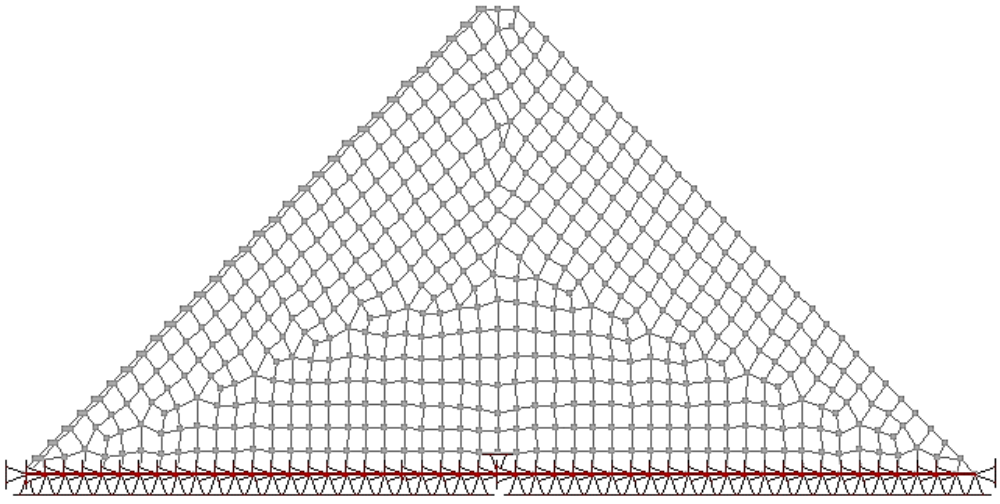

**Figure 2.6. Finite element mesh model of a dam cross section**

Assemblage of computer aided programs and numerical calculation methods, provide easiness to figure out the deformation characteristics and dynamic response of embankments and slopes. This method enables to simulate complex geometries and to apply strain dependent properties of soil as damping ratio and shear modulus degradation to analyses. Thus, nonlinear behavior of soil can be represented. Although three dimensional finite element based software like FLUSH , ABAQUS, ANSYS are available, two dimensional ones like LUSH, QUAD-4, PLAXIS, QUAKE/W are mostly preferred.

Since the third dimension of embankment is relatively large, 2D analysis is preferred for sake of ease. In two dimensional analysis, dam material is assumed to behave according to plain strain conditions.

Finite element method is mostly preferred and sufficient approach for the stability assessment of slopes and embankments under either static or dynamic loads. Capability of analyzing time dependent deformations by using strain compatible parameters provides advantage over limit equilibrium based methods.

### 2.2.5. Equivalent linear method

Dynamic properties of soil profiles vary due to cyclic loading generated by earthquake. Since the initial conditions of materials are changed by propagated waves through the soil strata, dynamic response of soil evolves. When the soil is expected to exhibit very small strains under increasing stress, linear elastic soil model can be used. However, if the soil undergoes medium and higher strains due to the loading, this behavior is known as nonlinear behavior. In other words, while the stiffness/shear modulus of soil shows tendency to decrease, damping of soil increases. Equivalent linear approach combines the linear approach with nonlinear soil properties by using strain dependent assumptions.

Cyclic loading causes soil to reveal a hysteretic loop as shown in Figure 2.7. As seen in the figure, while the strain increases, secant shear modulus decreases. The alteration of secant shear modulus is represented by backbone curve connecting the tips of stress paths. Herein, tangent of the initial point of this curve represents the maximum shear modulus.

Besides, maximum secant shear modulus can be evaluated by using shear wave velocity ($V_s$) and density of soil ($\rho$) as given in Equation 2.18.

$$G_{max} = \rho V_s^2 \tag{2.18}$$

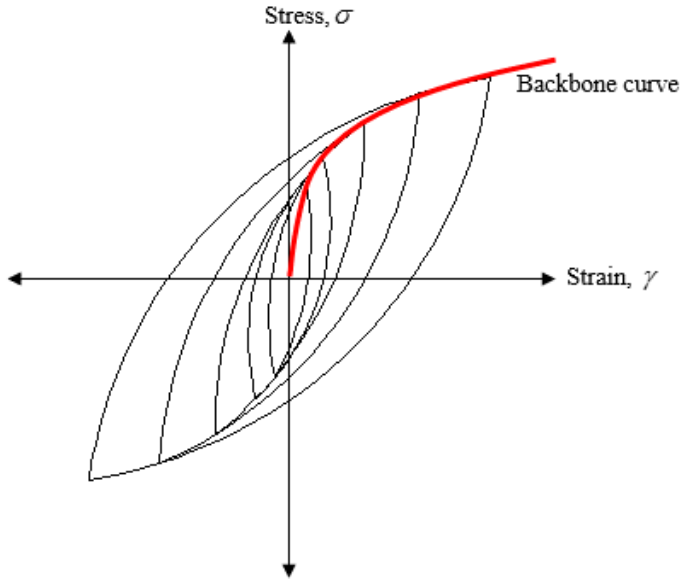


**Figure 2.7. Hysteretic curve of cyclic loading**

The equivalent material properties as equivalent shear modulus and equivalent damping ratio are obtained by using this hysteresis loop shown at Figure 2.8. and the dissipated energy can be calculated by using Equation 2.19.

$$\xi = \frac{1}{4\pi}\frac{W_D}{W_S} = \frac{1}{2\pi}\frac{A_{loop}}{G\gamma^2} \tag{2.19}$$

Where $W_D$ is dissipated energy, $W_S$ is maximum strain energy, $A_{loop}$ is the area of the hysteresis loop, $\gamma$ is current strain, $\xi$(D) is damping ratio and G is corresponding shear modulus.

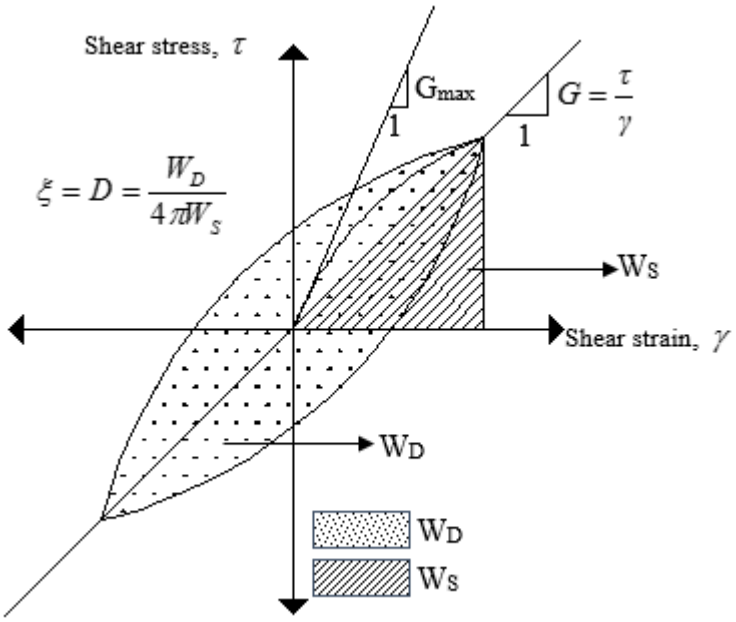


**Figure 2.8. Representation of the energy dissipation (Ishiara, 1996)**

As the strain evaluations based on equivalent linear properties, an iterative procedure is required for calculations. This procedure captures following steps (Kramer 1996):

- Initial assumptions for the value of G and $\xi$ for small strains in each layer.
- These initial values are required to calculate the maximum shear strain in each layer.
- A reduction factor (e.g.65%) is applied to maximum shear strain to have an effective shear strain in each layer.
- This effective shear strain is used to select new equivalent linear properties for the following iteration.
- Step 2 to 4 are repeated until the permissible error value is reached.

Computer programs as SHAKE, SOILWORKS can execute this iterative procedure effectively and easily for ground response analysis of layered soils.

Moreover, shear modulus degradation and damping curves are available to be used in equivalent linear analysis. These recommended curves present the stiffness and damping fashion of soil under increasing strain. Seed et al. (1986), Vucetic and Dobry (1991), Ishibashi and Zhang (1993), Silva et al. (1996), Darendeli (2001) are proposed some curves for this method (Figure 2.9.).

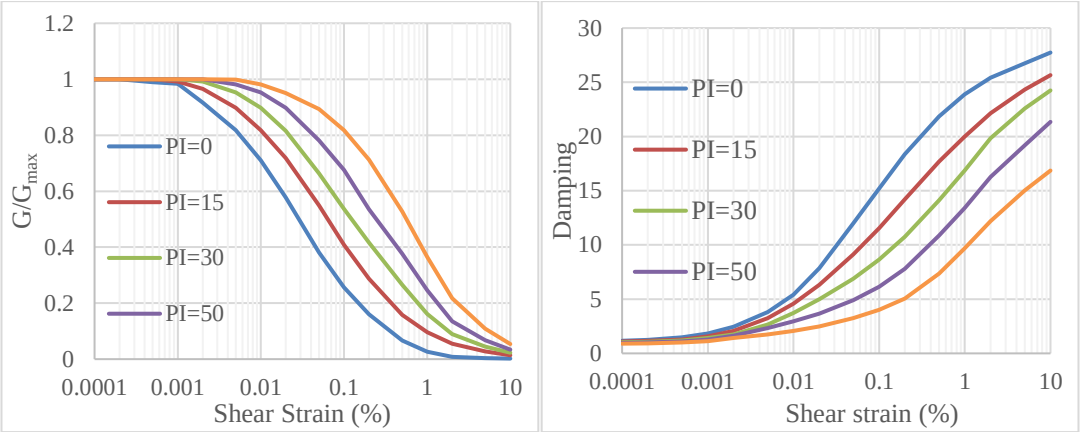


**Figure 2.9. Recommended modulus reduction and stress-strain curves (Vucetic and Dobry, 1991)**

### 2.2.6. Earthquake induced permanent displacement method

The earth creates numerous earthquakes during its endless evaluation process. Since there is no way to obtain the frequency of occurrence of earthquakes, the only topic to be focused is prediction of possible failure, according to this, designing earthquake-resistant structures. Proper seismic hazard assessment requirements generate many approaches for decades.

In early times, labeling the structures as safe or unsafe was the most essential necessity. Consequently, an index is defined by proportioning driving forces and resisting forces. This index is called factor of safety and used to categorize the structures if they are safe or not. Cyclic loads generated by earthquake are integrated to force equilibrium equations by pseudo-static approach (Terzaghi, 1950). This limit equilibrium and pseudo-static approaches are used for a while for static and dynamic analysis of slopes and embankments. However, this safety based classification is insufficient for seismic hazard assessments.

The analysis methods progress to development of permanent displacement based methods with Newmark (1965). Numerous other studies are originated from this approach. Makdisi and Seed (1978), Sarma (1975), and Ambraseys (1973) carried out some analysis and present some curves for permanent displacement calculations. Likewise, Hynes-Griffin and Franklin (1984) represent the displacement in terms of critical and peak accelerations.

Newmark's sliding block based studies show that this method is sufficient for the simulation of the seismic compression of large compacted earth fills (Stewart et al., 2001). In contradiction to rigid sliding block approach, Makdisi and Seed (1978) proposed a deformable soil model under dynamic loadings to consider the dynamic response of sliding soil mass. Lin and Whitman (1983), Rathje and Bray (2000) suppose this assumption because of being more realistic, however, this decoupled approach has some limitations because of overestimation probability for resonance and underestimation possibility for the case in which the structure has large fundamental period. Moreover, Ambraseys and Menu (1988), Yegian et al. (1991), Bray and Travasarou (2007), Rathje and Saygılı, (2009), work on the probability of potential permanent displacement that the slope can perform during the earthquake.

Nowadays, advanced computer techniques add another dimension to seismic slope stability assessments. Furthermore, considering equivalent linear material behavior, finite element based dynamic limit equilibrium analysis can be performed with new software. PLAXIS, SLOPE/W, QUAKE/W can be example of these kind of software.

#### *2.2.6.1. Newmark sliding block method*

Permanent displacement prediction is one of the most important part for seismic hazard assessment of dams and embankments. The early most used method is pseudo-static analysis in order to evaluate the dynamic safety of these structures. Since this method results in safety factor of potential sliding mass it can be used to identify the slope as safe or unsafe. However the real challenge is determination of the level of safety or unsafety. At this point, Newmark (1965) chances the way of improvements of stability approaches.

Against the lack of reliability in limit equilibrium based procedures, Newmark suggested a new concept to predict the seismic safety of slopes in terms of earthquake induced permanent displacement. Newmark's sliding block analysis is originated from pseudo-static analysis and the sliding portion is assumed as a rigid block with definite edges. This rigid block linearly moves along the slip surface as it is on an inclined surface (Figure 2.10.).

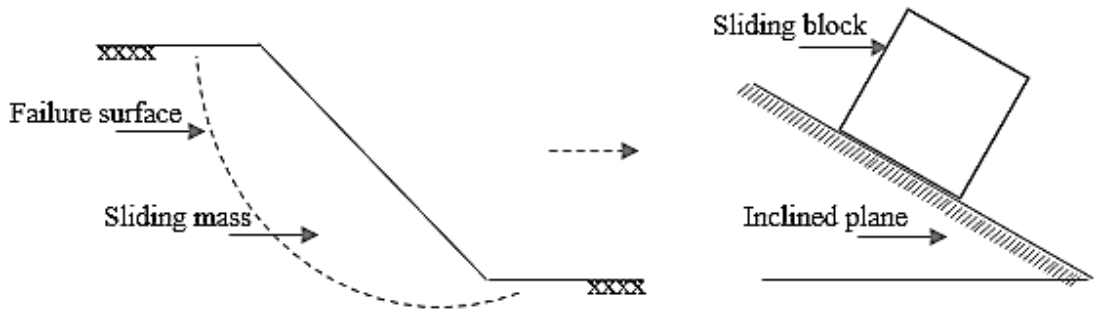


**Figure 2.10. Newmark sliding block analysis**

Initially, a yield acceleration is defined for the slope to be analyzed which is the maximum acceleration value that slope can withstand. The slopes are assumed safe as long as the driving and resisting forces are equal to each other (FS=1) or resisting forces are bigger than driving forces (FS>1). For the case of driving forces are higher than the resisting ones (FS<1), beyond the elastic phase, a permanent deformation is observed. Calculation of this permanent displacement, based mainly on double integration of earthquake induced accelerations that exceed the yield acceleration of related sliding portion.

Permanent displacement calculation steps according to Newmark's sliding block analysis can be written as below;

- Pseudo-static analysis procedure is conducted to show the earthquake induced forces act on the slope.
- A yield acceleration is defined. Under dynamic loadings, this yield acceleration makes the factor of safety 1. It can be said that yield acceleration is the minimum value of pseudo-static acceleration. Yield acceleration can be defined as in following equation.

  $$a_y = k_y g \qquad (2.20)$$

  $a_y$: yield acceleration

  $k_y$: yield coefficient

  g: gravitational acceleration
- The accelerations that exceed the yield acceleration cause movement of sliding prone parts of slopes. This movement creates permanent displacement. Double

integration of exceeding accelerations gives permanent displacement values (Figure 2.11.)

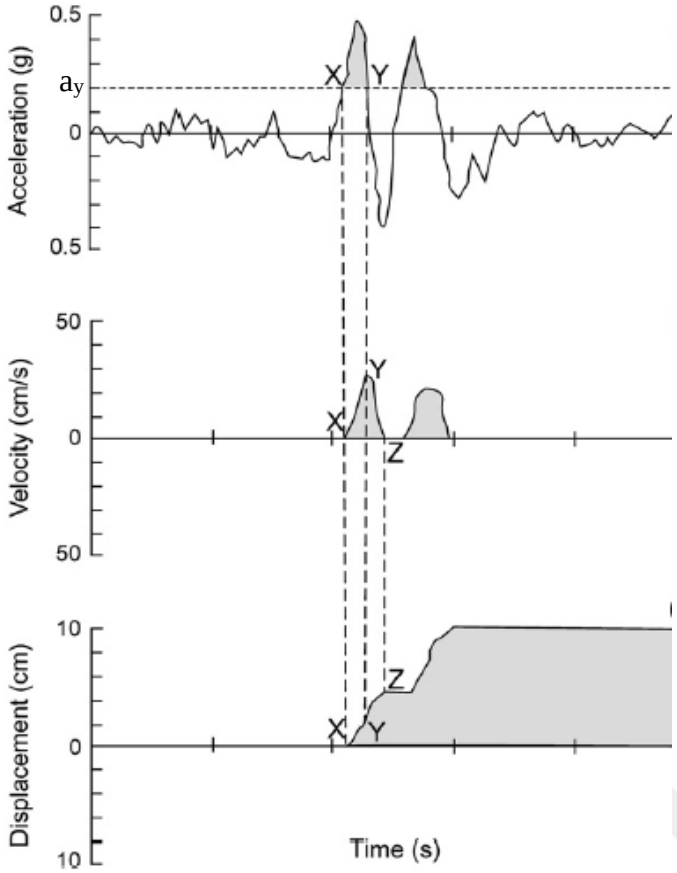


**Figure 2.11. Illustration of Newmark integration algorithm (Jibson, 2011)**

Furthermore, at every step of the analysis, finite element based computer programs can be used to provide a detailed reconnaissance. Dividing the sliding strata into smaller pieces by finite element mashes and calculating the earthquake induced acceleration in mash sized soil basis, make contribution to the accuracy of analyses.

*2.2.6.2. Makdisi and Seed (1978)*

Makdisi and Seed (1978) combined two methods to calculate the earthquake induced permanent displacements of slopes. Calculation of the average acceleration is made with the method proposed by Chopra (1966) and Newmark (1965) sliding block analysis is conducted for permanent displacement evaluation. These procedures are recommended if only the strength reduction of material is not significant.

The specified allowable strength loss is 10% to 20% of maximum undrained shear strength for safe designs.

Furthermore, a number of assumed and present dams are subjected to some real and artificial earthquake records after scaling to various magnitudes. The results are used to associate the permanent displacements with yield acceleration ($a_y$) and maximum earthquake induced crest acceleration ($a_{max}$) (Figure 2.12.).

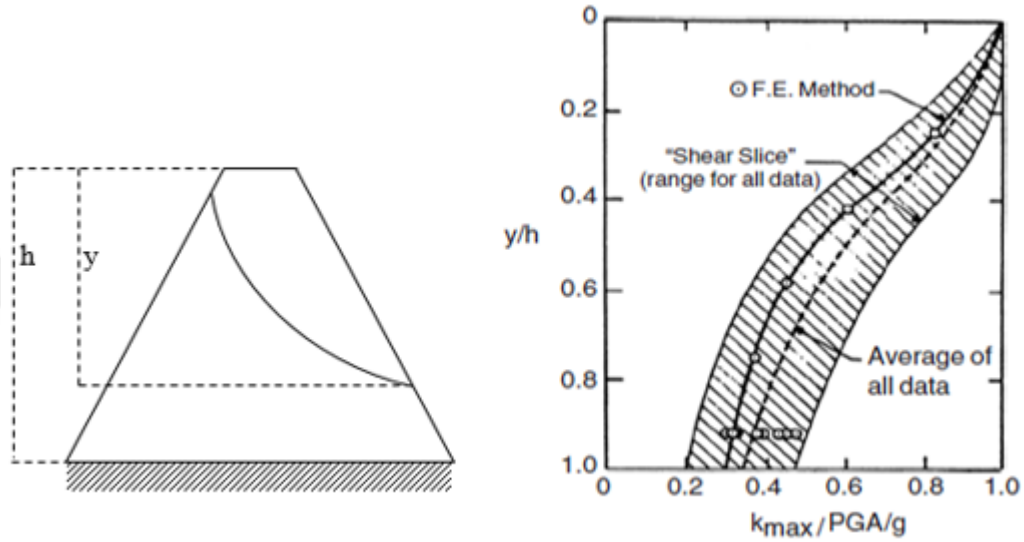


**Figure 2.12. Variation of average maximum acceleration with depth of slip surface (After Makdisi and Seed, 1978)**

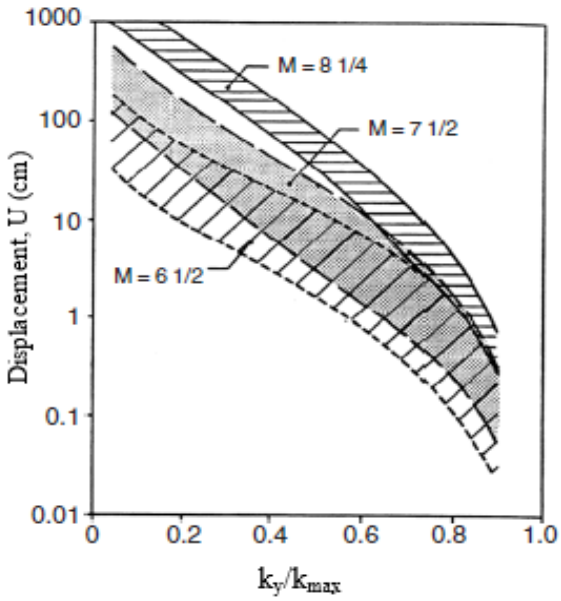


**Figure 2.13. Variation of permanent displacement with yield acceleration (Bray, 2007)**

Steps to be followed for permanent displacement prediction according to this method are listed below.

- By using pseudo-static approach a yield acceleration ($a_y$) that satisfies factor of safety 1.0, is determined.
- Earthquake induced maximum crest acceleration ($a_{max}$) is evaluated utilizing computer programs, suggested charts or other proposed methods. Then fundamental period of corresponding sliding portion is calculated.
- In order to calculate the average maximum acceleration ($a_{max,avg}$) of sliding mass, Figure 2.12 is used.
- Finally, Figure 2.13. is used to calculate the permanent displacement for the magnitude range to be considered.

Since the composed chats contain case study results, the authors suggested the researchers to update the charts with available data. Sarma (1975) and Ambraseys (1973) examined this method for earthquakes with magnitude of about 6.5 and Figure 2.14. shows the comparison of results.

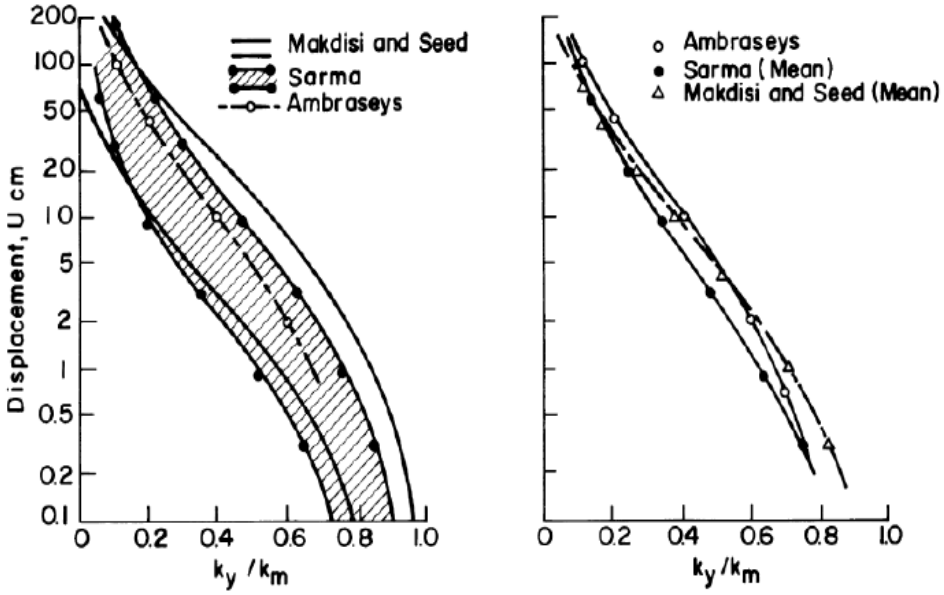


**Figure 2.14. Computed displacement of embankment dams subjected to magnitude 6.5 earthquakes having little or no loss of strength due to earthquake induced deformations (Seed, 1979)**

*2.2.6.3. Jibson (2007)*

Jibson (2007) proposed a simple regression model utilizing Newmark sliding block model for seismic displacement evaluation. 2270 strong motion records were used for these regression equations. Critical acceleration ($a_c$) which is same with yield acceleration, maximum acceleration ($a_{max}$ or PGA), moment magnitude of earthquake (M), Arias intensity ($I_a$) were included in the equations. Since the model has a standard deviation of 0.5, it is recommended to use for seismic landslide hazard mapping or rapid preliminary assessment of site. It is not useful to apply for site specific designs. Different regression models composed of various ground motion parameters can be seen in Equation 2.21 to Equation 2.24.

$$\log D_n = 0.215 + \log\left[\left(1-\frac{a_c}{a_{max}}\right)^{2.341}\left(\frac{a_c}{a_{max}}\right)^{-1.438}\right] \pm 0.510 \quad (2.21)$$

$$\log D_n = -2.710 + \log\left[\left(1-\frac{a_c}{a_{max}}\right)^{2.335}\left(\frac{a_c}{a_{max}}\right)^{-1.478}\right] + 0.424M \pm 0.454 \quad (2.22)$$

$$\log D_n = 2.401 \log I_a - 3.481 \log a_c - 3.230 \pm 0.656 \quad (2.23)$$

$$\log D_n = 0.5611 \log I_a - 3.833 \log(a_c/a_{max}) - 1.474 \pm 0.616 \quad (2.24)$$

*2.2.6.4. Bray and Travasarou (2007)*

In order to consider the unpredictable nature of earthquakes Bray and Travasarou (2007) combined the Newmark's framework with probabilistic point of view. This method based on nonlinear fully coupled stick-slip sliding block model and can be applied to earth dams, natural slopes, compacted earth fills and waste fills. Earthquake induced deviatoric displacements expressed in terms of yield coefficient ($k_y$), initial fundamental period ($T_s$), and spectral acceleration of ground motion at degraded period ($1.5T_s$). Probability of the exceedance of permanent displacements are

calculated with the proposed method. Besides, probability of zero displacements that are less than 1 cm are excluded during the calculations. Equation (2.25) can be used for earthquake induces permanent displacement evaluation.

$$\ln(D) = -0.22 - 2.83\ln(k_y) - 0.333(\ln(k_y))^2 + 0.566\ln(k_y)\ln(a_{max}) + 3.04\ln(a_{max}) - 0.244(\ln(a_{max}))^2 + 0.278(M-7) \quad (2.25)$$

*2.2.6.5. Saygılı and Rathje (2009)*

One other interpretation of Newmark's sliding block was made by Saygılı and Rathje (2009) for the seismic displacement assessments of natural slopes. Yield acceleration ( $k_y$), maximum ground acceleration (PGA) and earthquake magnitude are necessary parameters for the earthquake induced displacement calculations. Yield acceleration is calculated according to the Equation 2.26 proposed by Saygılı and Rathje (2009). Herein, $\alpha$ is slope angle, $\varphi$ is internal friction angle of material.

$$k_y = \frac{(FS-1)*g}{\cos\alpha * \tan\phi + 1/\tan\alpha} \quad (2.26)$$

$$\ln D = 4.89 - 4.85\left(\frac{k_y}{a_{max}}\right) - 19.64\left(\frac{k_y}{a_{max}}\right)^2 + 42.49\left(\frac{k_y}{a_{max}}\right)^3 - 29.06\left(\frac{k_y}{a_{max}}\right)^4 + 0.72\ln(a_{max}) + 0.89(M-6) \quad (2.27)$$

# 3. ANALYSES OF NUMERICAL DAM MODELS

## 3.1. Analyses Procedure

As mentioned before, this thesis is a numerical study and contains a series of finite element analyses. 1728 dynamic analyses were conducted for the dynamic response and earthquake induced permanent displacement prediction of concrete faced rockfill dams. Tabulated form of parameters used in this numerical study is presented in Table 3.1. Steps to be followed for the analyses procedure are stated below.

Effects of dam height, slope inclination, crest width and material properties on the response of rockfill dams were planned to investigate. Thus, dam models used in analyses were set off with different geometric and material properties.

Required seismic excitations were provided from real earthquake records obtained from Pacific Earthquake Engineering Research Center (PEER) ground motion database. Input motions were expected to contain different frequency content. The selection was made by comparing the response spectra of excitations. To investigate the effect of maximum ground acceleration, acceleration records were used after scaling them to different PGAs.

To determine the yield acceleration ($a_y$) and factor of safety (FS) of critical slip surfaces, pseudo-static analyses were conducted by using the limit equilibrium based computer program SLIDE. Predefined potential slip surfaces with three different depths were searched and, 1/3 and 1/2 of maximum ground acceleration were applied as horizontal seismic coefficient.

Dam models were divided into layers and maximum shear modulus calculations were made at the midpoints of layers. Damping and modulus degradation curves were defined for the iterations of equivalent linear analysis procedure. Acceleration records of nodes were saved and used for the study.

Initial stress conditions are essential for the dynamic analyses. Initial static analysis option of QUAKE/W was used for the static analyses of dam models to obtain the developed mean effective stresses. Then, dynamic analyses were performed utilizing the equivalent linear analysis option of QUAKE/W. Dynamic material properties were added to static analyses, then same mesh properties and boundary conditions were used in dynamic analyses.

Finally, earthquake induced permanent displacements were calculated using Newmark Sliding Block analysis. By integrating the accelerations above the yield acceleration ($a_y$), permanent displacements were obtained.

Prior to the dynamic analyses of dam models, Sürgü Dam was simulated with QUAKE/W to check its suitability for dynamic cases.

**Table 3.1. Used parameters in dam models**

| | |
|---|---|
| **Dam height** | 50 m – 100 m – 150 m – 200 m |
| **Crest width** | 5 m – 10 m – 15 m – 20 m |
| **Slope inclination** | 1:1.2 - 1:1.4 - 1:1.6 - 1:1.8 |
| **Internal friction angle** | $35^\circ$ - $40^\circ$ - $45^\circ$ - $50^\circ$ |
| **Earthquake** | 6 records |
| **Peak ground acceleration** | 0.2g - 0.4g – 0.6g |
| **Horizontal seismic coefficient** | $a_{max}/2$ – $a_{max}/3$ |

## 3.2. Simulation of Sürgü Dam

Improvement of computer aided programs eases the simulation of structures and computations of structural behavior under various situations. Within the geotechnical scope, a lot of alternatives are present for every kind of problem with numerical options as finite element, finite difference or material models as nonlinear, equivalent linear and so forth. However, it should not be forgotten, software are tools for only calculations, not for final decision. According to the outputs of programs, an engineering judgement is required for a proper design and reliability. Simulating the

case studies and comparing the results with actual values, in other words validations, help to prove reliability of programs and users to develop a point of view about the strengths and weaknesses of programs.

Although the results of previous studies conducted with QUAKE/W are logical, a validation is made by modelling Sürgü Dam. Sürgü Dam locates on Sürgü stream of Malatya in southeast Turkey. This rockfill with inclined clay core type dam is 55 m high from the ground level with a crest of 736 m length and 10 m width (Özkan et.al 1996). Location of dam is given in Figure 3.1. Inclined impermeable core is a composition of sandy and silty clay, and weathered gneiss material is used for rockfill parts. Slopes of downstream and upstream show changes at upper and lower elevations of dam body. Details of zones and the slopes are illustrated in Figure 3.2.

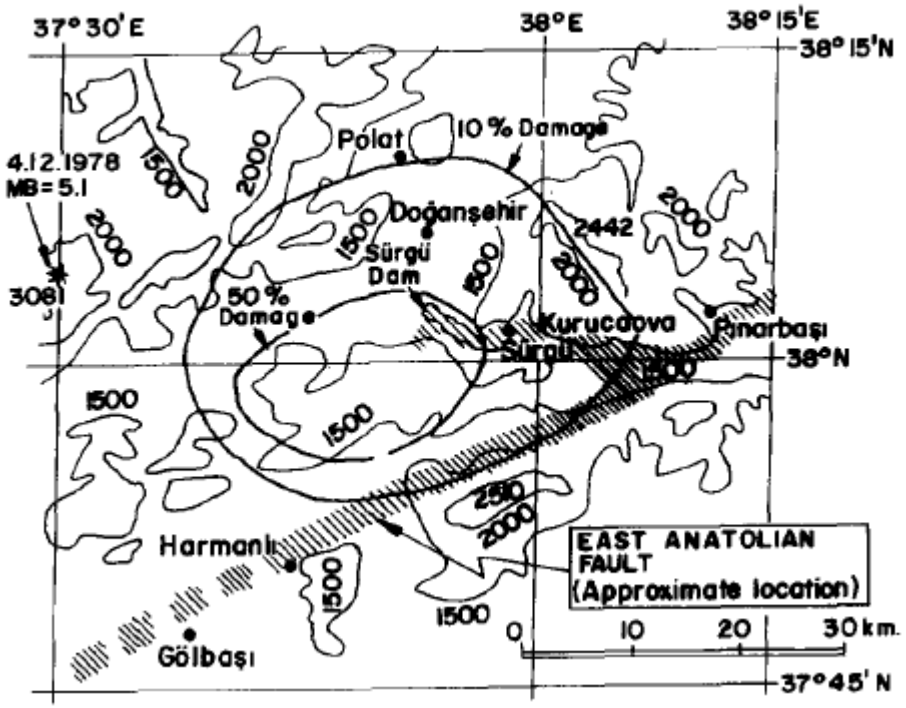


**Figure 3.1. Location of Sürgü Dam**

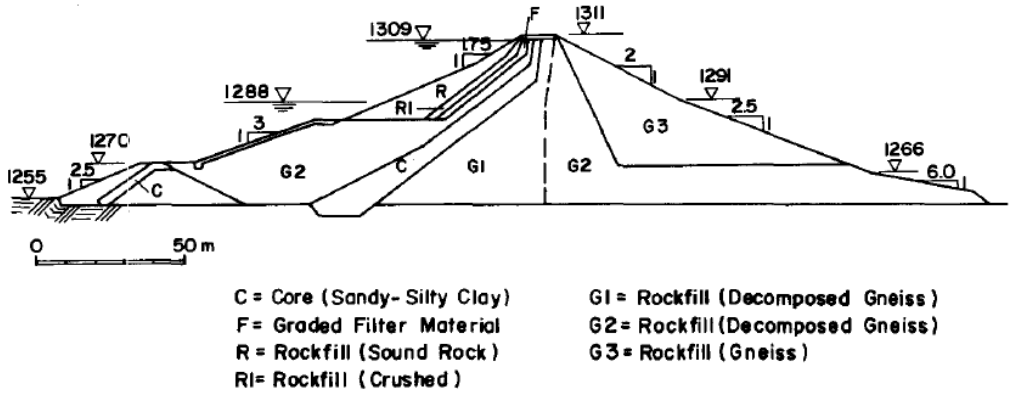


**Figure 3.2. Cross-section of Sürgü Dam embankment**

East Anatolian Fault, one of the major strike-slip fault mechanism of Turkey, ruptured on May 5, 1986 and created an earthquake with a magnitude of 5.8 ($M_b$) and epicentral distance of 10 km. According to report of Özkan et.al. (1996), there were longitudinal cracks on the crest up to 20 cm widths.

The maximum elongation of a continuous crack observed at crest was 150 m. Observed openings were scattered near the edges of upstream part with the depth of 0.5 m to 3.0 m from the crest. Moreover, settlement of the upstream part of crest was about 15 cm.

In the presence of these information, a numerical model was prepared to establish the dynamic response of Sürgü Dam with QUAKE/W. Observed deformations after Malatya earthquake and the numerical simulation outputs were compared. Thus, both algorithm of QUAKE/W and applicability of Newmark method were checked for the usage of seismic slope stability estimations of rockfill dams.

### 3.2.1. Numerical model

QUAKE/W maintains a good drawing interface for modelling the structures. Thus, according to the cross section shown in Figure 3.2., a numerical model of dam was prepared as given in Figure 3.3. Zonation of dam was in accordance with the original structure and the material properties are given in Table 3.2.

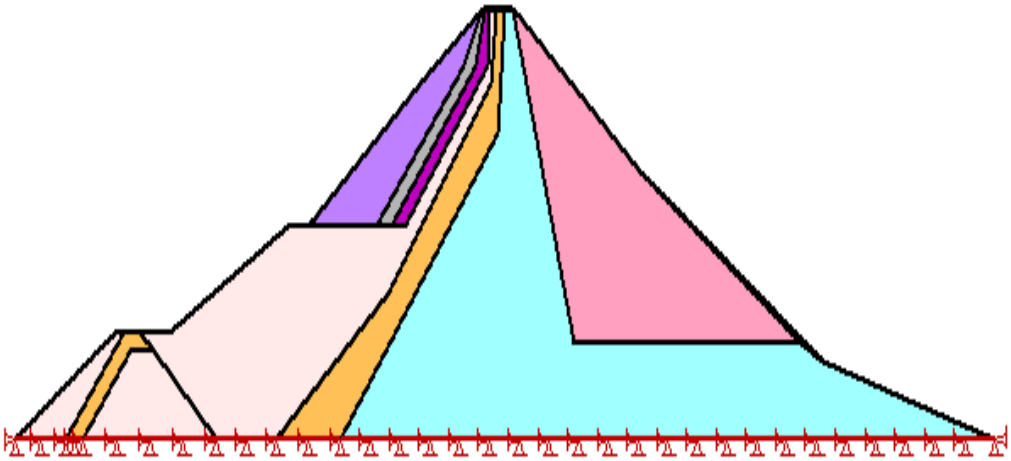

**Figure 3.3. QUAKE/W model of Sürgü Dam**

**Table 3.2. Material properties of Sürgü Dam**

| Material type | Internal friction angle | Cohesion kN/m$^2$ | Poisson's ratio ℣ | Dry Unit weight kN/m$^3$ |
|---|---|---|---|---|
| Core (C) (sandy and silty clay) | 22 | 10 | 0.42 | 19.5 |
| Rockfill (G1) (decomposed gneiss) | 27 | 0 | 0.3 | 19.5 |
| Rockfill (G2) (decomposed gneiss) | 33 | 0 | 0.3 | 19.5 |
| Rockfill (G3) (gneiss) | 35 | 0 | 0.3 | 19.5 |
| Rockfill (sound rock) | 40 | 0 | 0.3 | 19.5 |
| Filter | 33 | 0 | 0.38 | 19.5 |

### 3.2.2. Input motion

Although, records of Malatya Earthquake were gathered from different stations, they were not coherent with site conditions of Sürgü Dam. In this study, 6 real earthquake records obtained from PEER Strong Motion Database were used. The earthquakes were selected from the records generated by strike slip type faults with the magnitude range of 5.0 to 6.0. When the dam location and closest fault are considered about 10 km epicentral distance is suitable for selections.

Detailed information of earthquakes are written in Table 3.3. Acceleration-time histories and response spectra for 5% damping are presented in Figure 3.4. to Figure 3.9.

**Table 3.3. Earthquakes used in Sürgü Dam analyses**

| Name of event | Moment Magnitude | Arias intensity | Epicentral distance (km) | PGA (g) | Fault mechanism | Duration (s) |
|---|---|---|---|---|---|---|
| Coyote Lake-1 | 5.74 | 0.1 | 10.67 | 0.12 | Strike slip | 26.83 |
| Coyote Lake-2 | 5.74 | 0.5 | 9.02 | 0.26 | Strike slip | 26.86 |
| Mammoth Lakes-1 | 5.94 | 0.5 | 12.39 | 0.31 | Strike slip | 25.995 |
| Mammoth Lakes-2 | 5.94 | 1.0 | 12.39 | 0.38 | Strike slip | 11.5 |
| Parkfield-1 | 6.0 | 1.0 | 9.95 | 0.17 | Strike slip | 60 |
| Parkfield-2 | 6.0 | 1.0 | 9.34 | 0.20 | Strike slip | 60 |

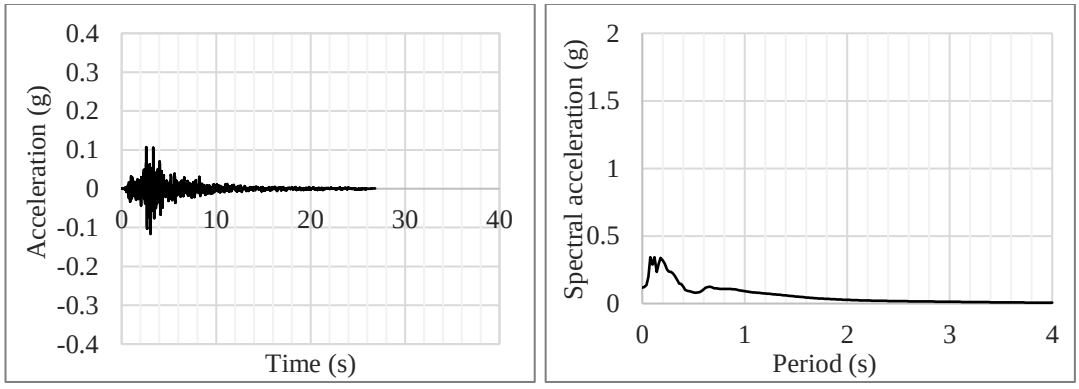


**Figure 3.4. Acceleration-time history and response spectrum of Coyoto Lake-1 earthquake**

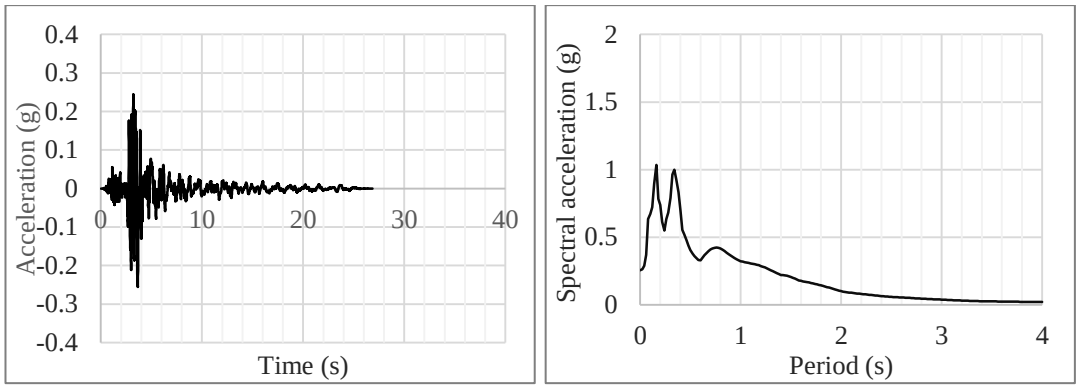


**Figure 3.5. Acceleration-time history and response spectrum of Coyoto Lake-2 earthquake**

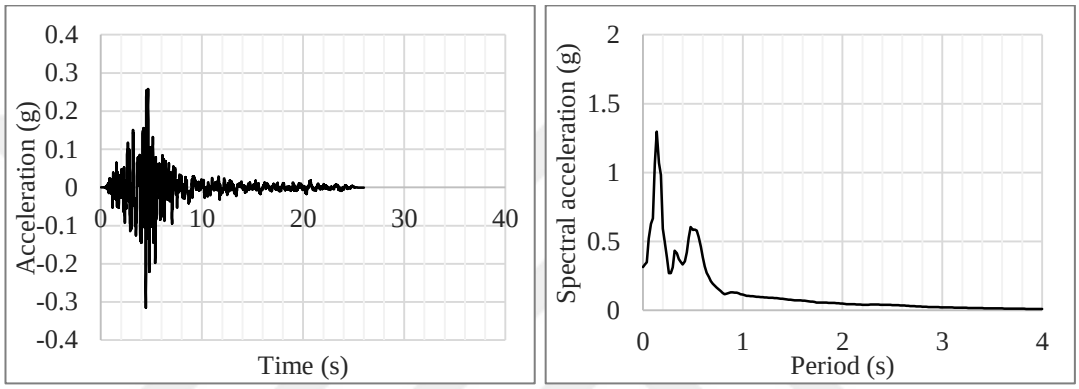


**Figure 3.6. Acceleration-time history and response spectrum of Mammoth Lakes-1 earthquake**

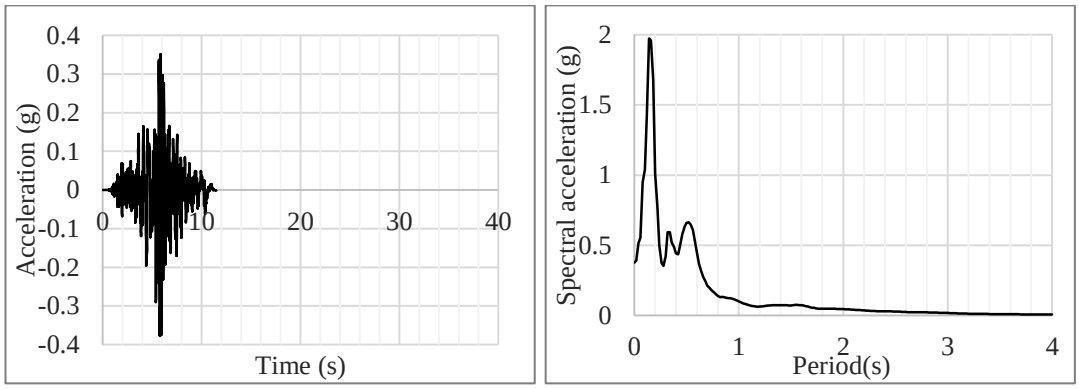


**Figure 3.7. Acceleration-time history and response spectrum of Mammoth Lakes-2 earthquake**

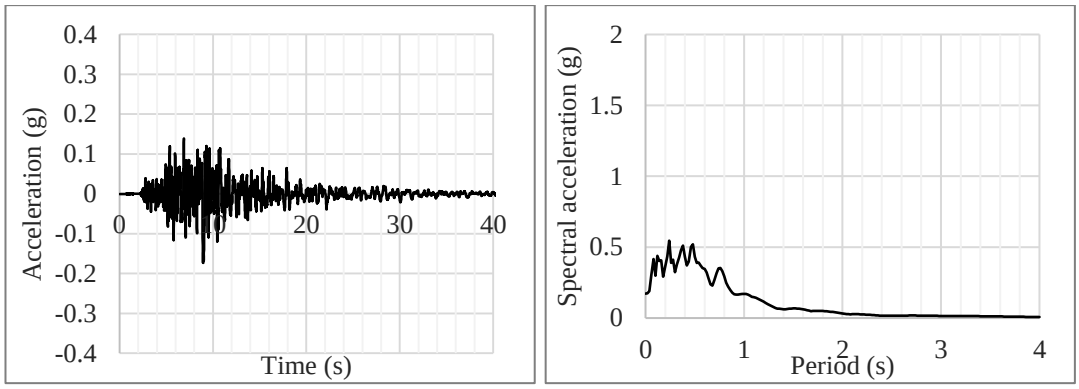


**Figure 3.8. Acceleration-time history and response spectrum of Parkfield-1 earthquake**

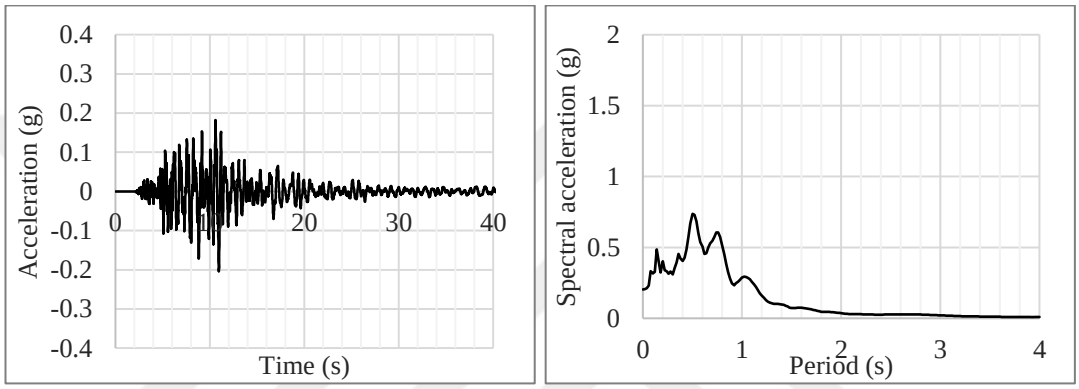


**Figure 3.9. Acceleration-time history and response spectrum of Parkfield-2 earthquake**

### 3.2.3. Static and dynamic analyses

Static and dynamic analyses were conducted under 2D plain strain conditions by using finite element based QUAKE/W. Initial static analyses performed according to the material properties noted in Table 3.2. 409 finite elements were generated for both static and dynamic analyses as seen in Figure 3.10.

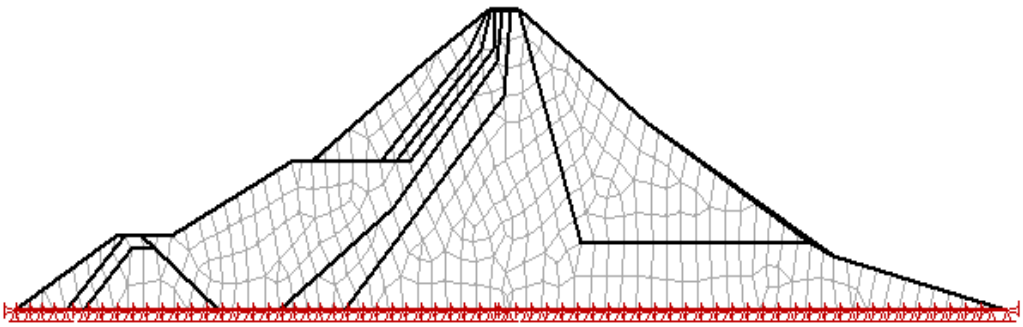

**Figure 3.10. Mesh generation of Sürgü Dam**

As mentioned previous chapters, dynamic material properties as damping and shear modulus degradation curves and maximum shear modulus are required for iterative procedure in equivalent linear analysis. Curves proposed by Jia and Chi (2012) were used for this requirement. Detailed information about selected curves will be given in Section 3.3.2.

Static analysis result can be seen in Figure 3.11.

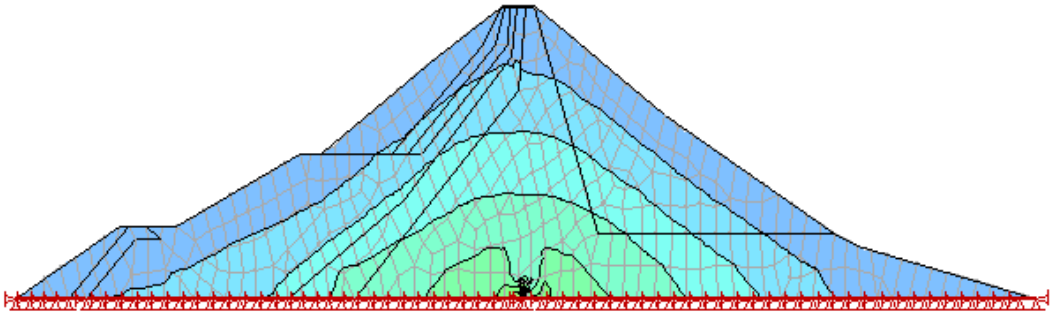

**Figure 3.11. Static analysis of Sürgü Dam**

The reconnaissance of Özkan et al. (1996) points out slip surface 1 for containing the observed failure. In this study 6 failure surfaces were determined as shown in Figure 3.12., however, the given results are belong to the slip surface 1 in order to give comparative results. According to the pseudo-static analyses, 0.12 g yield acceleration is determined as a threshold of slip surface 1.

Finally, earthquake induced accelerations in dam body and yield acceleration were utilized for permanent displacement calculations. The acceleration values greater than yield acceleration were integrated two times to conduct Newmark's permanent displacement procedure.

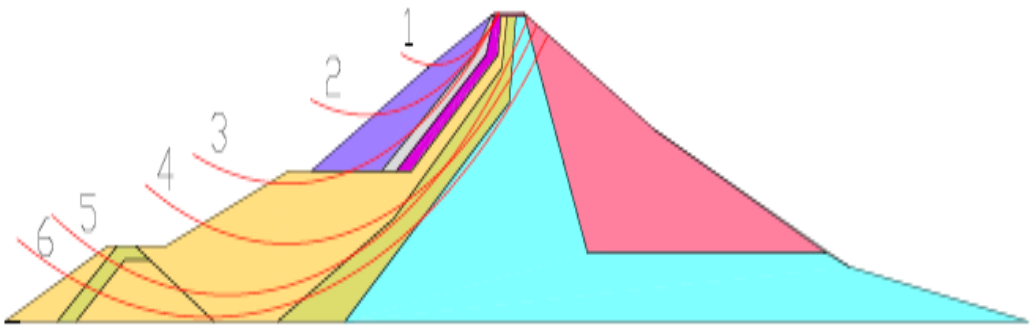


**Figure 3.12. Slip surfaces of Sürgü Dam**

### 3.2.4. Results

Through the dam body, acceleration alterations were recorded at 9 history points (Figure 3.13.) and obtained accelerations were represented in terms of normalized acceleration. Normalization was made according to the maximum ground acceleration. Outputs of six earthquakes in terms of normalized acceleration can be seen in Figure 3.14. As seen in the figure, amplification ratio of accelerations reached up to 2.5 times of ground acceleration. Özkan et.al. (1996) reported the maximum amplification as 3 times of ground acceleration.

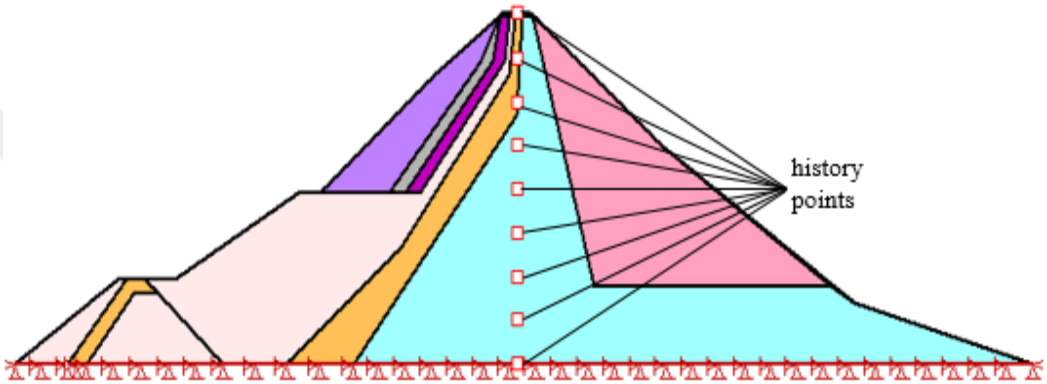


**Figure 3.13. History points locations**

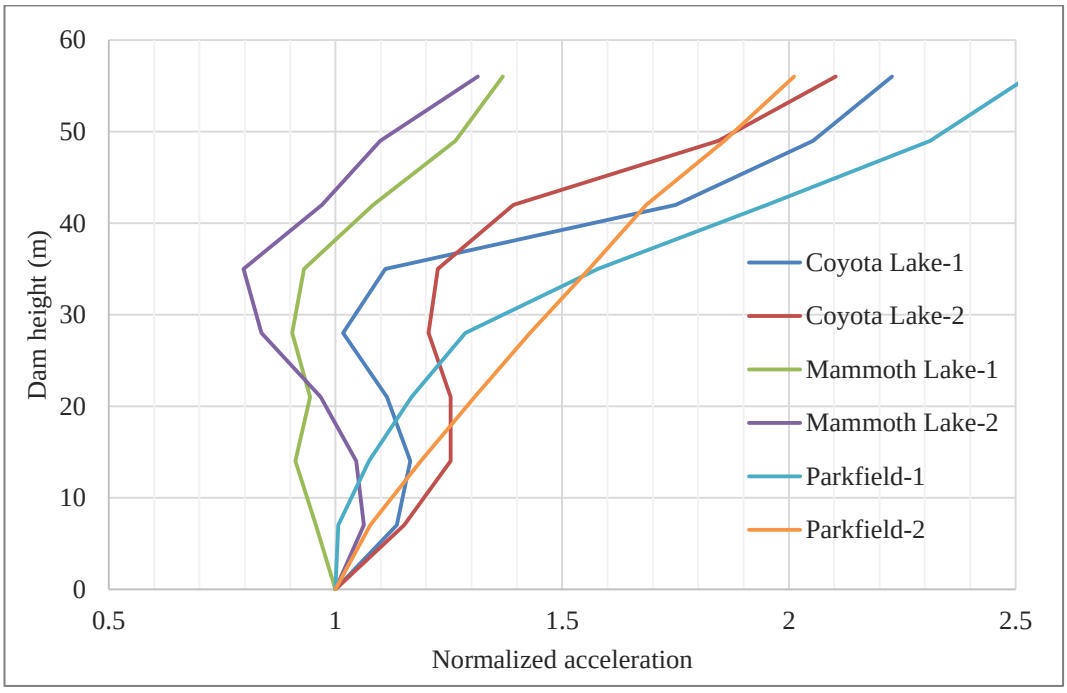


**Figure 3.14. Normalized acceleration variation through the dam body**

Finally, permanent displacements of slip surface 1 were calculated under six different dynamic loadings. Evaluated maximum displacement values are given in Table 3.4.

**Table 3.4. Comparison of maximum permanent displacements**

| Earthquake | Evaluated maximum permanent displacement with QUAKE/W(cm) | Observed maximum permanent displacement at site (cm) |
|---|---|---|
| Coyote Lake-1, 8/6/1979 | 1.00 | 20.00 |
| Coyote Lake-2, 8/6/1979 | 14.00 | |
| Mammoth Lakes-1, 5/27/1980 | 23.00 | |
| Mammoth Lakes-2, 5/27/1980 | 27.00 | |
| Parkfield-1, 9/28/2004 | 13.00 | |
| Parkfield-2, 9/28/2004 | 27.00 | |

### 3.2.5. Conclusion

Sürgü Dam on Sürgü Stream in Malatya, was reanalyzed according to the data represented in the research of Özkan et al. (1996) in order to check how reliable the results of finite element based dynamic analysis software, QUAKE/W is. Acceleration response of dam was evaluated under 2D plane strain conditions with six different actual earthquake records according to the equivalent linear analysis procedure. Then permanent displacements were calculated due to Newmark's method.

As noted before, after The Malatya Earthquake, recorded deformations in Sürgü Dam reached up to 20 cm. When the 1 cm deformation is neglected because of its low Arias intensity, evaluated results with QUAKE/W ranged from 14 cm to 27 cm.

Even so, with respect to the permanent displacement results shown in Table 3.4., QUAKE/W outputs are in reasonable agreement with the observed deformations by Özkan et.al (1996).

### 3.3. Numerical Analyses of CFRD Models

#### 3.3.1. Static material properties

Dams are massive structures so that a potential failure can cause fatal consequences. Under these conditions material selection becomes an important step for dam construction. Both static and dynamic properties of the fill material become crucial for the satisfaction of the required stability demands.

Rockfill type dams are generally preferred when the dam site is suitable to provide required material economically. However, there are some points to be considered before usage of available materials for such big hydraulic structures as water resistance against the dissolution, breakage resistance against the loading.

In the present study specifying no rock type, static material properties of rockfill were specified as given in Table 3.5. As seen in the table internal friction angle changes between $35^{\circ}$ to $50^{\circ}$. This range is compatible with previous studies.

**Table 3.5. Material properties of rockfill materials**

| | |
|---|---|
| Unit weight ($\gamma$) (kN/m$^3$) | 22 |
| Poisson's ratio ($\upsilon$) | 0.2 |
| Cohesion (C) (kN/m$^2$) | 0 |
| Internal friction angle ($\phi$) (degree) | $35^{\circ}$ - $40^{\circ}$ - $45^{\circ}$ - $50^{\circ}$ |

#### 3.3.2. Dynamic material properties

As mentioned before, strain dependent parameters are required for an equivalent linear analysis. Damping and shear modulus variations depending on cyclic load induced strains and maximum shear modulus are the most effective parameters for dynamic analysis.

In order to assure the relevance of computation process to real conditions in terms of strains, curves for damping and shear modulus suggested by Jia and Chi (2012) were used. Mentioned study contains statistical calculations of 35 kinds of rockfill and the results are arranged in terms of statistical curves including best fit curve, one standard

division curves and two times standard division curves. Strain dependency of shear modulus and damping are shown in Figure 3.15. and Figure 3.16., respectively. According to their study, following equations (Equation 3.1 and Equation 3.2) can be used for rockfill material.

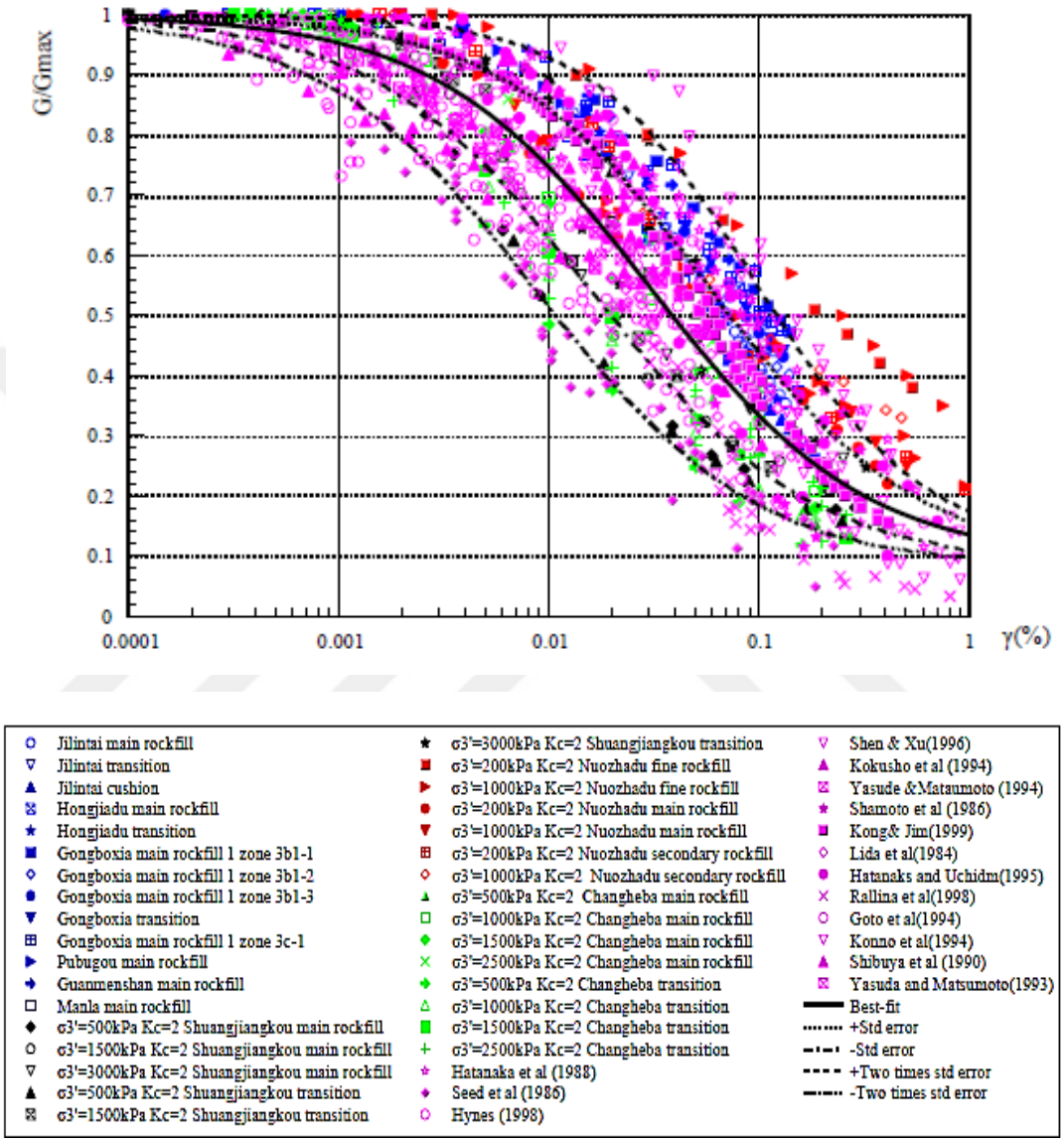


**Figure 3.15. Data points defining G/G0 versus g relationships for 35 kinds of rockfills based on testing along with the best-fit curve, ± one standard division curves and two times standard division curves (Jia and Chi, 2012).**

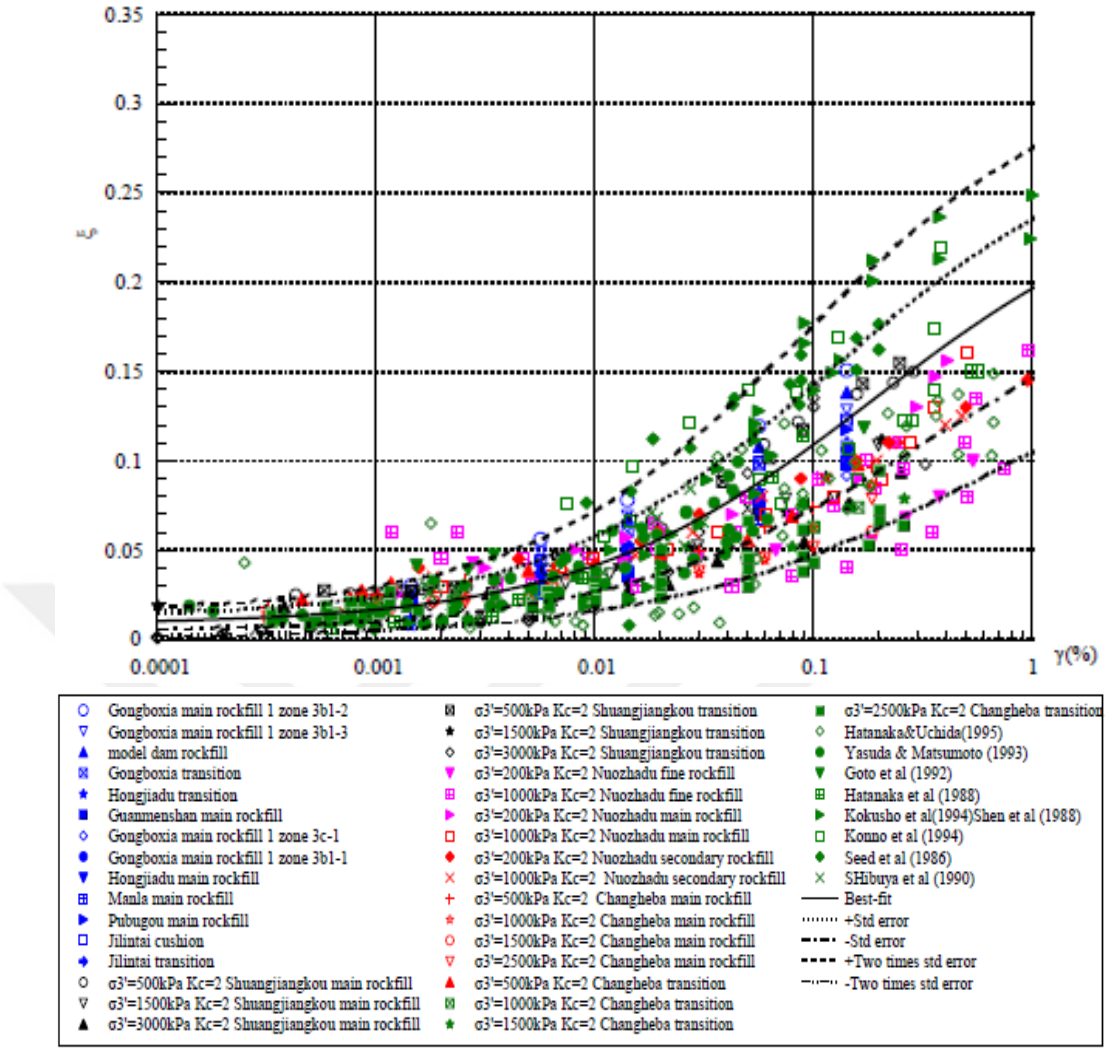


**Figure 3.16. Data points defining x versus g relationships for 35 kinds of rockfills based on testing along with the best-fit curve, ± one standard division curves and two times standard division curves (Jia and Chi, 2012).**

$$\xi = A_2 + \frac{A_1 - A_2}{1 + a\gamma^n} \tag{3.1}$$

$$G/G_0 = b + \frac{1-b}{1 + \left(\frac{\gamma}{x_0}\right)^m} \tag{3.2}$$

Where $\xi$ is damping ratio; $G$ is dynamic shear modulus; $G_0$ is initial dynamic shear modulus; $\gamma$ is shear strain; $A_1$ and $A_2$ are maximum and minimum $\xi$ versus $\gamma$ between

$10^{-6} \sim 10^{-1}$ respectively; $b$ is minimum $G/G_0$ $a$, $n$, $m$ and $x_0$ are fitting parameters. Herein, values of parameters are given in Table 3.6.

**Table 3.6. Parameters for statistic curves**

| Statistic curves | *b* | $x_0$ | *m* | $A_1$ | $A_2$ | *a* | *n* |
|---|---|---|---|---|---|---|---|
| **Best-fit** | 0.09123 | 0.03048 | 0.85218 | 0.00819 | 0.26123 | 2.90294 | 0.64172 |
| **+ one standard division** | 0.09345 | 0.05809 | 0.89702 | 0.01209 | 0.29204 | 3.95345 | 0.65595 |
| **- one standard division** | 0.08424 | 0.01596 | 0.84206 | 0.00418 | 0.21802 | 1.97530 | 0.61858 |
| **+ two standard division** | 0.11093 | 0.09673 | 1.08876 | 0.01526 | 0.32513 | 5.20375 | 0.68162 |
| **- two standard division** | 0.07955 | 0.00883 | 0.83877 | 0.00076 | 0.18467 | 1.30518 | 0.58710 |

Moreover, maximum shear modulus ($G_{max}$) was calculated by using the following equation (Equation 3.3) proposed by Hardin and Drnevich (1972).

$$G_{max} = 3230 \times \frac{(2.973 - e)^2}{(1+e)} \times OCR^K \times \sigma_m^{1/2} \quad (3.3)$$

Here, e is void ratio, OCR is over consolidation ratio, $\sigma_m$ is mean principle effective stress, K is a constant related with plasticity index, PI, and the tabulated form of K values are given in Table 3.7., and both $\sigma_m$ and $G_{max}$ are in kPa.

**Table 3.7. Proposed values for K (Hardin and Drnevich, 1972).**

| PI | K |
|---|---|
| 0 | 0 |
| 20 | 0.18 |
| 40 | 0.30 |
| 60 | 0.41 |
| 80 | 0.48 |
| ≥100 | 0.50 |

According to the equations proposed by Jia and Chi (2012), following curves were constructed with suitable values. Damping and shear modulus alterations for rockfill material can be seen in Figure 3.17. and Figure 3.18., respectively.

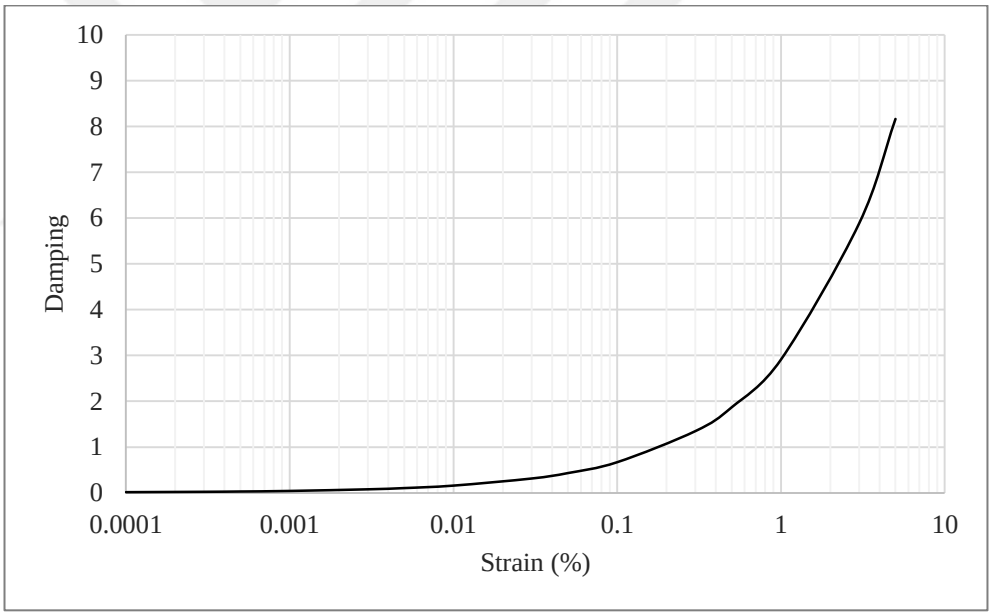


**Figure 3.17. Damping versus strain values used in analyses**

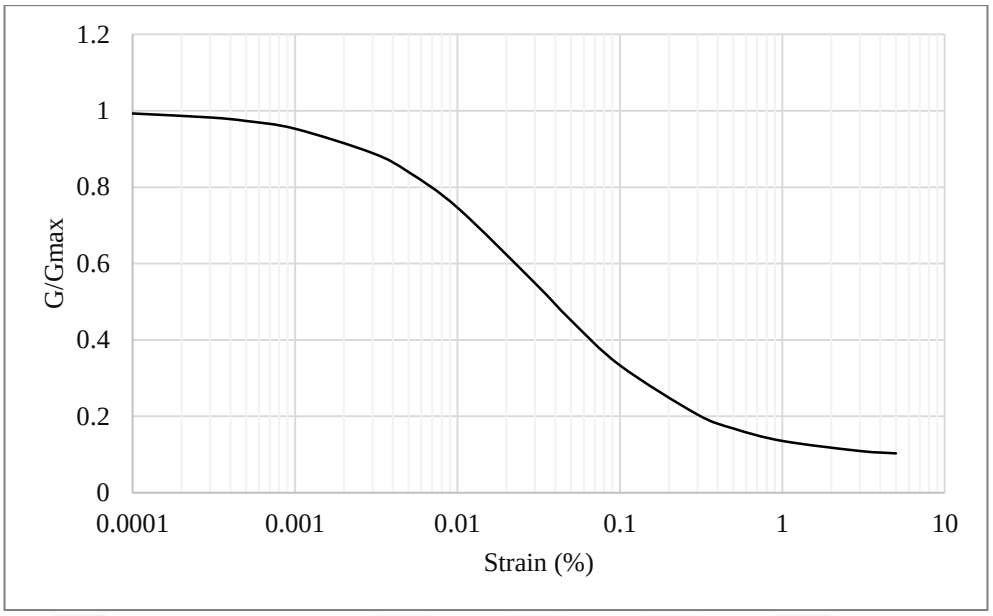


**Figure 3.18. Shear modulus versus strain curve used in analyses**

### 3.3.3. Input motion

Earthquakes are main source of dynamic loading of dams. Produced waves are propagated through the dam body and dynamic properties of embankment soil vary due to the cyclic loading. Variations in dynamic properties affect the peak ground acceleration, duration and frequency content of travelling waves from ground surface to crest and seismic response of dam. For earthquake resistant structure design, representative earthquakes are required. Either synthetic acceleration-time series can be produced by computer programs or real earthquake acceleration-time records from databases are accessible and can be used for dynamic analyses.

In this study, acceleration-time records of six different real earthquakes were used. Required accelerograms were obtained from Pacific Earthquake Engineering Research Center (PEER) Strong Ground Motion Database. Horizontal component of records were used for the analyses. Earthquakes generated by strike slip and thrust fault mechanism with the moment magnitude range of 6.5 to 7.5 were preferred. Detailed information about the earthquakes are given in Table 3.8. As seen in the table, frequency contents of earthquakes were expected to be different from each other, thus, earthquakes with different predominant periods were selected.

Further information about the acceleration time histories and response spectra of motions for 5% damping are given in from Figure 3.19. to Figure 3.24.

**Table 3.8. Earthquakes used in analyses**

| Earthquakes | Date | Fault Mechanism | PGA | Predominant Period (s) | Moment Magnitude (Mw) |
|---|---|---|---|---|---|
| **Cape Mendocino** | 1992 | Thrust | 0.39 | 0.24 | 7.2 |
| **Düzce** | 1999 | Strike Slip | 0.35 | 0.82 | 7.2 |
| **Kobe** | 1995 | Strike Slip | 0.50 | 0.44 | 6.9 |
| **Landers** | 1992 | Strike Slip | 0.65 | 0.08 | 7.3 |
| **Northridge** | 1994 | Thrust | 0.40 | 0.22 | 6.7 |
| **Tabas** | 1978 | Thrust | 0.11 | 0.54 | 7.4 |

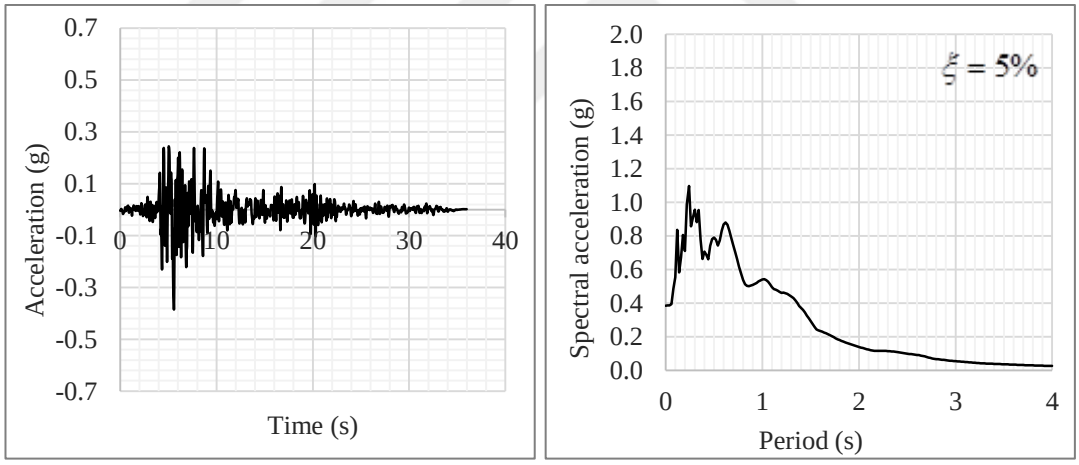


**Figure 3.19. Acceleration time history and response spectrum of Cape Mendocino earthquake**

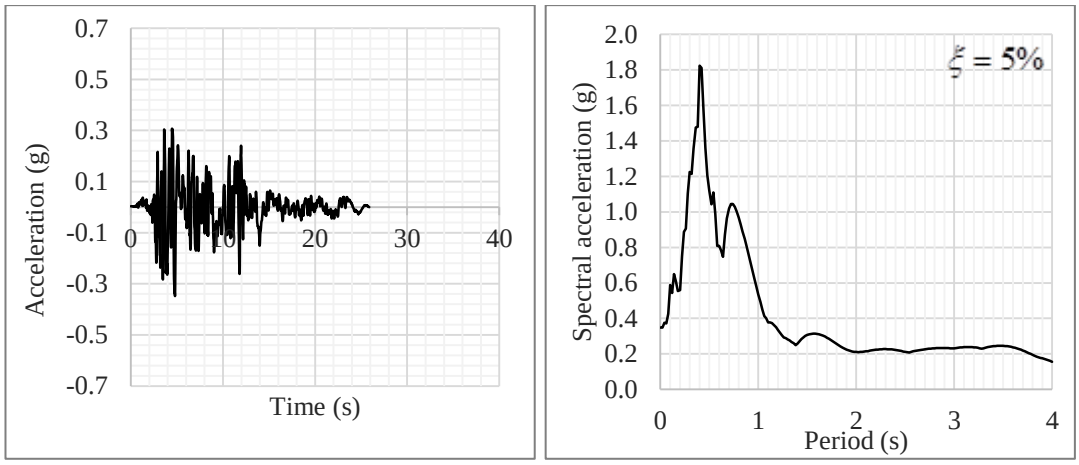


**Figure 3.20. Acceleration time history and response spectrum of Düzce earthquake**

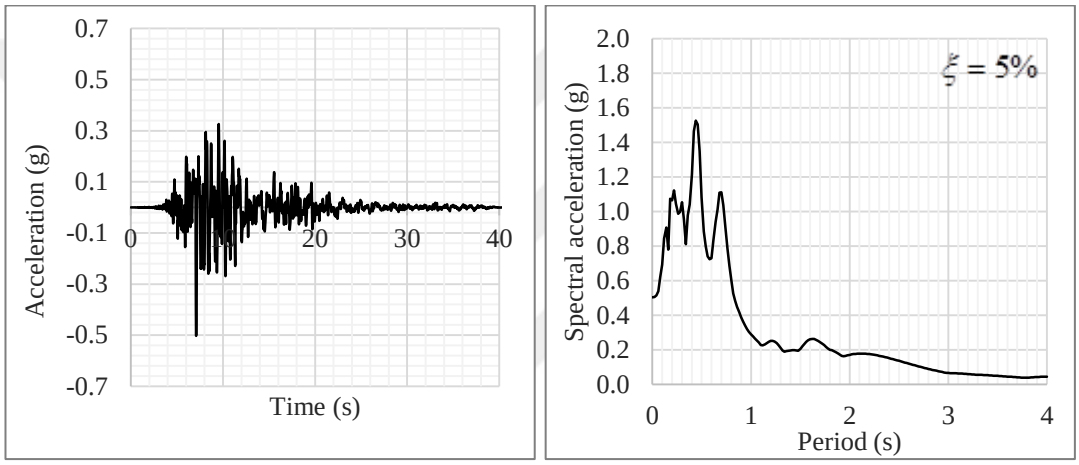


**Figure 3.21. Acceleration time history and response spectrum of Kobe earthquake**

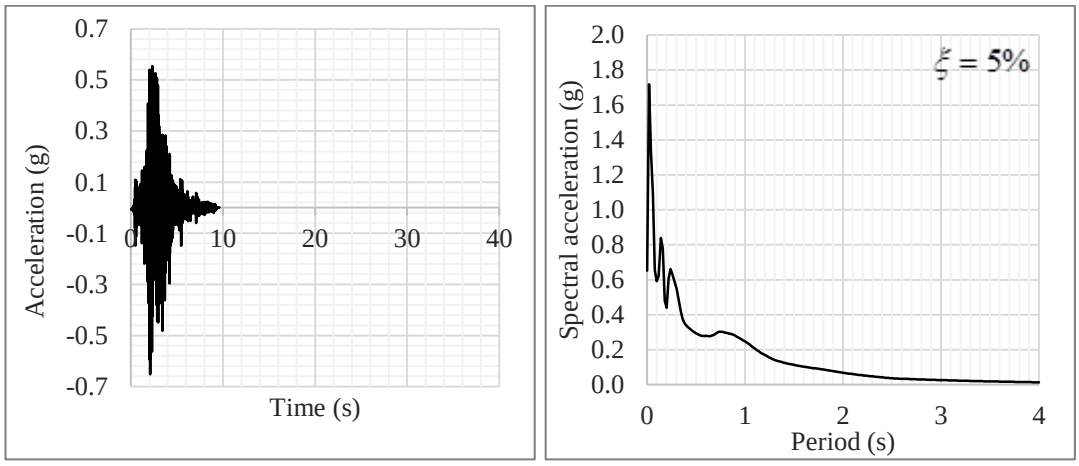


**Figure 3.22. Acceleration time history and response spectrum of Landers earthquake**

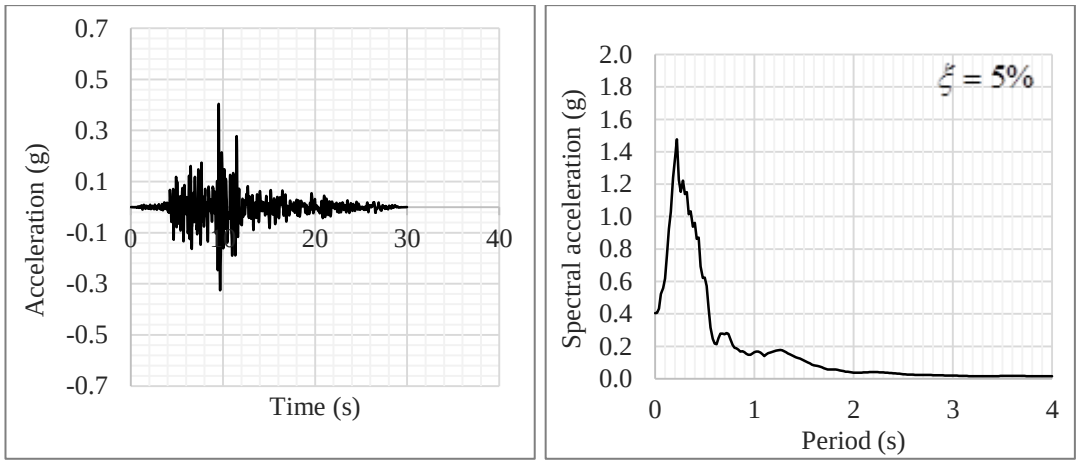


**Figure 3.23. Acceleration time history and response spectrum of Northridge earthquake**

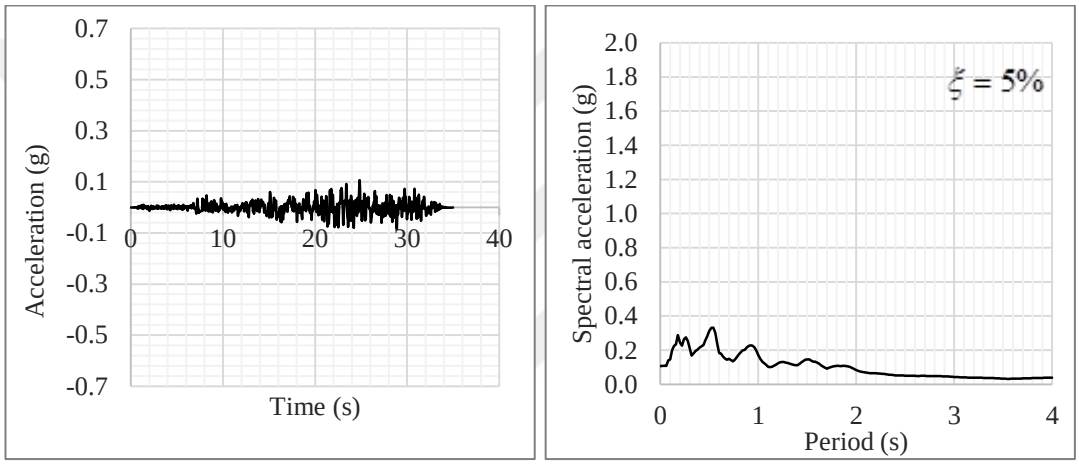


**Figure 3.24. Acceleration time history and response spectrum of Tabas earthquake**

Since this numerical study also aims to represent the influence of maximum ground acceleration on dynamic response of concrete faced rockfill dams, available PGA data were scaled to 0.2g, 0.4g, and 0.6g. A sample for this scaling is given for Cape Mendocino earthquake in Figure 3.25.

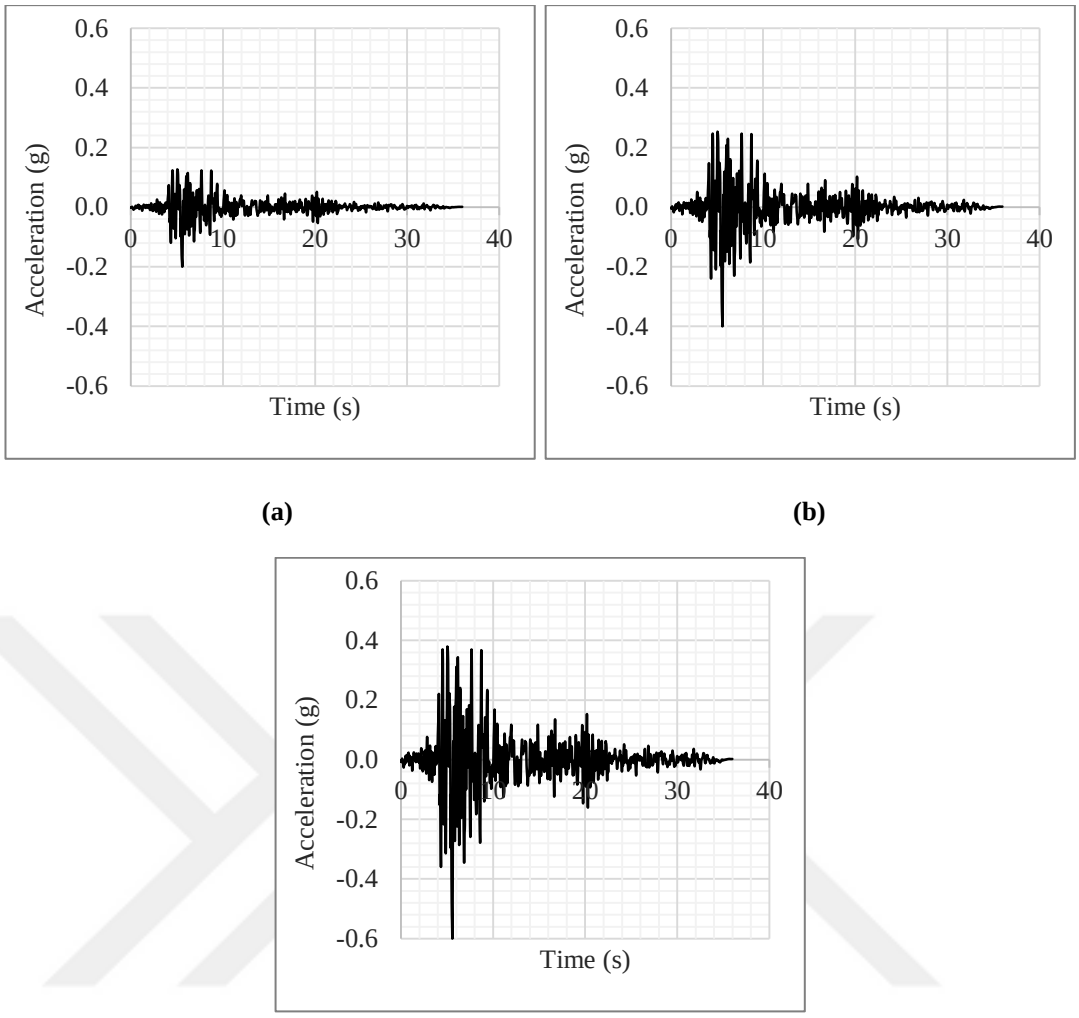


**Figure 3.25. Scaled accelerations for Cape Mendocino earthquake a)PGA=0.2g b)PGA=0.4g c)PGA=0.6g**

### 3.3.4. Static analyses

Initial stress conditions within the dam body are essential for the dynamic analyses. According to the results of static analysis, dynamic material properties are calculated. Static analyses of numerical dam models with empty reservoir were conducted by utilizing QUAKE/W. QUAKE/W is included in GeoStudio geotechnical software package. This finite element based geotechnical software is used for the dynamic analyses of structures subjected to earthquake shaking or other impact loading. Analyses were performed under 2-D plain strain conditions. A sample of initial stress distribution is given in Figure 3.26.

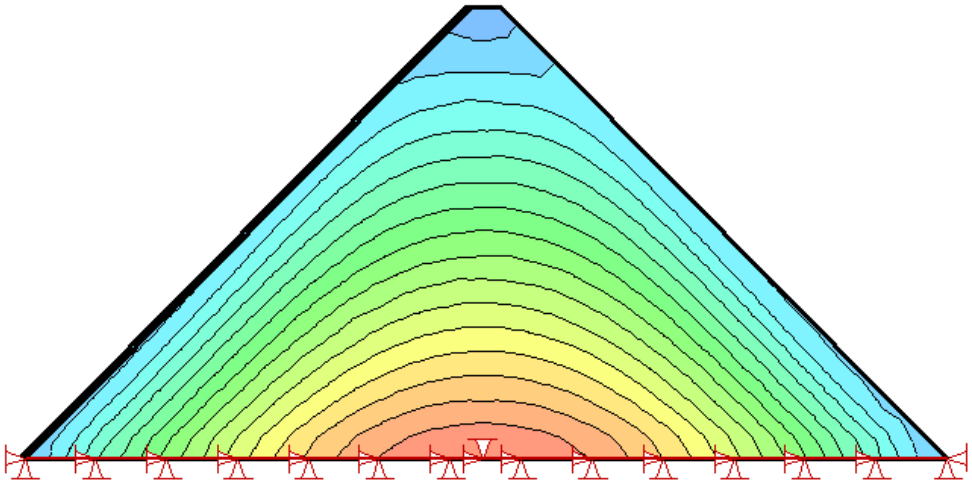

**Figure 3.26. Initial stress distribution of a dam model**

For the initial static analysis, unit weight and Poisson's ratio of materials are mandatory parameters. Poisson's ratio is required to calculate the coefficient of earth pressure at rest condition ( $K_0$ ) and this coefficient affects the mean effective stress, ($\sigma'_m$). QUAKE/W assumes the following equation for the evaluation of $K_0$ .

$$K_0 = \frac{\nu}{1-\nu} \tag{3.4}$$

Mean effective stress is expressed with Equation 3.5 and Equation 3.6 according to the stresses shown in Figure 3.27.

$$\sigma'_m = \frac{\sigma'_1 + \sigma'_2 + \sigma'_3}{3} \tag{3.5}$$

$$\sigma'_2 = \sigma'_3 = K_O \times \sigma'_1 \tag{3.6}$$

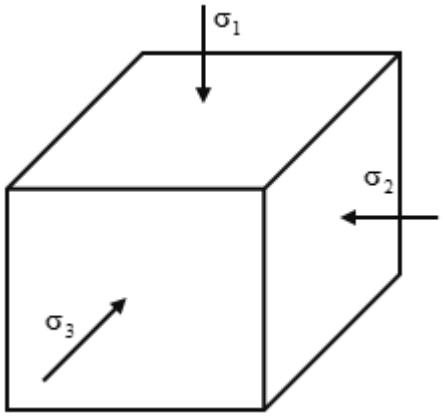


**Figure 3.27. Stresses acting on a soil element**

### 3.3.5. Pseudo-static analyses

Pseudo-static approach is one of the earliest application for slope stability assessments starting with Terzaghi (1950). The methodology, advantages and disadvantages of this approach were expressed in Section 2.2.2. Nowadays, this method integrated into computer programs. SLIDE is one of these software and utilized in this research.

SLIDE is a two dimensional limit equilibrium based software for slope stability analyses. The program is applicable for soil or rock slopes with circular or non-circular failure surfaces. SLIDE allows definition of external loads, groundwater, surcharge or pseudo-static earthquake forces. The output of this program is factor of safety. During the analyses, a lot of slip surfaces are generated with their factor of safeties.

In this study, yield accelerations were established for the predefined critical slip surfaces. Starting from the crest of the dam models three potential slip surfaces passing through 0.25h, 0.50h and 0.75h were specified, where h is dam height (Figure 3.28., Figure 3.29., Figure 3.30.). The accelerations which made the factor of safety "1" were accepted as yield acceleration. These yield accelerations were used for the calculation of permanent displacements according to Newmark's approach.

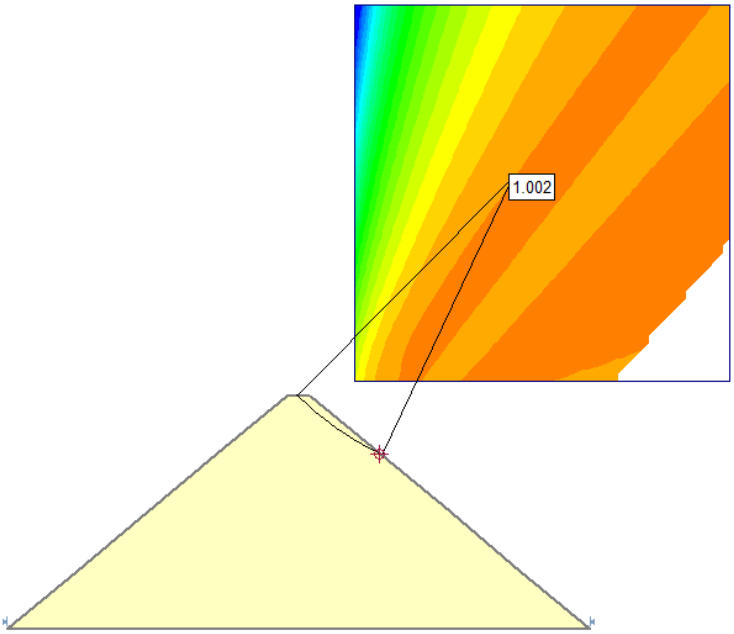


**Figure 3.28. SLIDE model for 0.25h**

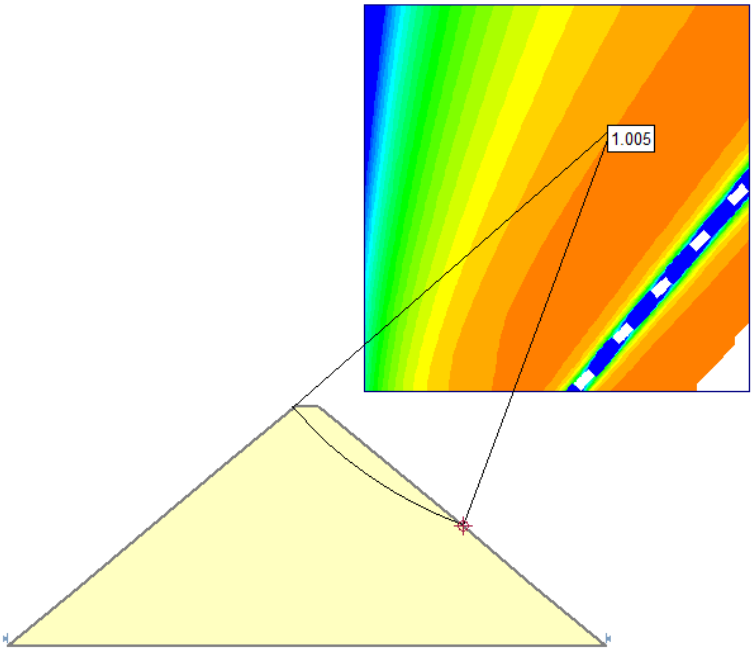


**Figure 3.29. SLIDE model for 0.50h**

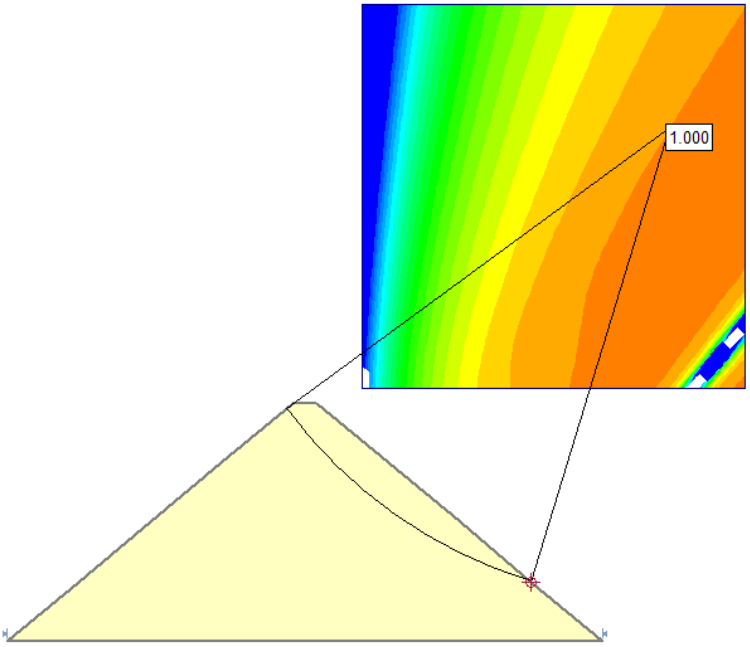


**Figure 3.30. SLIDE model for 0.75h**

A wide range of material model is available in the database of program and internal friction angle, cohesion, unit weight are required material properties for the pseudo-static analyses. Mohr-Coulomb material model was selected for rockfill with the properties shown in Table 3.5. The compelling part of a pseudo-static analysis is the uncertainty about the selection of seismic coefficient ($k_h$). While some researchers suggest to use an exact value, some of them suggest to select seismic coefficient related with earthquake itself. From the recommended values in Table 2.2. peak horizontal acceleration (PHA) based correlation proposed by Marcuson was preferred. According to this equations, used seismic coefficients are given in Table 3.9.

**Table 3.9. Used horizontal seismic coefficients**

| PGA($a_{max}$) | $a_{max}/2$ | $a_{max}/3$ |
|---|---|---|
| 0.2 | 0.1 | 0.067 |
| 0.4 | 0.2 | 0.133 |
| 0.6 | 0.3 | 0.2 |

### 3.3.6. Dynamic analyses

QUAKE/W was used for both static and dynamic analyses. Initial static, equivalent linear dynamic and nonlinear dynamic are available analysis types in QUAKE/W. Furthermore, three constitutive material models including linear elastic model, equivalent linear model and non-linear model are involved in this finite element method (FEM) based software. Dynamic loading occasioned nonlinear behavior of rockfill in the embankment can be modelled with equivalent linear analysis approach under 2-D plain strain conditions. As is known, cyclic loadings change the dynamic material properties of soil. Shear strength and damping capacity of fill material differ after the shock waves passing. QUAKE/W allows application of user-defined damping and modulus degradation curves, thus, the alterations of material properties due to the seismic loads can be considered in the analyses, as in site conditions.

Dynamic analysis steps of QUAKE/W are listed below:

- Initial static analysis:

  To evaluate the dynamic response of a dam, a static analysis is followed by a dynamic one. Stress results of static analysis are used to calculate effective stress dependent dynamic parameters as cyclic stress ratio and shear modulus, G.

- Input motion:

  Six actual earthquake records from PEER Strong Motion Database were used for the analyses (Table 3.8.). Selection of excitations were made according to the frequency content, predominant period, focal depth and moment magnitude range from 6.5 to 7.5.

- Material Properties:

  Rock is the only fill material used in models and its properties are given in Table 3.5. Additionally, as noted before, damping and shear modulus degradation curves of rockfill material shown in Figure 3.17 and Figure 3.18. were defined to observe how the shear modulus and damping change during the excitation and affect the dam behavior. Furthermore, maximum shear modulus ($G_{max}$) was calculated according to the Equation 3.3

As seen in Equation 3.3, maximum shear modulus ($G_{max}$) depends on mean effective stress ($\sigma_m^{'}$). Since mean effective stress varies with depth, $G_{max}$ shows differences due to these changes. For a more accurate calculation, dam body was divided into equal layers with a ten meter thickness and the maximum shear modulus was calculated at the midpoint of these layers.

- As mentioned before, 24 different numerical models are included in this study and the amounts of mesh vary depending upon the dam models. However, mesh dimensions were determined considering the wavelength. Kuhlemeyer and Lysmer (1973) focused on selection of mesh size for an accurate analysis and proposed Equation 3.7. Where λ is the wave length and ΔL is the length of element. A sample of mesh generation is given in Figure 3.28.

$$\lambda \leq \frac{\Delta L}{10} \tag{3.7}$$

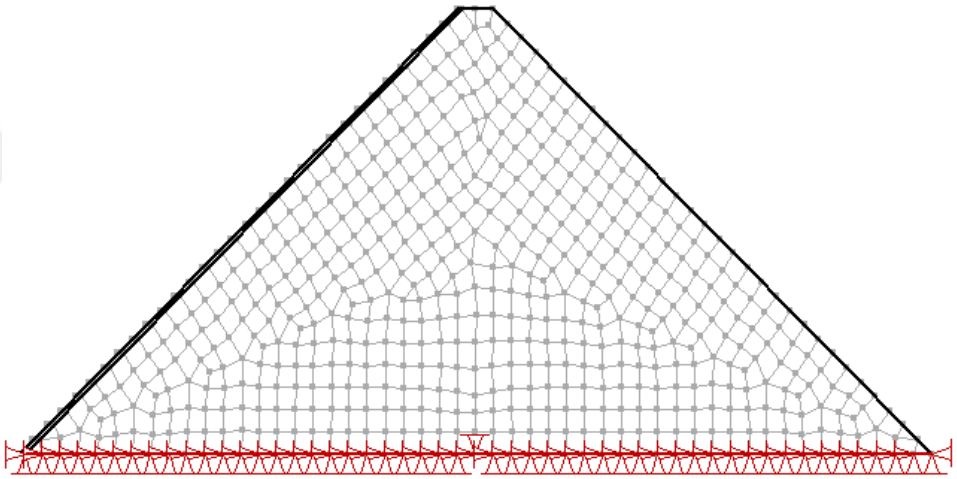

**Figure 3.31. A sample of mesh generation**

- History points:

  Acceleration, velocity, displacement, strain, stress, pore pressure data are available outputs of QUAKE/W. Besides, two types of data collection are possible; one of them is node based the other one is history point based. As it is understood from the expression, node based one can provide information at every node point. However, data sets of nodes do not contain every time step of motion. For the simplicity, QUAKE/W rearrange the time step of output to be given. In return/whereas, history point results are compatible with time step of

motion. History points can be defined by entering the coordinates of point where the user wants to collect the data. Even so, number of history points are limited, maximum nine points can be defined.

In order to compare the same kind of results, history point definition was preferred in this study. Nine points were placed at every dam model with equal distances, from bottom to crest as seen in Figure 3.32.

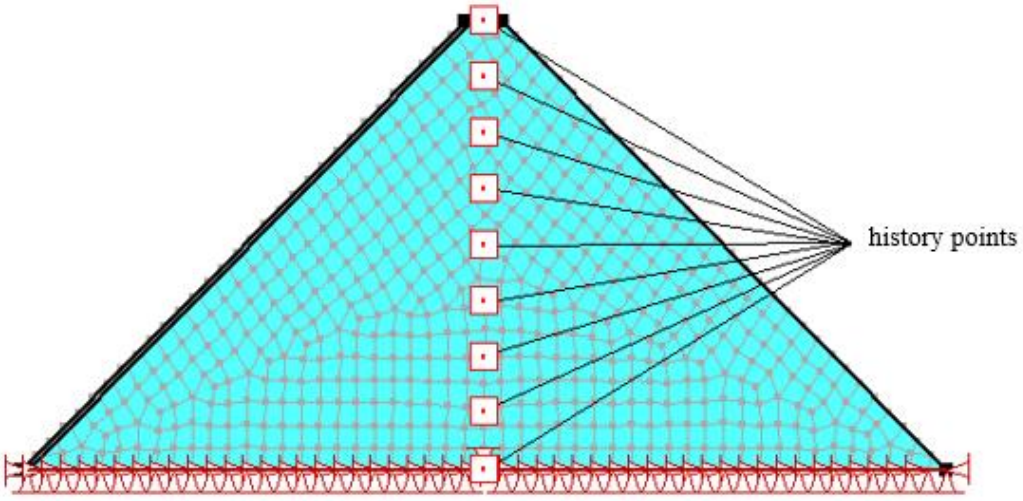


**Figure 3.32. History point locations**

- Dynamic analysis: Initial stress levels, mesh properties, boundary conditions were transferred to dynamic analysis by cloning the initial static analysis and then, after applying the input motion, dynamic analysis was conducted. A sample of dynamic analysis output can be seen in Figure 3.33.

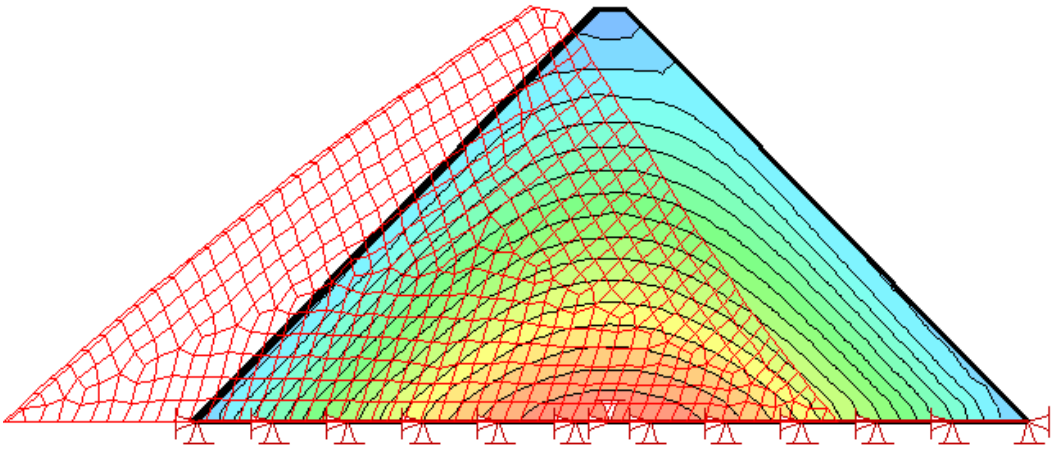

**Figure 3.33. Exaggerated for of deformed shape**

### 3.3.7. Permanent displacement calculation

In order to evaluate the earthquake induced permanent displacements of embankments, Newmark's method (1965) was used in this study. As detailed before, acceleration-time history and yield acceleration of sliding block are required for this calculations. Acceleration response of numerical models under six earthquake records with scaled peak ground accelerations to 0.2g, 0.4g and 0.6g, were obtained by using QUAKE/W and the yield accelerations were evaluated by using SLIDE. For the acceleration values exceeding yield acceleration, a double integration procedure was applied to achieve the permanent displacements of models.

Average acceleration-time histories from the nodes lie within the defined slip surfaces were calculated. Yield accelerations of sliding portions were obtained from SLIDE. For the double integration of the exceeding accelerations, MATLAB codes were used. One of these codes is given in the appendix A.

# 4. RESULTS

## 4.1. Factor of Safety

Factor of safety calculations by writing moment equilibrium or force equilibrium is one of the simplest way for preliminary assessment of a slope stability problem. Unity is a generally accepted threshold for factor of safety approach, however, recommended value for a statically safe slopes is 1.5 (Anonymous, 1989).

Following results are interpreted in terms of dynamic factor of safety. Results having less than 1.5 static factor of safety are included and excluded in figures. Dynamic factor of safety is directly related with horizontal seismic coefficient, thus, two different seismic coefficients were used to see which one should be preferred for safe and economic design. The other limitation against the failure is permanent displacement. Despite the inaccuracy, 100 cm permanent displacement is proposed by Hyness-Griffin and Franklin (1984) as tolerable maximum deformation. In the light of these information, relation between dynamic factor of safety and permanent displacement with the horizontal seismic coefficients given in Table 3.9. are represented in terms of dam height. As stated in Figure 4.1. to Figure 4.16., although the factor of safeties are less than "1", upper limit of permanent deformation is not reached for most cases. These results build up suspicion about factor of safety based decisions. In other words, factor of safety is not adequate alone, additional evaluations are required for a proper risk assessment. When a comparison is made between the horizontal seismic coefficients, it is clear that using $k_h$ as 1/2 of PGA generally gives satisfactory results. However, it sometimes seems to cause overdesigned structures, so suitability of other recommendations can be checked with a deformation based evaluations. If Figure 4.1. and Figure 4.2. or Figure 4.3. and Figure 4.4. are compared, although the number of data points with dynamic factor of safety less than 1 increases, permanent displacement values are mostly in the allowable limits for the case of seismic coefficient equal to 1/3 of PGA.

Moreover the findings show that permanent displacements decrease slightly with increasing dam height under these seismic coefficients. This difference can be attributed to the natural period and damping characteristics of dams.

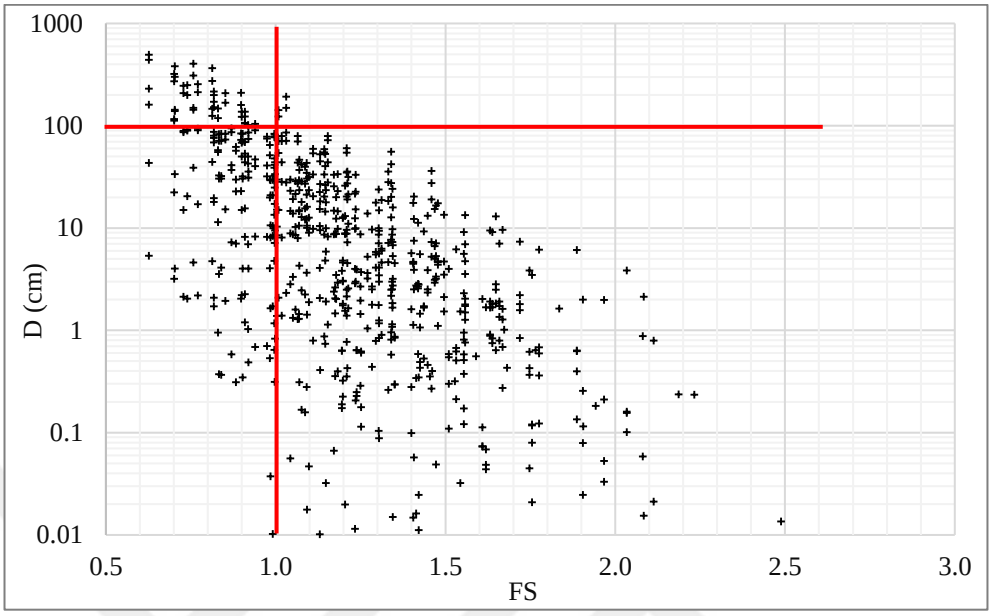


**Figure 4.1. Relation between D and FS for 50 m dam with $k_h=a_{max}/2$**

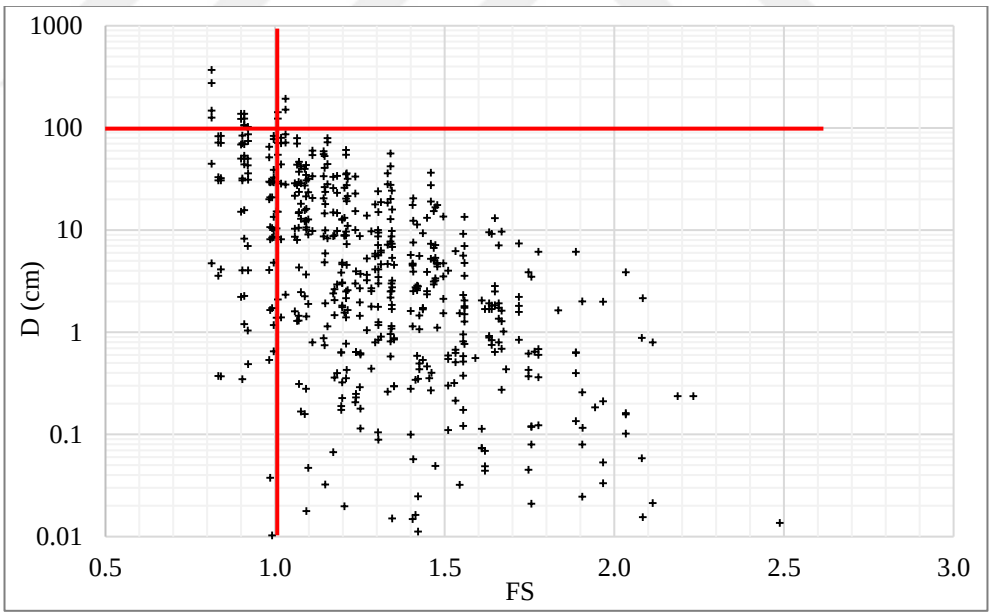


**Figure 4.2. Relation between D and FS for 50 m dam with $k_h=a_{max}/2$ (Static FS>1.5)**

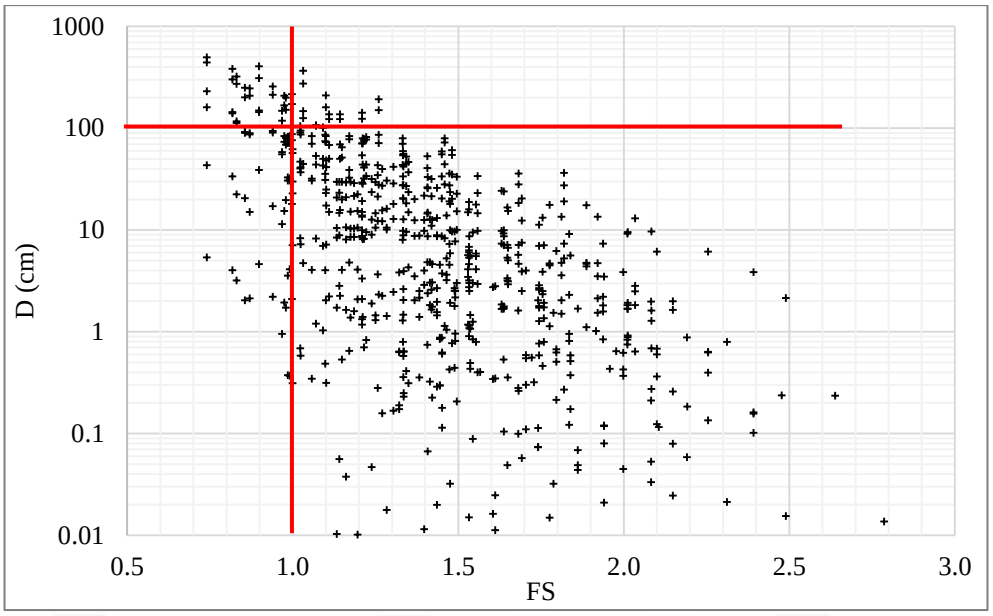


**Figure 4.3. Relation between D and FS for 50 m dam with $k_h=a_{max}/3$**

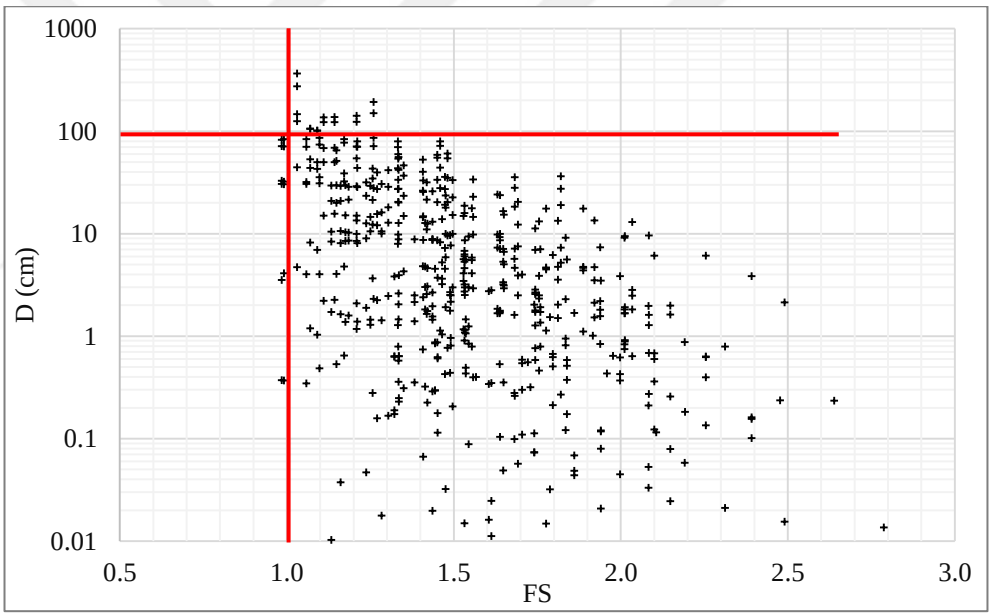


**Figure 4.4. Relation between D and FS for 50 m dam with $k_h=a_{max}/3$ (Static FS>1.5)**

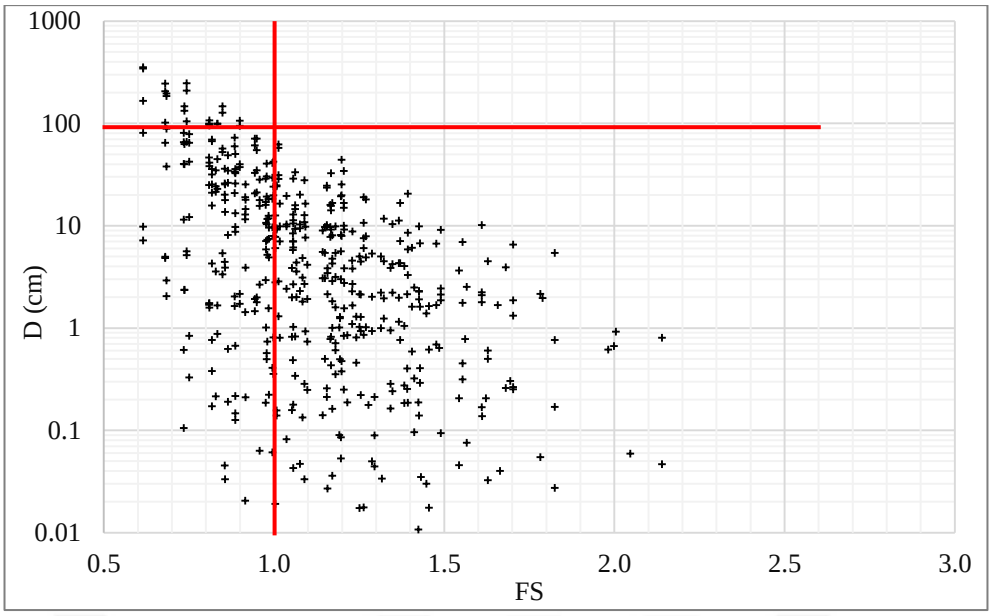


**Figure 4.5. Relation between D and FS for 100 m dam with $k_h=a_{max}/2$**

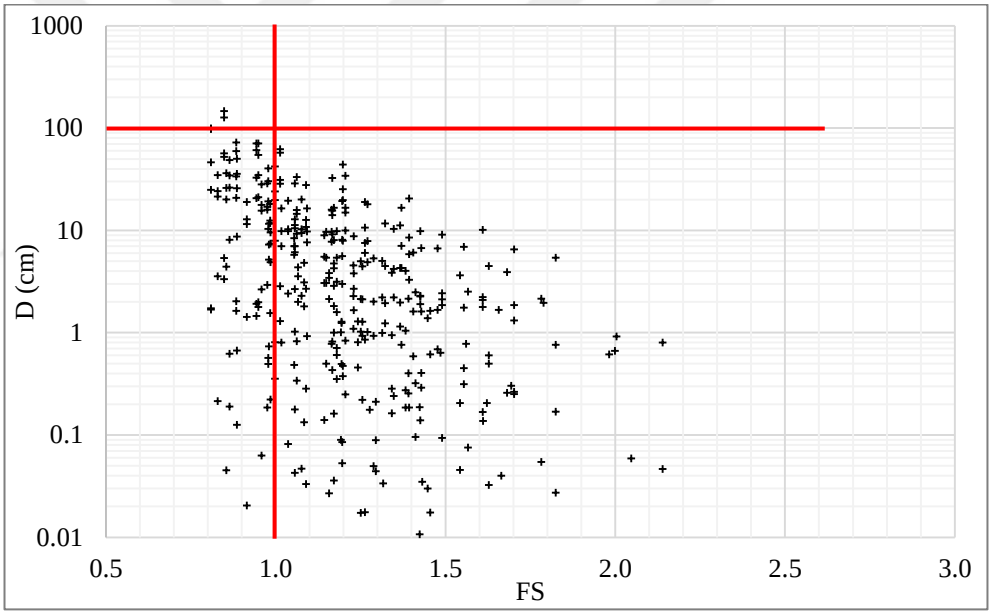


**Figure 4.6. Relation between D and FS for 100 m dam with $k_h=a_{max}/2$ (Static FS>1.5)**

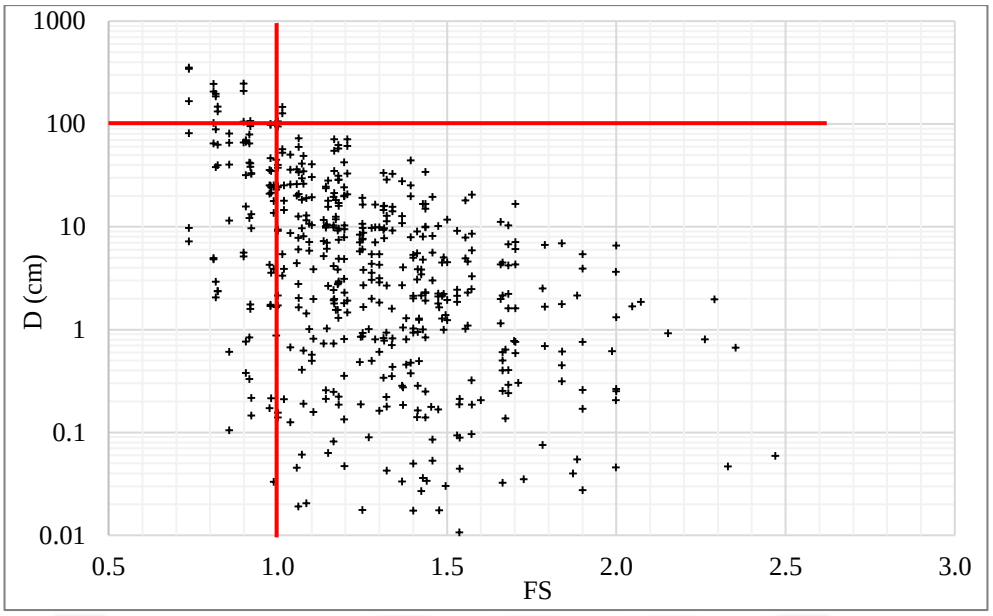


**Figure 4.7. Relation between D and FS for 100 m dam with $k_h=a_{max}/3$**

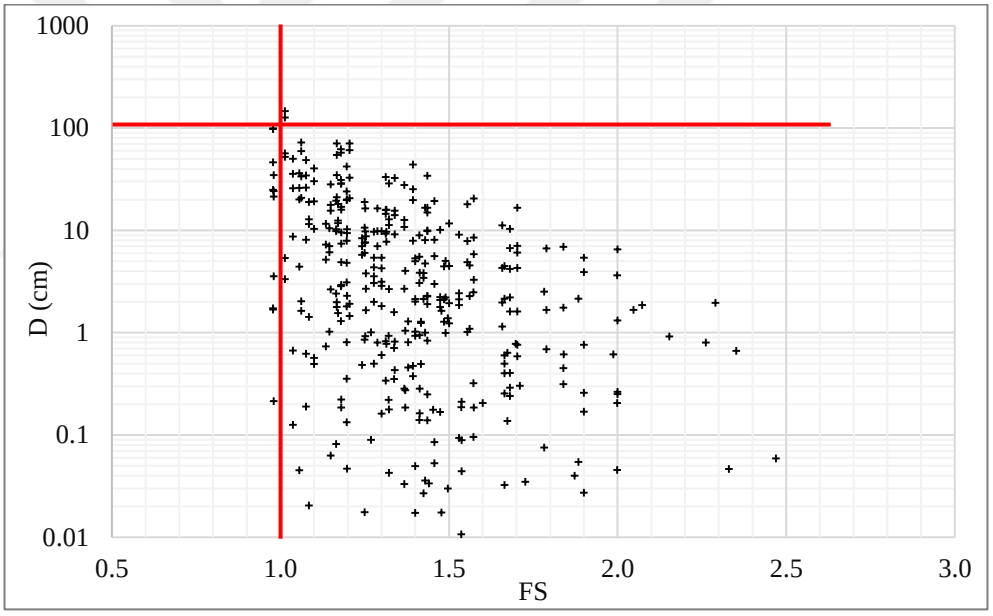


**Figure 4.8. Relation between D and FS for 100 m dam with $k_h=a_{max}/3$ (Static FS>1.5)**

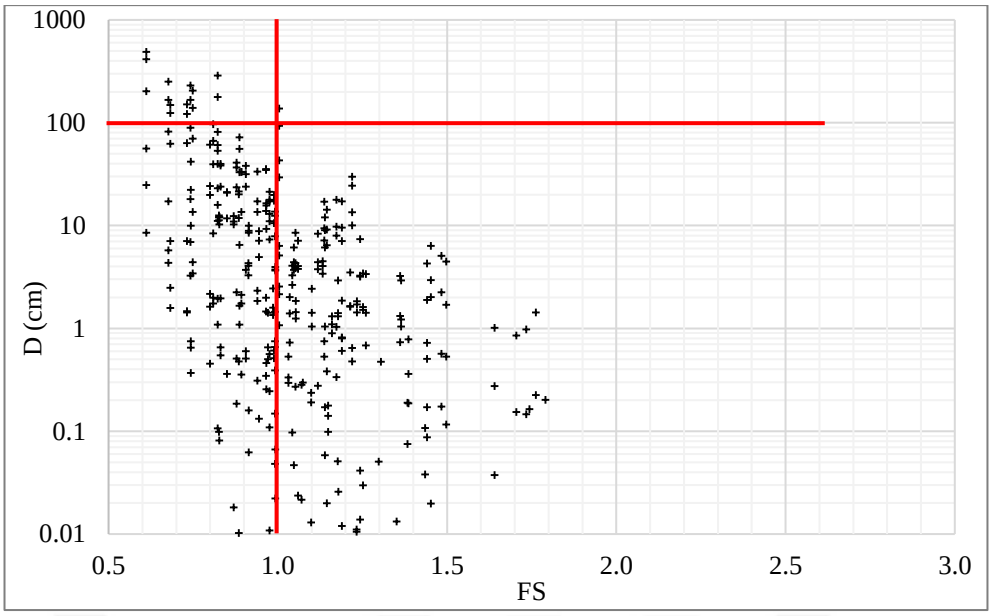


**Figure 4.9. Relation between D and FS for 150 m dam with $k_h=a_{max}/2$**

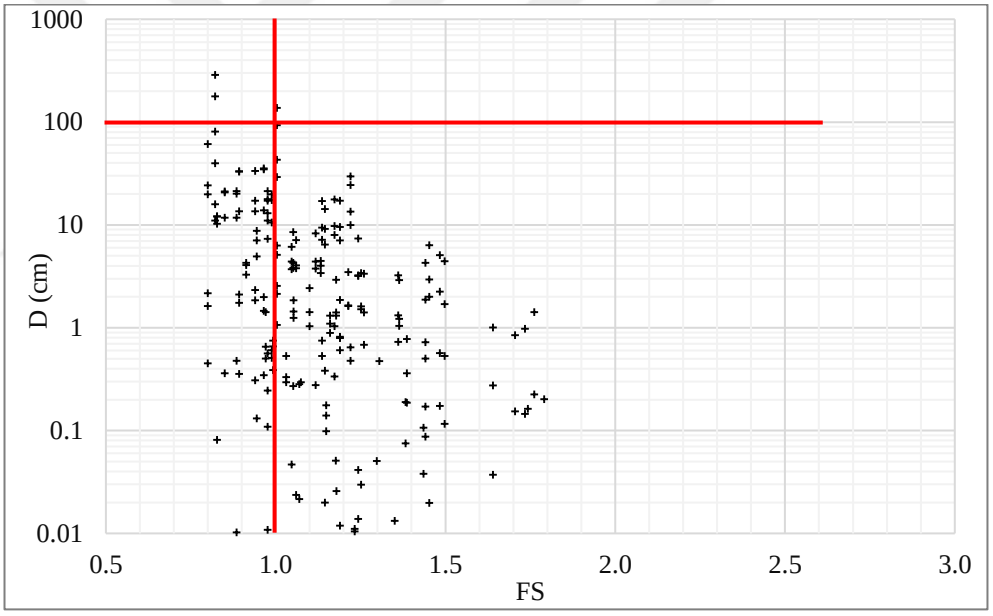


**Figure 4.10. Relation between D and FS for 150 m dam with $k_h=a_{max}/2$ (Static FS>1.5)**

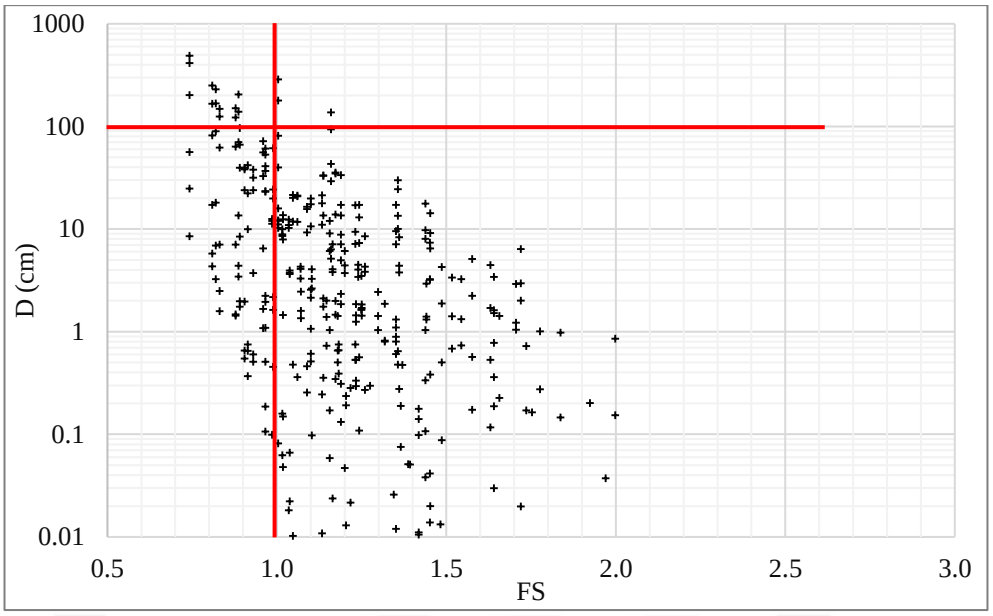


**Figure 4.11. Relation between D and FS for 150 m dam with $k_h=a_{max}/3$**

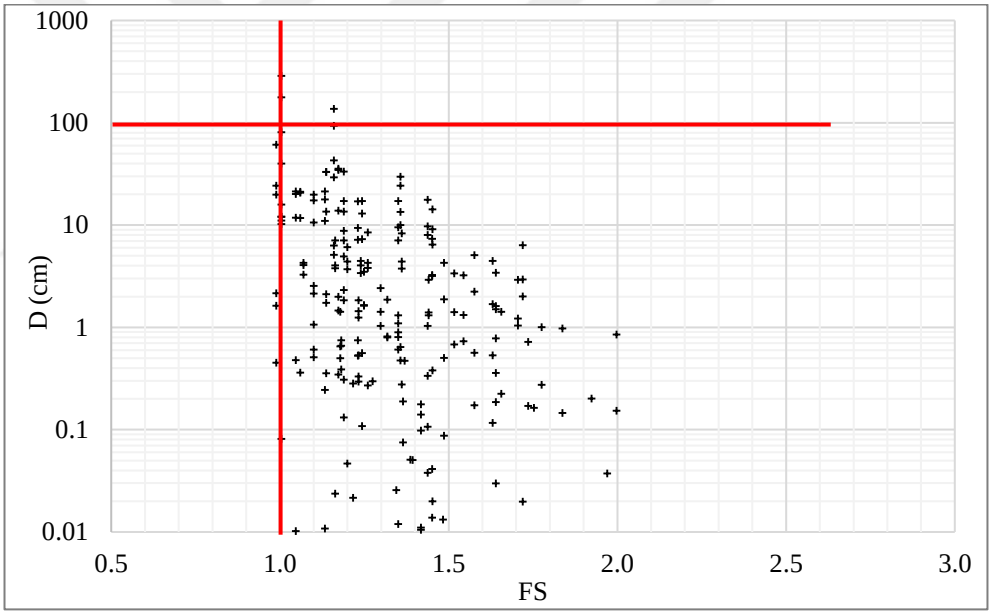


**Figure 4.12. Relation between D and FS for 150 m dam with $k_h=a_{max}/3$ (Static FS>1.5)**

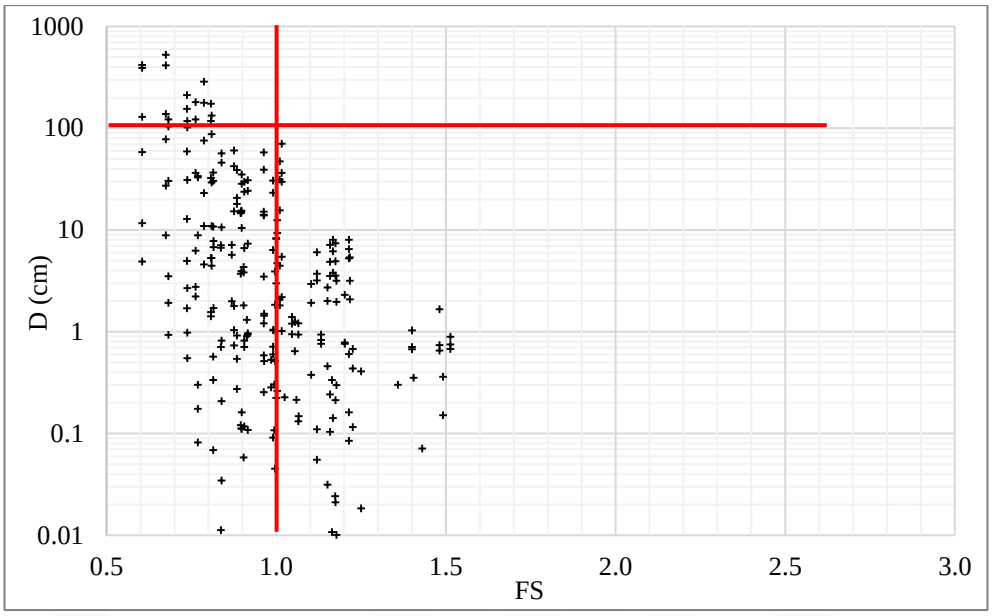


**Figure 4.13. Relation between D and FS for 200 m dam with $k_h=a_{max}/2$**

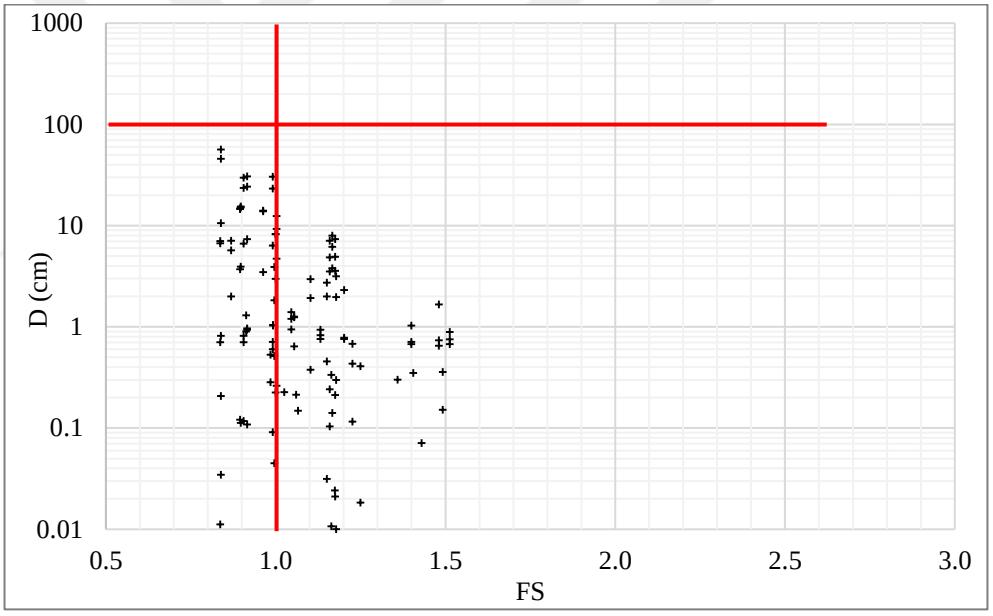


**Figure 4.14. Relation between D and FS for 200 m dam with $k_h=a_{max}/2$ (Static FS>1.5)**

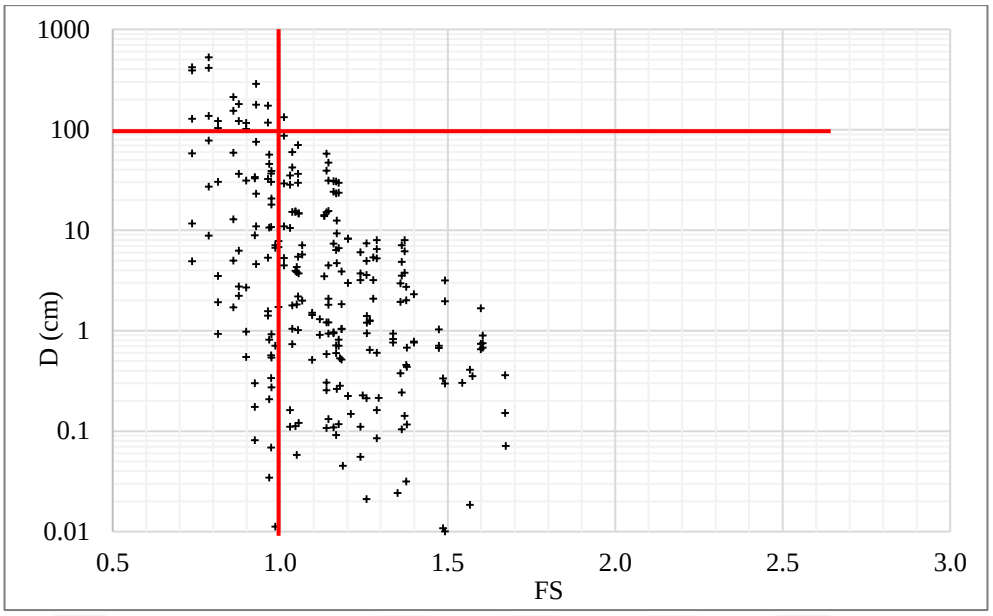


**Figure 4.15. Relation between D and FS for 200 m dam with $k_h=a_{max}/3$**

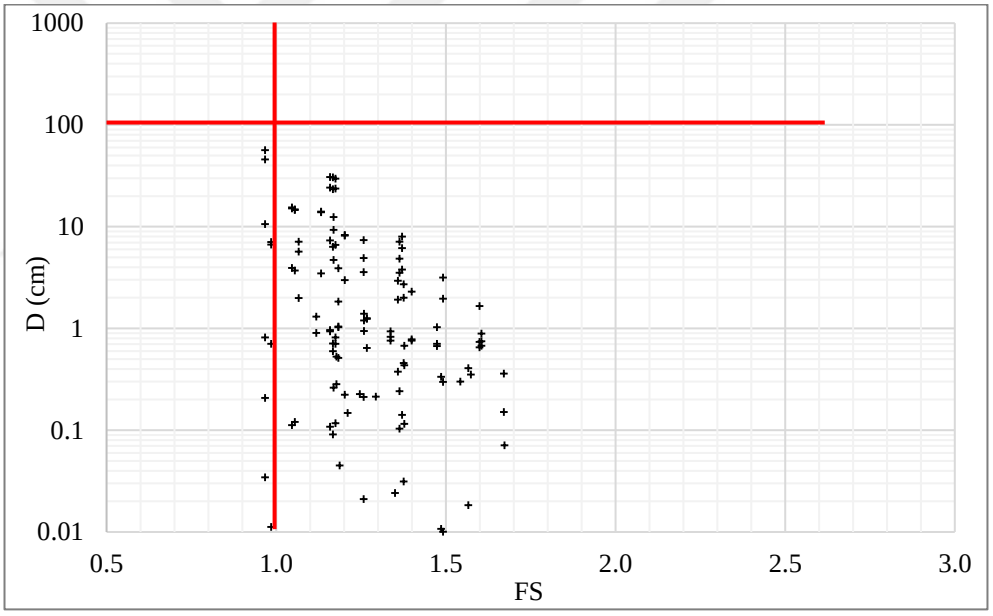


**Figure 4.16. Relation between D and FS for 200 m dam with $k_h=a_{max}/3$ (Static FS>1.5)**

Another finding is about the effect of slip surface depth. As mention before, three slip surfaces were searched including 0.25h, 0.50h, 0.75h and the results are represented in Figure 4.17 and Figure 4.18. Results of 0.75h slip surface contains more data points with factor of safety less than 1. While number of exceedance of 100cm permanent displacement are nearly same for three slip surfaces, data points that have factor of safety less than 1 decreases with increasing slip surface depth. This can be related with the weight of sliding mass. Since the increase in weight cause an increment in driving

force component of force equilibrium, FS decreases. Besides, when Figure 4.17. and Figure 4.18. are searched in terms of the points that have FS less than "1", it is seen that many of the points have less than 100 cm displacement. This result indicates the inadequacy of FS alone for slope stability assessments.

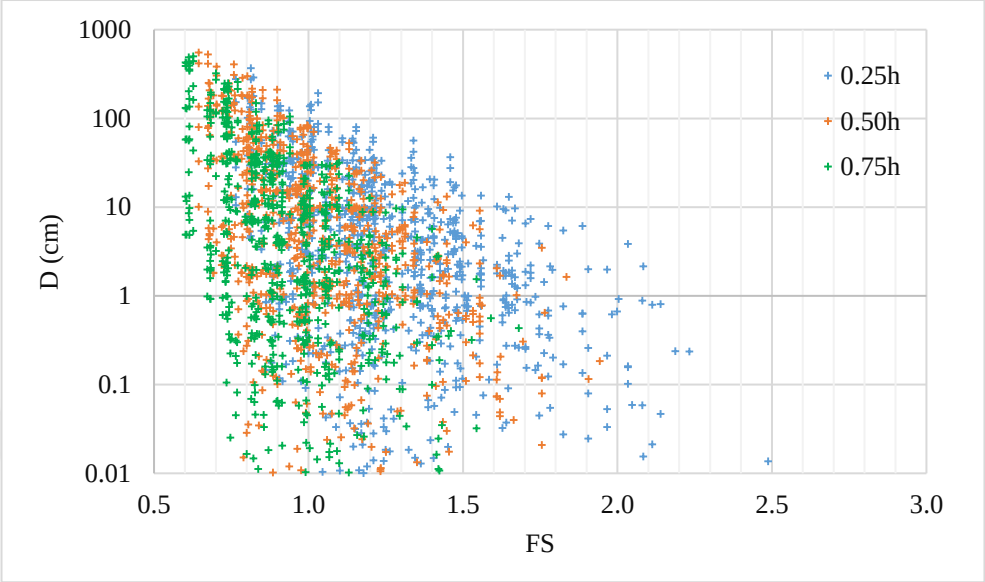


**Figure 4.17. Relation between D and FS in terms of slip surface depth with $k_h=a_{max}/2$ for all data**

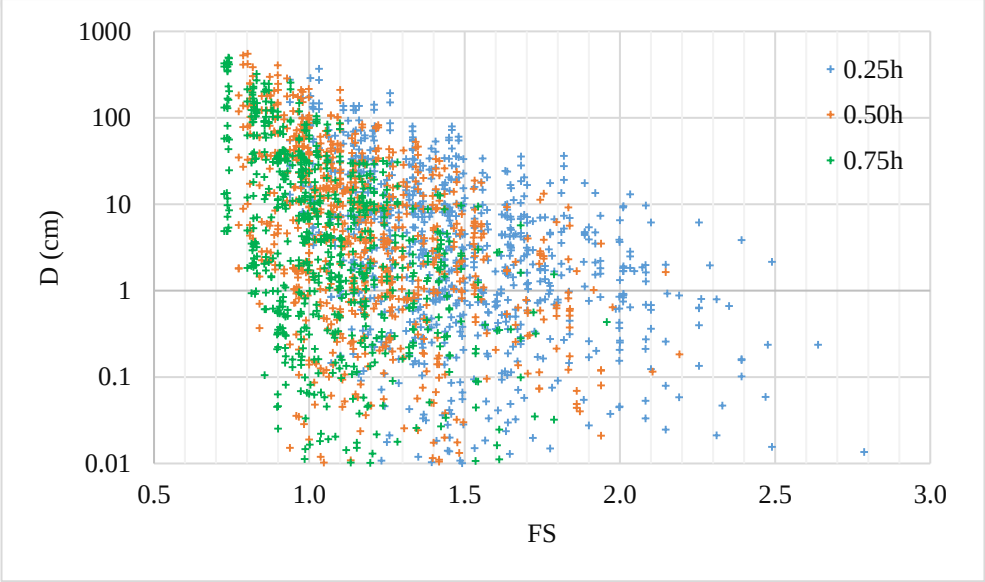


**Figure 4.18. Relation between D and FS in terms of slip surface depth with $k_h=a_{max}/3$ for all data**

### 4.2. Acceleration Response and Amplifications

Evaluated accelerations were normalized with maximum ground accelerations and the results expressed in terms of variations of normalized accelerations along the dam body. Illustrated results belong to dam models that subjected to same earthquake excitation for the accurateness of comparisons. Figure 4.19., Figure 4.20., Figure 4.21., and Figure 4.22. represent the effect of slope inclination on acceleration response of rockfill dams. As seen in the figures, data points of different slopes nearly follow same path for every dam height. However as the dam height increases effect of slope inclination increases and steeper slopes show more amplification. It can be said that the seismic response of rockfill dams are less affected by variation of slopes.

As is known, input motion characteristics as peak ground acceleration, frequency content and duration are most effective parameters on the dynamic behavior of embankments. Results of dam models with 1:1.2 slope, 50 m height and $40^{\circ}$ internal friction angle were investigated by subjecting 0.2g, 0.4g and 0.6g maximum ground accelerations (PGA) (Figure 4.23., Figure 4.24., Figure 4.25. and Figure 4.26.). Given results are obtained from the analyses made with Düzce earthquake. As seen in the figures, acceleration amplifications of dam models decrease with increasing PGA and dam height. This behavior can be explained with increment of natural period of dams. Additionally, smaller dams are more rigid than higher ones and flexibility of higher dams influence the shear strain that affects shear modulus and damping of material. Consequently the damping of fill material increases with increasing PGA. All these parameters are causes of weakening the acceleration along the dam body so a decrement can be seen in amplification.

Another finding from all these figures is the amplification variation along the dam body. Indiscriminately, amplifications show a dramatic increment after the 3/4 of dam height from the bottom at every dam model. Thus, dam crest undergoes more deformation than remaining part of dam body. This behavioral difference points the requirement of a structural treatment approach during the construction of crest.

Reinforcement of crest part of dam with geogrids proposal of Liu et.al (2014) is a pertinent precaution against the dam failures.

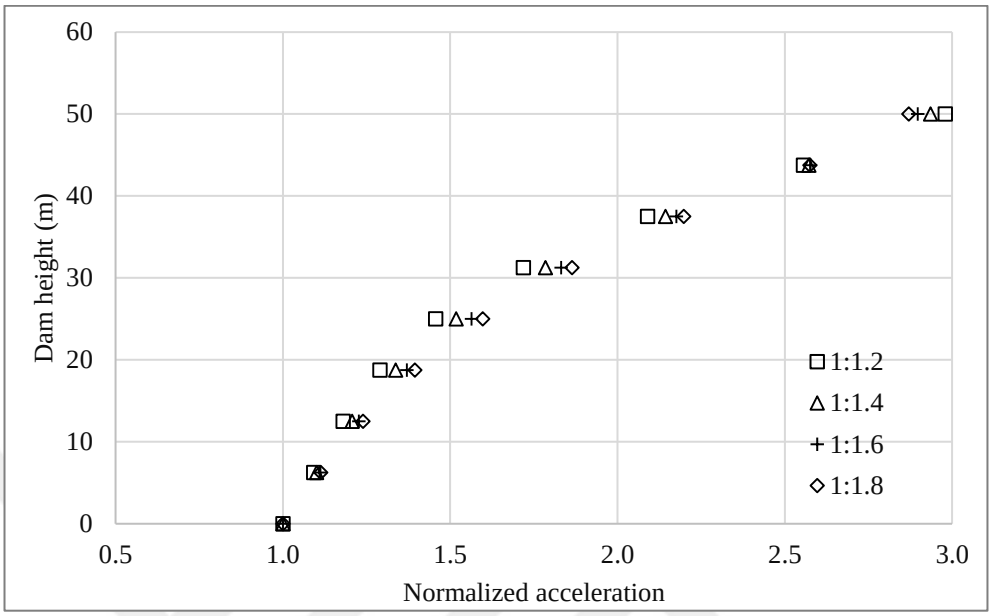


**Figure 4.19. Effect of slope inclination on variation of normalized acceleration along the dam height for 50 m dam**

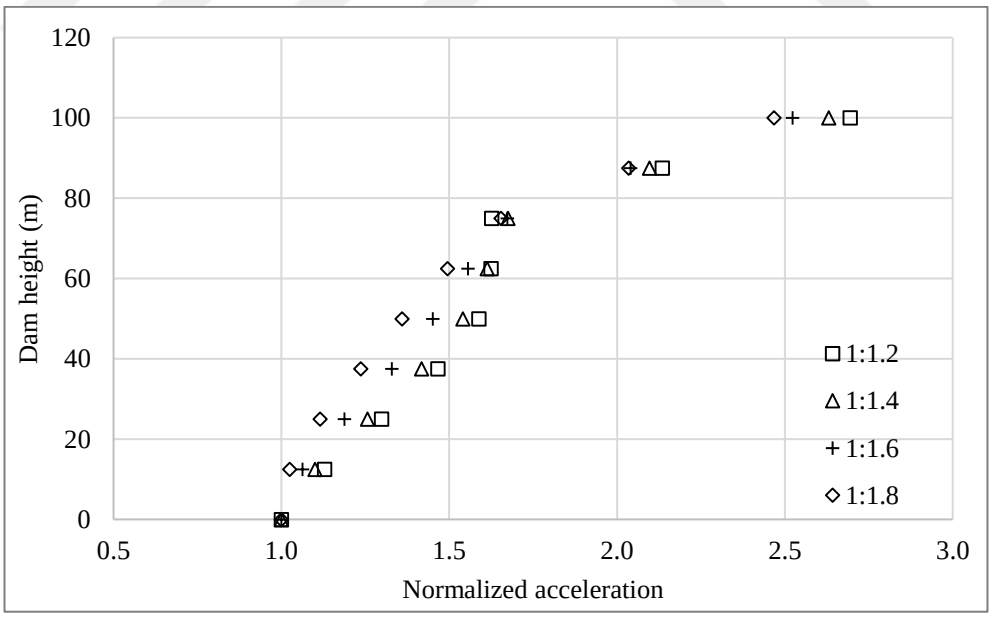


**Figure 4.20. Effect of slope inclination on variation of normalized acceleration along the dam height for 100 m dam**

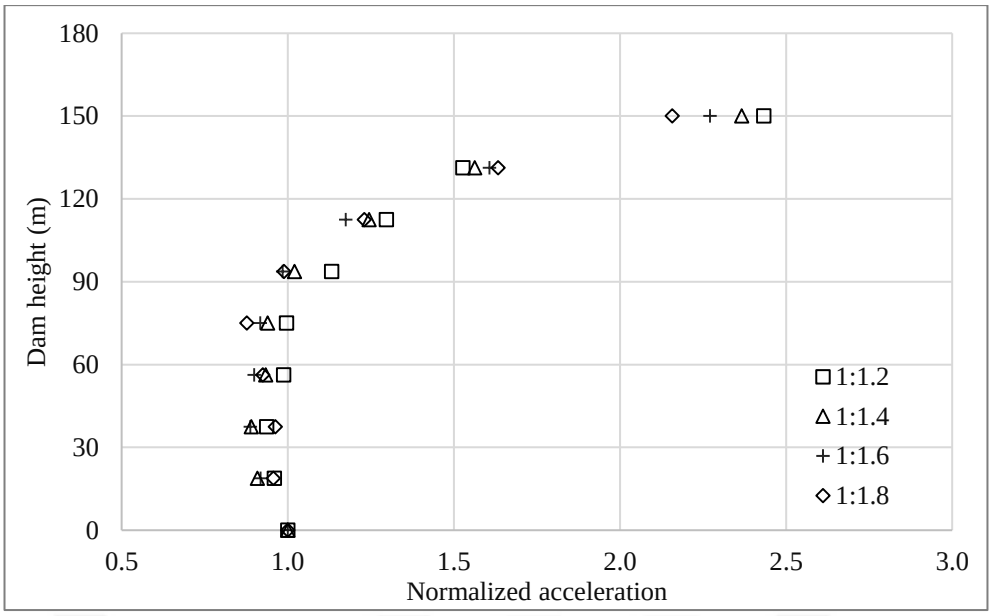


**Figure 4.21. Effect of slope inclination on variation of normalized acceleration along the dam height for 150 m dam**

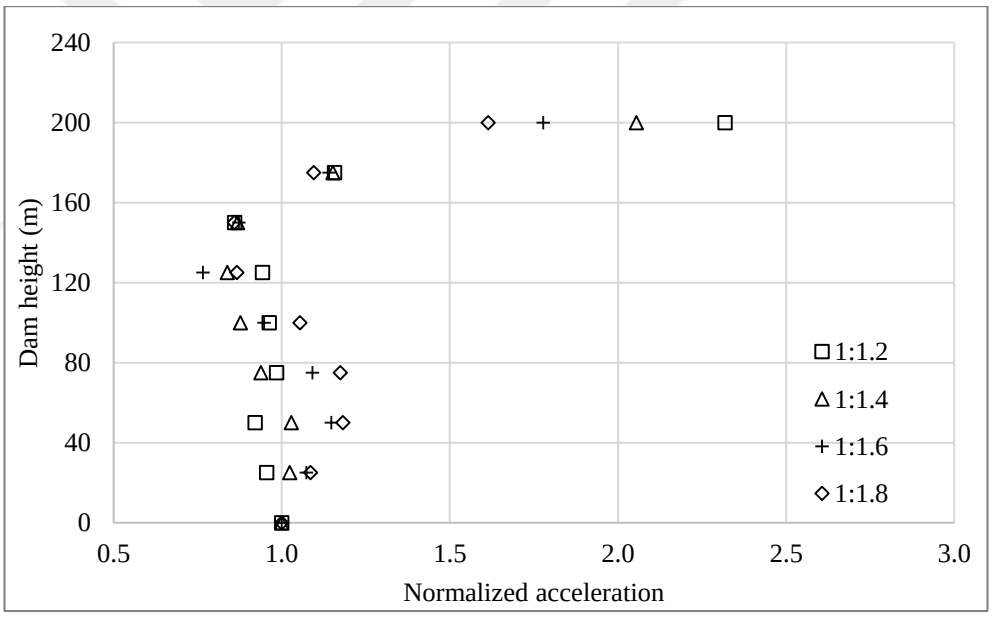


**Figure 4.22. Effect of slope inclination on variation of normalized acceleration along the dam height for 200 m dam**

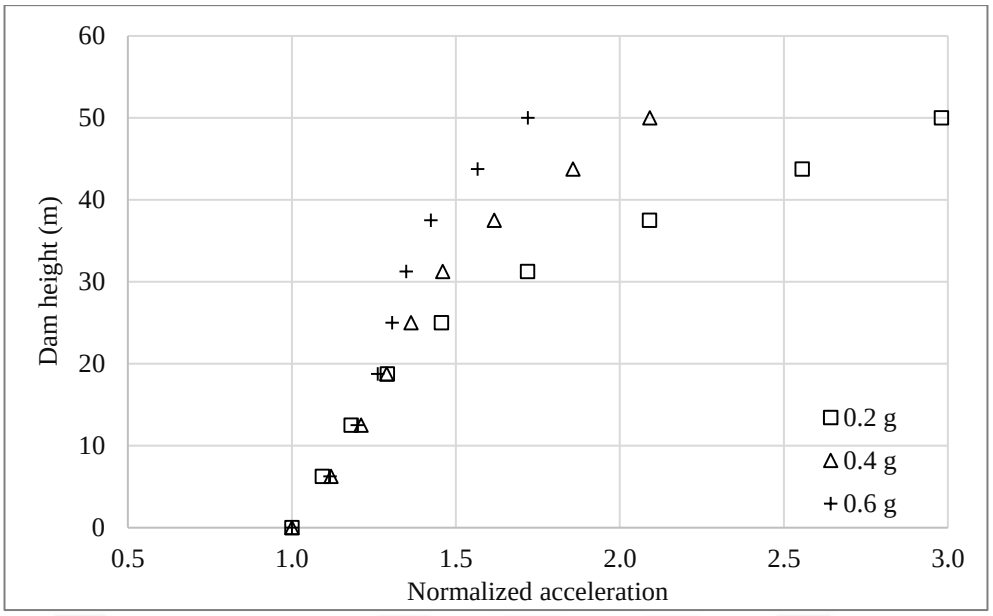


**Figure 4.23. Effect of maximum ground acceleration on variation of normalized acceleration along the dam height for 50 m dam**

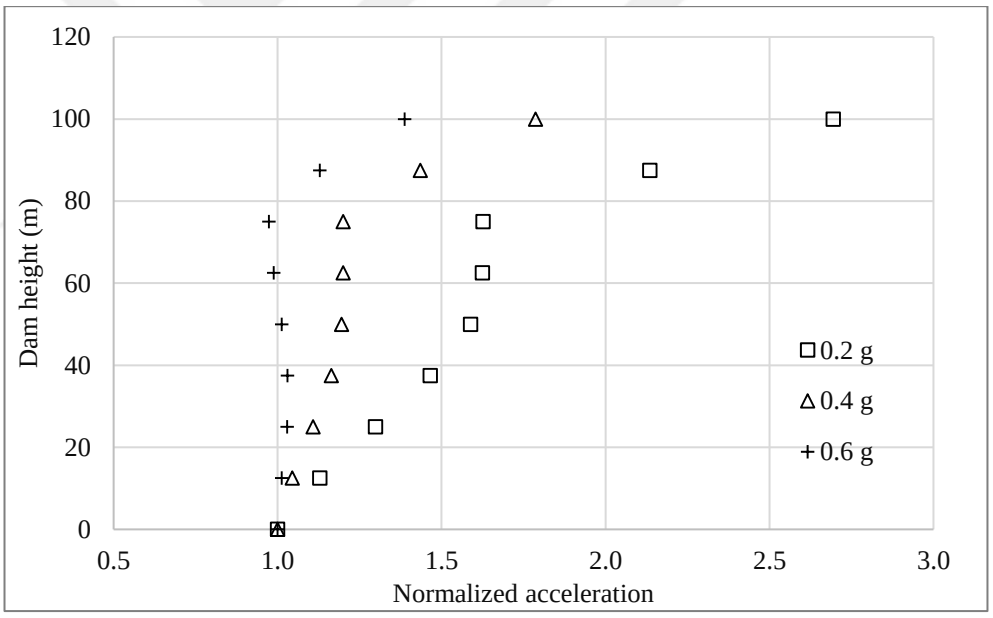


**Figure 4.24. Effect of maximum ground acceleration on variation of normalized acceleration along the dam height for 100 m dam**

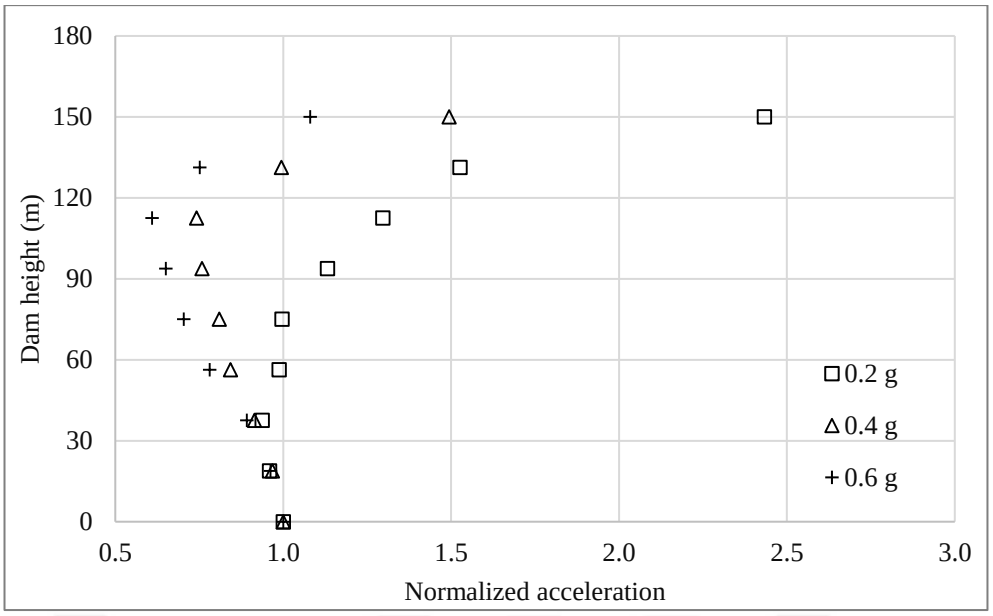


**Figure 4.25. Effect of maximum ground acceleration on variation of normalized acceleration along the dam height for 150 m dam**

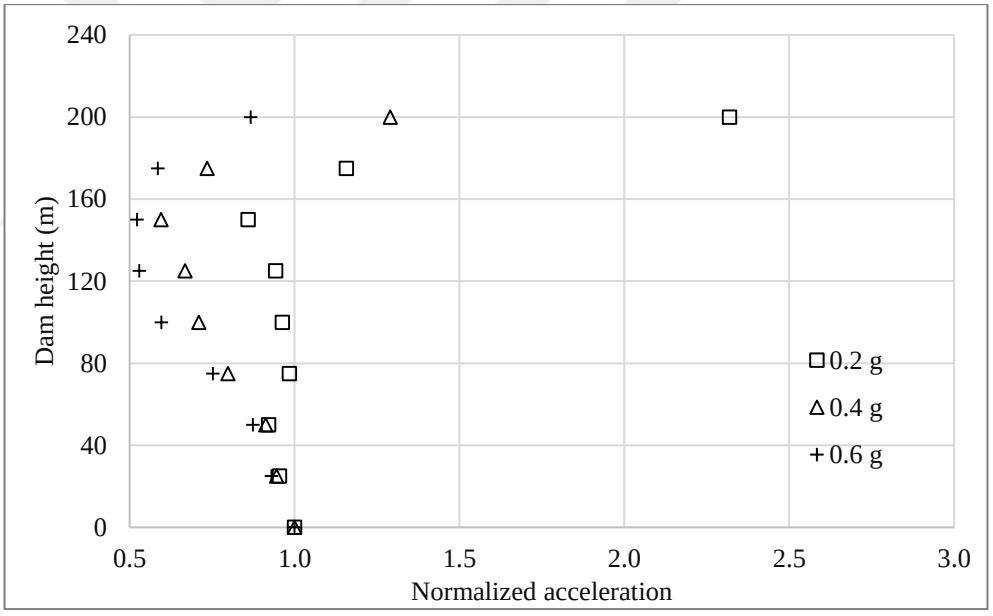


**Figure 4.26. Effect of maximum ground acceleration on variation of normalized acceleration along the dam height for 200 m dam**

Relation between maximum crest acceleration and maximum ground acceleration is given in Figure 4.27., Figure 4.28., Figure 4.29., Figure 4.30. according to the dam height. As the dam height increases, range of maximum crest acceleration is widen, however, amplification ratios decreases. These figures can be used to guess crest accelerations induced by earthquakes for different dam heights, at preliminary design stage.

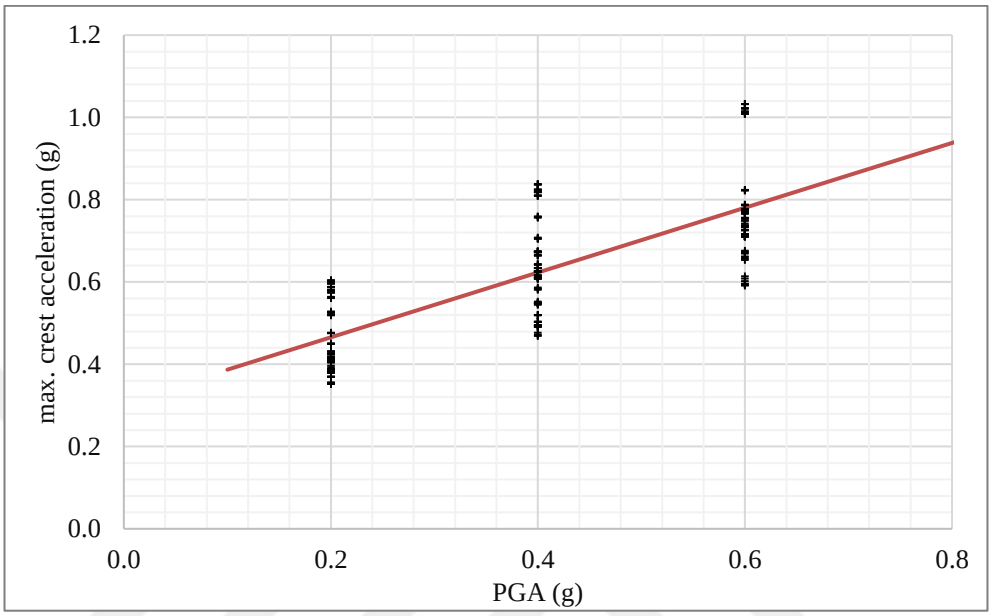


**Figure 4.27. Relation between maximum crest acceleration and maximum ground acceleration for 50 m dam**

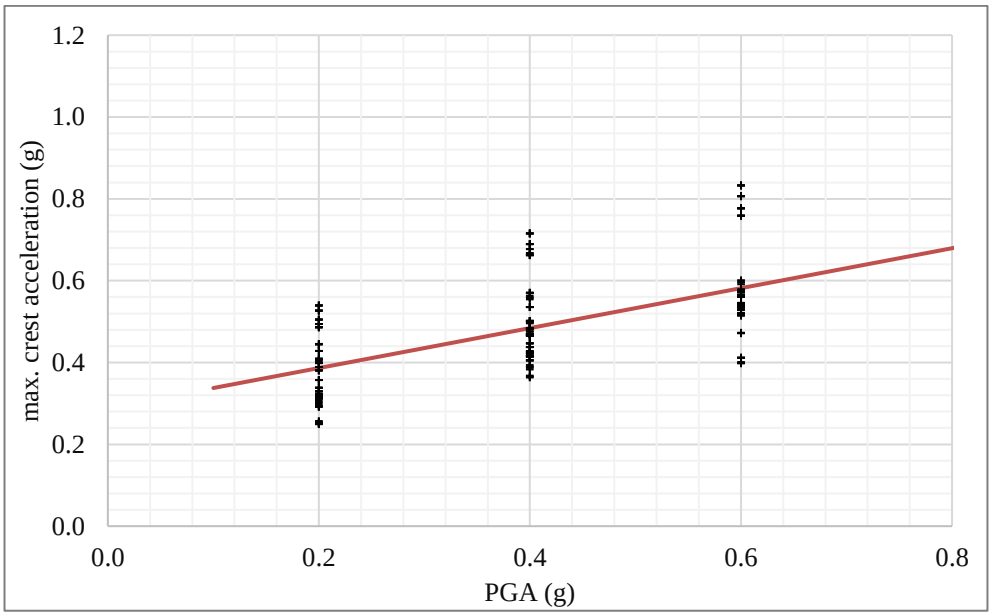


**Figure 4.28. Relation between maximum crest acceleration and maximum ground acceleration for 100 m dam**

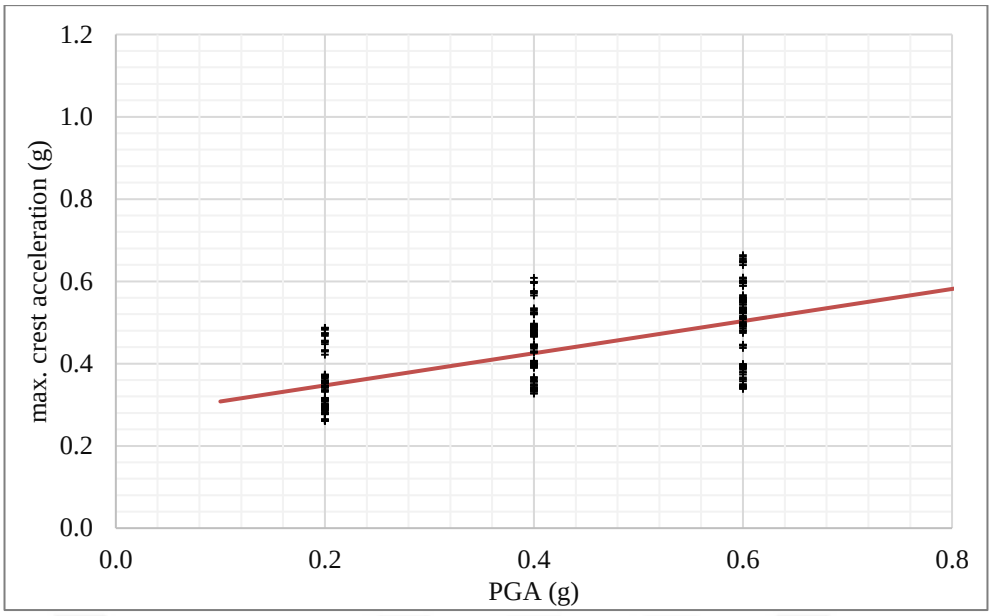


**Figure 4.29. Relation between maximum crest acceleration and maximum ground acceleration for 150 m dam**

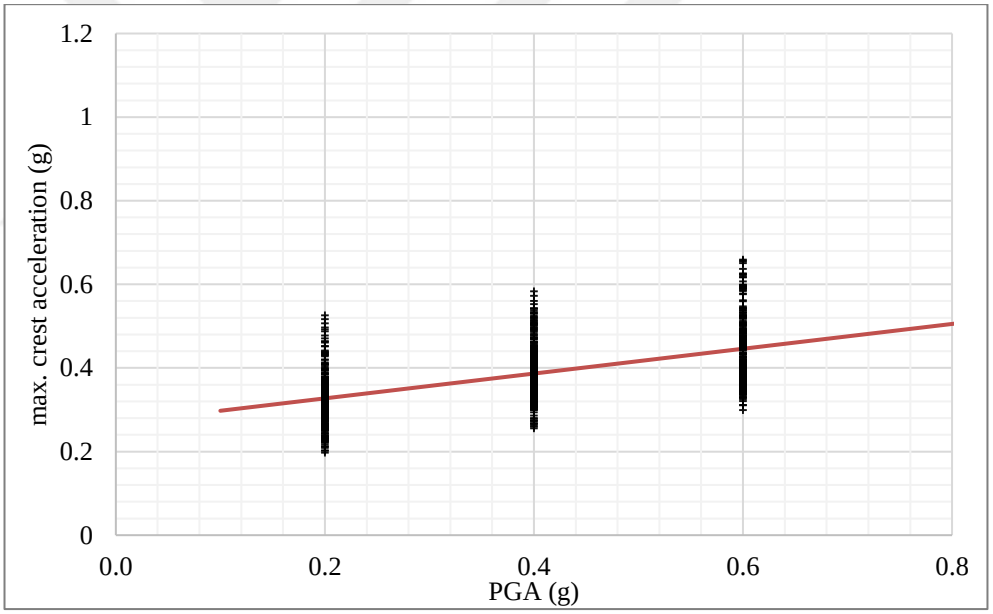


**Figure 4.30. Relation between maximum crest acceleration and maximum ground acceleration for 200 m dam**

Variation of maximum average acceleration of sliding mass and maximum crest acceleration ratio with depth is given in Table 4.1. Maximum and minimum values are stated for the acceleration ratios in the table. Once the maximum crest acceleration or maximum average acceleration of sliding mass at a specified depth is determined, the other one can be predicted by utilizing Table 4.1.

**Table 4.1. Variation of average acceleration and crest acceleration ratio with slip surface depth**

| | max. average acceleration/ max. crest acceleration | | |
|---|---|---|---|
| | **0.25h** | **0.50h** | **0.75h** |
| **50 m dam** | 0.45 – 1.11 | 0.32 – 1.05 | 0.28 – 0.97 |
| **100 m dam** | 0.34 – 1.10 | 0.27 – 0.93 | 0.2 – 0.88 |
| **150 m dam** | 0.28 - 0.90 | 0.29 – 0.78 | 0.26 – 0.82 |
| **200 m dam** | 0.24 – 0.93 | 0.24 – 0.84 | 0.2 – 0.77 |

## 4.3. Permanent Displacement

Conventional methods for permanent displacement calculations are generally recommended for cored earth dams or waste fills (Bray and Rathje, 1998). Since the rockfill dams are relatively new, researches on their seismic performance are limited. According to the analyses made on rockfill dams within this study, following permanent displacement based figures are evaluated. Figure 4.31. is constructed to reveal the relationship between permanent displacement, yield acceleration and maximum crest acceleration. As noted in Section 4.1., minimum required factor of safety is 1.5 for statically stable slopes, thus, data points having more than 1.5 static factor of safety are plotted in the figure. Average data points are sketched on the figure with a black trendline. Since Newmark approach is based on yield acceleration and the crest acceleration is affected by relation between natural period of dam and frequency content of earthquake, these parameters are preferred to state in the figure. This figure can be used in combination with the figures plotted in terms of maximum crest acceleration and maximum ground acceleration for deformation calculation. Once a maximum crest acceleration is determined according to the maximum ground acceleration of causative earthquake due to the dam heights from Figure 4.27., Figure 4.28., Figure 4.29., or Figure 4.30. Then, a yield acceleration is calculated considering the recommended yield coefficients. Finally, utilizing these findings, a permanent displacement can be calculated from Figure 4.31. Besides, detailed illustration of dam

height based results can be seen in Figure 4.32., Figure 4.33., Figure 4.34., Figure 4.35. for 50m, 100m, 150m, 200m dam heights, respectively.

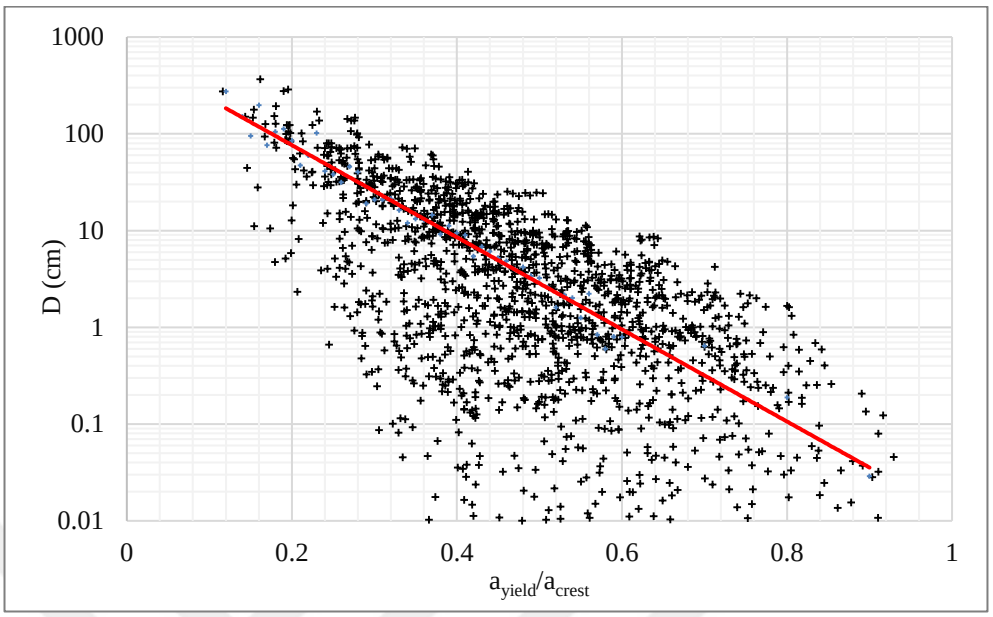


**Figure 4.31. Variation of permanenet displacement with the ratio of yield and maximum crest acceleration**

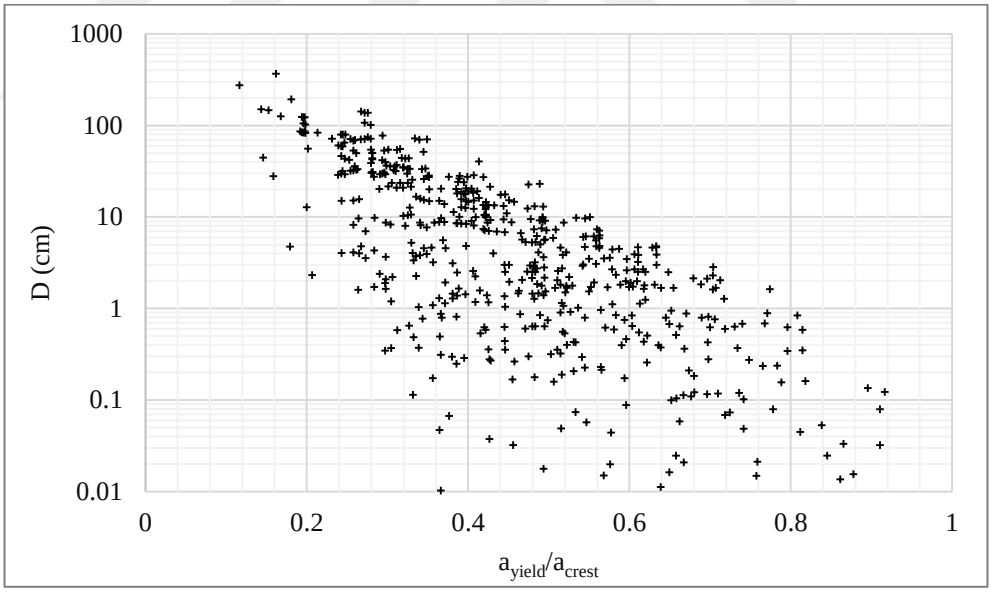


**Figure 4.32. Variation of permanenet displacement with the ratio of yield and maximum crest acceleration for 50 m dam**

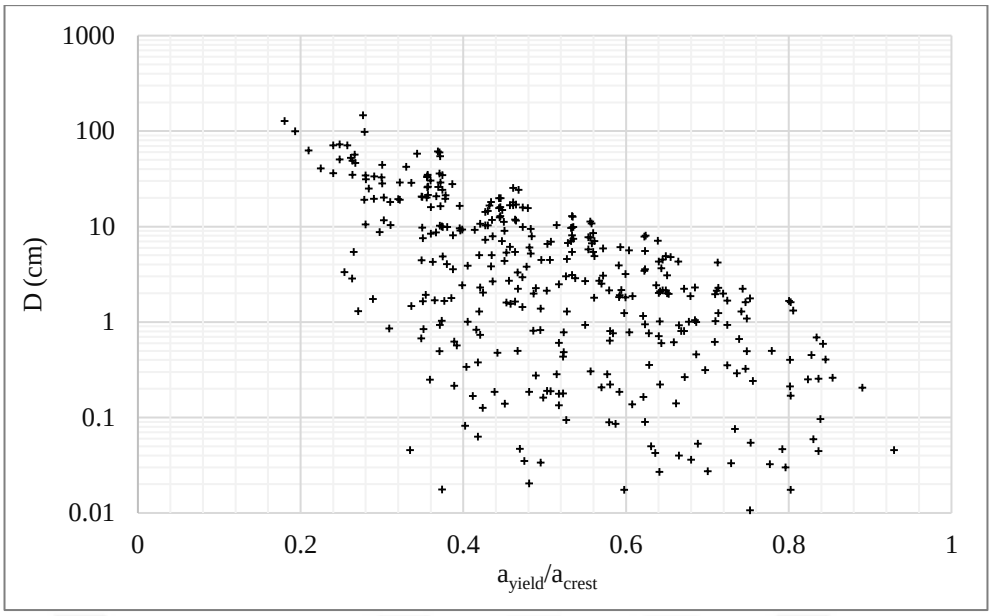


**Figure 4.33. Variation of permanenet displacement with the ratio of yield and maximum crest acceleration for 100 m dam**

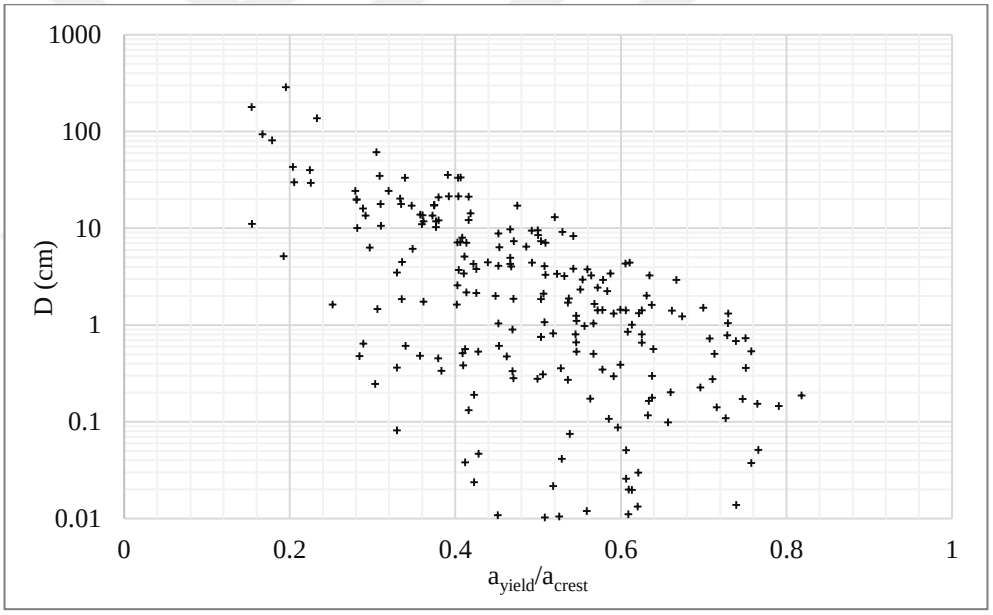


**Figure 4.34. Variation of permanenet displacement with the ratio of yield and maximum crest acceleration for 150 m dam**

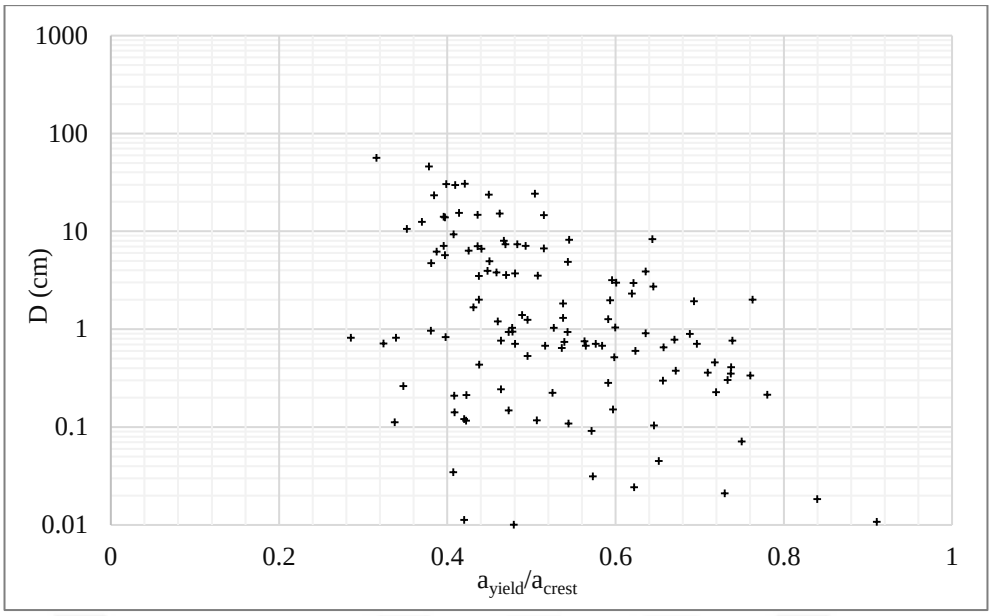


**Figure 4.35. Variation of permanenet displacement with the ratio of yield and maximum crest acceleration for 200 m dam**

Additionally, variation of permanent displacement due to the earthquake induced average acceleration and yield acceleration is plotted in Figure 4.36., Figure 4.37. and Figure 4.38. for 0.75h, 0.50h and 0.25h slip surface depths, respectively. As noted before, as the slip surface depth increases permanent displacements decrease. Again, this can be associated with natural period. The deeper slip surface means higher period and structures with higher periods absorb the seismic energy more than small ones. Thus, evaluated permanent displacements may decrease.

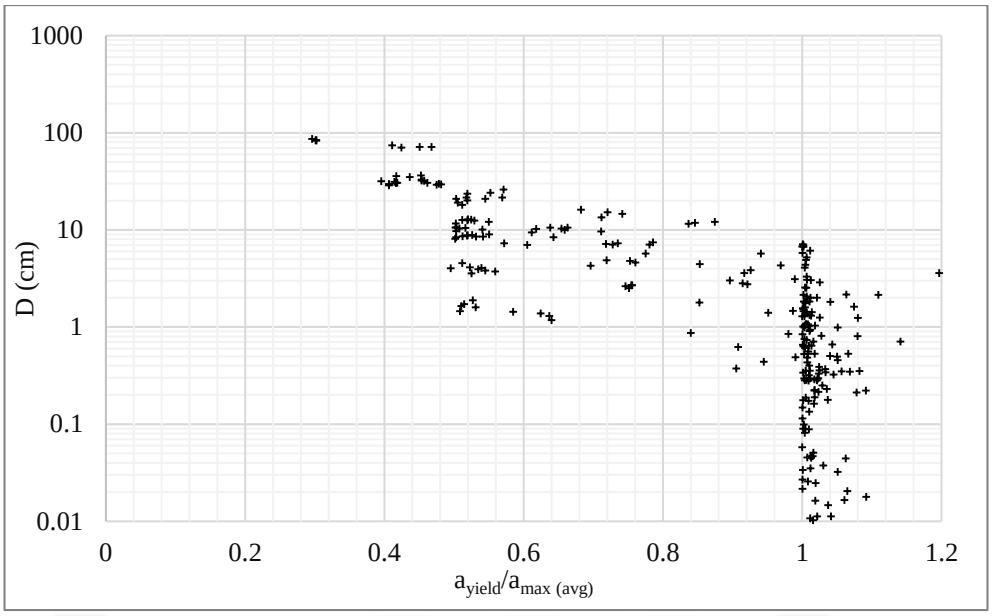


**Figure 4.36. Variation of permanent displacement with the ratio of yield and maximum average acceleration for 0.75h slip surface depth**

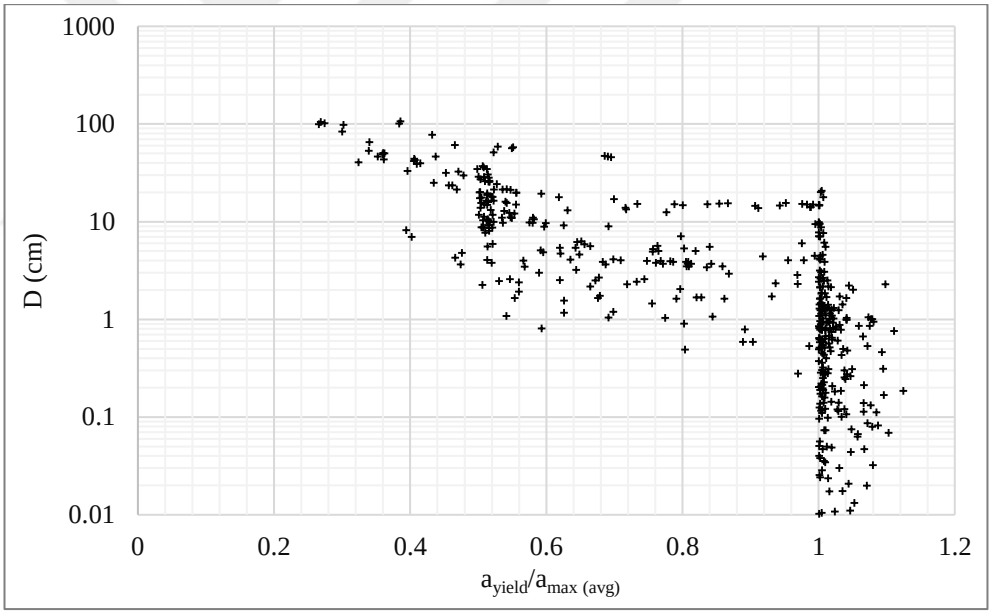


**Figure 4.37. Variation of permanent displacement with the ratio of yield and maximum average acceleration for 0.50h slip surface depth**

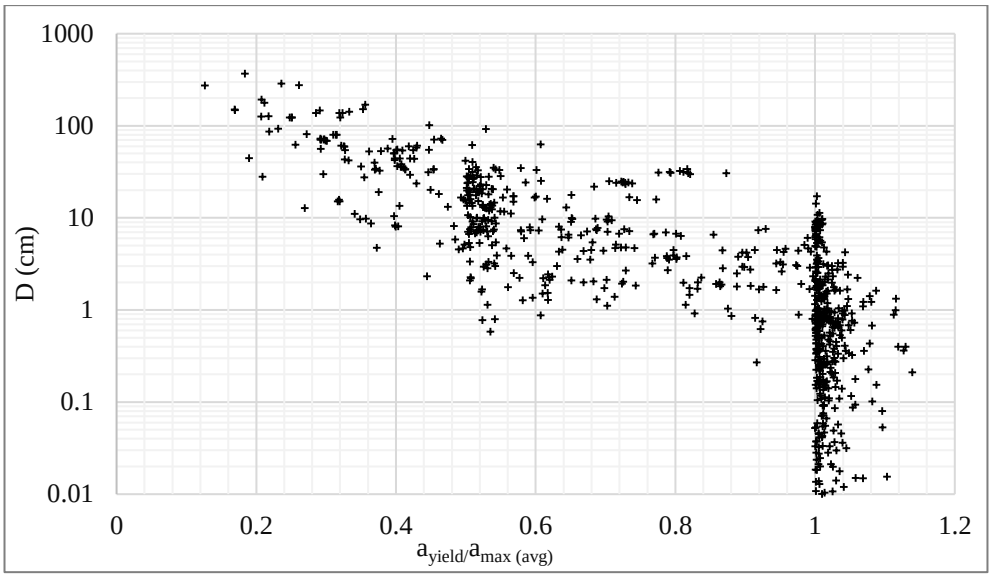


**Figure 4.38. Variation of permanent displacement with the ratio of yield and maximum average acceleration for 0.25h slip surface depth**

In Figure 4.39., yield acceleration is normalized with maximum ground acceleration and permanent displacement is plotted against this ratio. Even the maximum ground acceleration is two times of yield acceleration, 100 cm displacement limit is not achieved. For the values with the ratio less than 0.4, only a few points exceed the maximum limit displacement. A permanent displacement prediction can be made by using this figure. Figure 4.39. is reconstructed in terms of dam height. For a dam height based evaluation Figure 4.40, 4.41., 4.42. and 4.43. can be used for 50 m, 100 m, 150 m, 200 m dam heights , respectively.

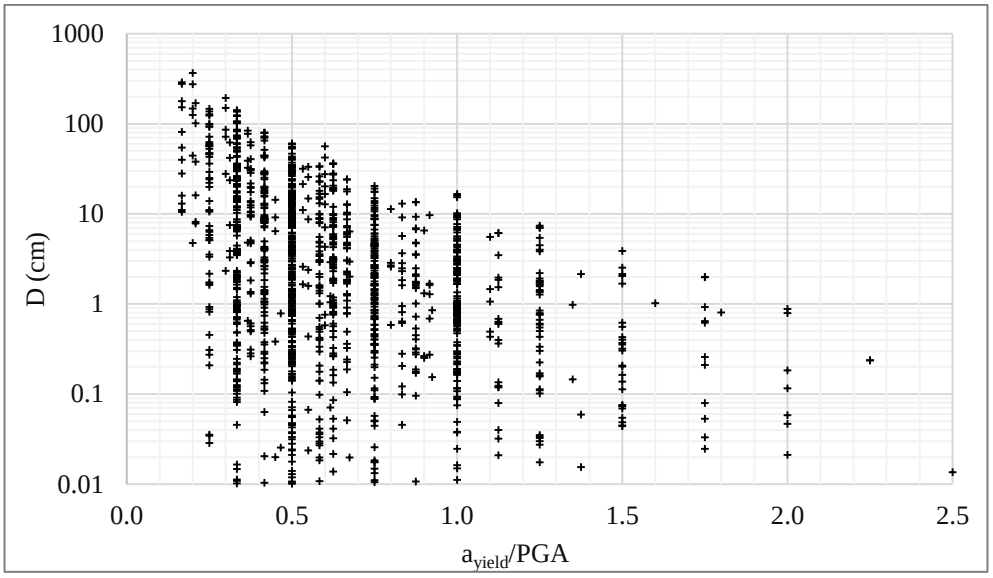


**Figure 4.39. Variation of permanent displacement with the ratio of yield and maximum ground acceleration for all dam heights**

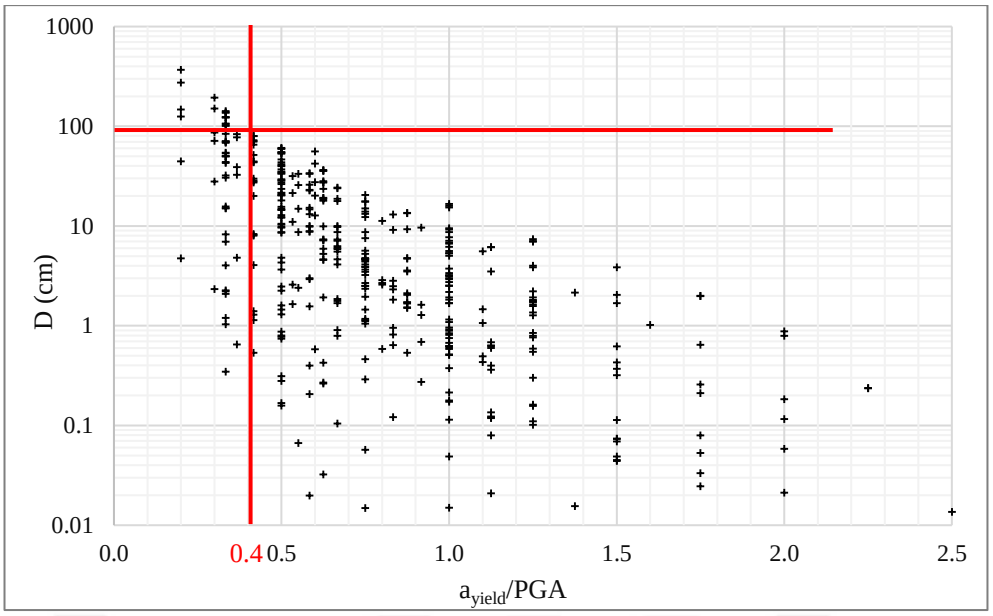


**Figure 4.40. Variation of permanent displacement with the ratio of yield and maximum ground acceleration for 50 m dam**

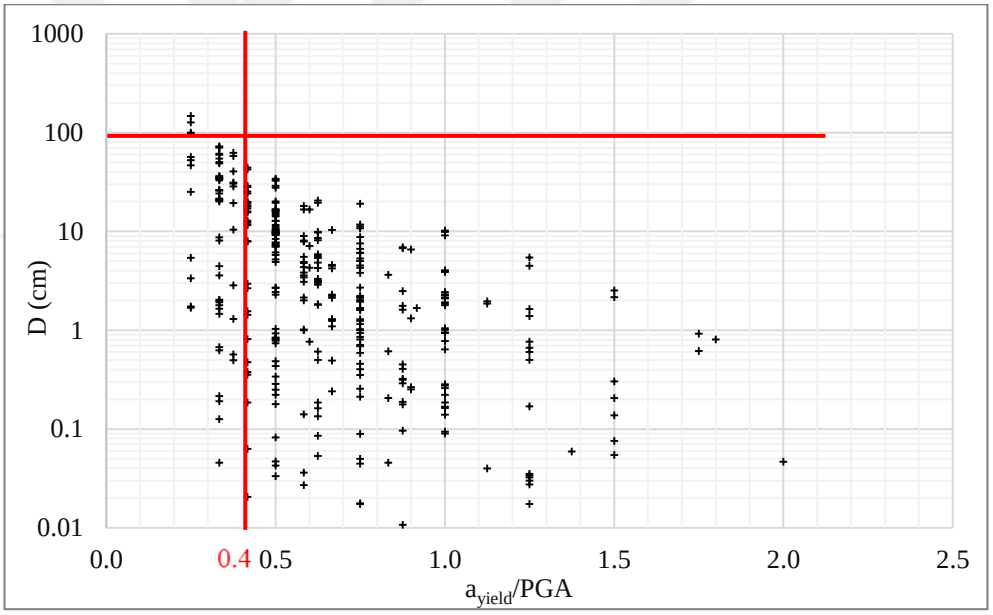


**Figure 4.41. Variation of permanent displacement with the ratio of yield and maximum ground acceleration for 100 m dam**

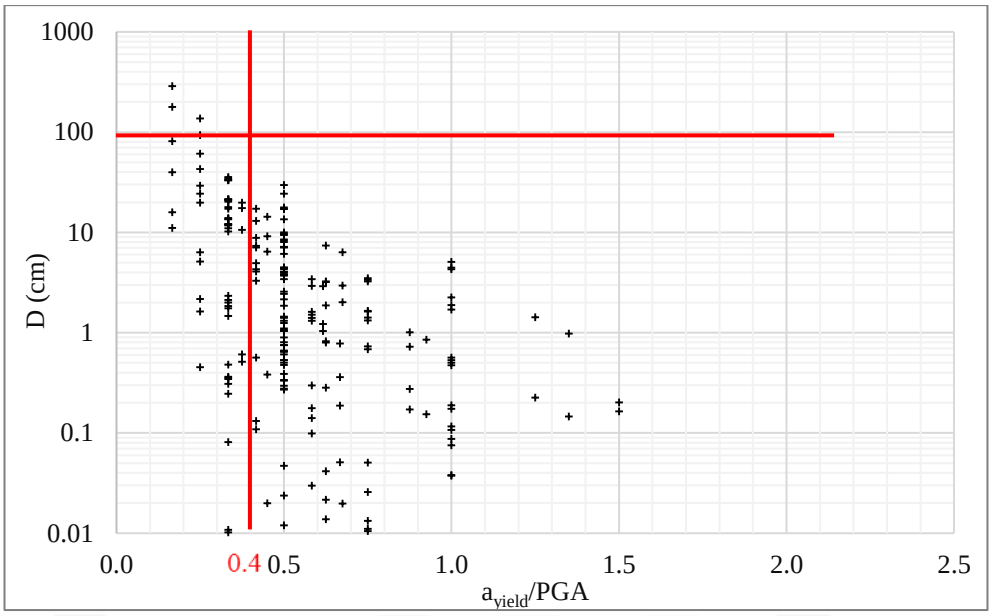


**Figure 4.42. Variation of permanent displacement with the ratio of yield and maximum ground acceleration for 150 m dam**

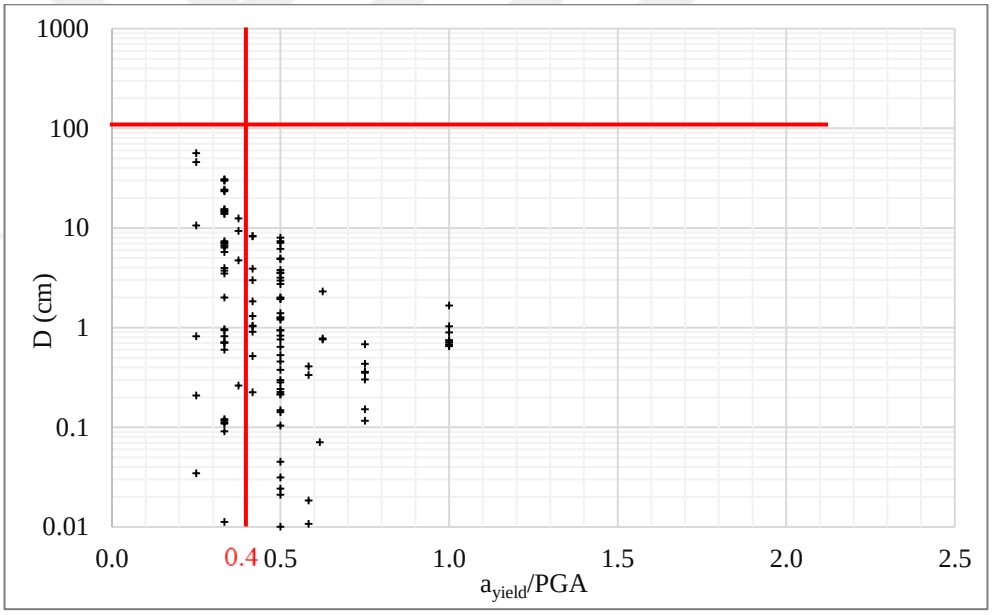


**Figure 4.43. Variation of permanent displacement with the ratio of yield and maximum ground acceleration for 200 m dam**

# 5. CONCLUSIONS AND COMMENTS

In this study a series of pseudo-static and dynamic analyses were performed to investigate the dynamic response of concrete faced rockfill dams (CFRD). After the invention of seismic resistant features, construction of rockfill type dams increase especially at earthquake prone areas. Subsequently, earthquake exposures of constructed rockfill dams show the deficiency of applications. However, available researches and approaches are generally applicable for other cored type dams or embankments not for only rockfill dams. This study aims to fulfill this requirement and to reveal the seismic behavior of rockfill dams. For this purpose, many numerical analyses under various conditions were conducted. Combination of different dam geometries that are formed with different material properties are analyzed under varied excitations. In consequence of analyses, earthquake induced permanent displacements, seismic coefficients and acceleration responses of CFRDs are scrutinized.

- Since QUAKE/W was planned to use for this study, appropriateness of software was checked by modelling Sürgü Dam. Experienced deviatoric deformations acceleration amplifications under Malatya Earthquake were reevaluated and the results of QUAKE/W analyses are in reasonable agreement with the observed deformations by Ozkan et.al (1996).
- Comparisons of horizontal seismic coefficients to be used for dynamic analyses are studied upon two options. Selection of 1/2 of PGA may lead overdesign of structures. When the horizontal seismic coefficient is used as 1/3 of PGA, exceedance of 100 cm limit value is calculated at a few number of analyses. Thus, horizontal seismic coefficient can be used as 1/3 of PGA.
- Effects of slip surface depth are examined under three likely conditions. While number of exceedance of 100cm permanent displacement are nearly same for three slip surfaces, data points that have FS less than 1 decreases with increasing slip surface depth. This can be related with the travelling duration of wave inside the sliding portion. Since the duration is longer in larger slip surface, this part undergoes more deformation than others, thus stability decreases.

- In the analyses, data points of different slopes nearly follow same path for every dam height. However as the dam height increases effect of slope inclination increases and steeper slopes show more amplification. Results indicate that acceleration response of dam is less affected by the slope inclination.
- Amplification of accelerations decrease with both increasing PGA and dam height. This tendency can be associated with the natural period of dam and damping of the rockfill material. As the dam height increases, natural period of the dam increase and accordingly there is deamplification of higher frequency contents in earthquake motion. Moreover, damping in rockfill material increases with the shear strain at higher PGAs. Hence, acceleration amplification decreases with increase damping.
- It is seen that the most significant parameters acting on response of CFRDs and that can jeopardize overall stability are earthquake parameters (duration, frequency, PGA). Accordingly, selection of input motion at design stage is thought to be very important.
- A behavioral difference draw attention when the acceleration variations are viewed. 1/4 height of dam from the crest react different in comparison with remaining parts. A remarkable increment in the acceleration is seen around the crest. Thus, reinforcement of the upper regions of dam can be suggested as a precaution to prevent the excessive deformations that can endanger overall stability of dam.
- Slip surface depth(y) affects the ratio of maximum crest acceleration and average acceleration. Increasing slip surface depth decreases the acceleration ratio.
- Estimated permanent displacements of 200 m CFRD are slightly lower than those of 50 m CFRD. If it is generalized, deviatoric displacements decrease with increasing dam height. The most likely reasons for that difference are the natural periods and the damping characteristics of dam.
- A thorough investigation on the seismic behavior of concrete faced rockfill dams and the role of different parameters has been assessed in this study. By utilizing the results, earthquake induced permanent displacement of concrete faced rockfill dams can be predicted at preliminary design stage.

## REFERENCES


Abramson, L. W. (2002) *Slope stability and stabilization methods*, John Wiley & Sons, 703.

Ambraseys N.N., Menu J.M. (1988) Earthquake-induced ground displacements, *Journal of Earthquake Engineering and Structural Dynamics*, 16: 985–1006.

Ambraseys, N.N. (1972) Behaviour of foundation materials during strong earthquakes, *Proceedings 4th European Symposium on Earthquake Engineering*, London, Vol 7, 11-12.

Anonymous, (1989) *Advanced dam engineering for design, construction, and rehabilitation*, Springer US, 816.

Anonymous, (2015) *Perspectives on Earthquake Geotechnical Engineering*, Springer US, 484.

Aryal, K.P. (2006) *Slope stability evaluations by limit equilibrium and finite element methods*, Doctor of Philosophy, Norwegian University of Science and Technology, Norway, 146.

Bayraktar, A., Kartal, M. E., (2010) Linear and nonlinear response of concrete slab on CFR dam during earthquake, *Soil Dynamics and Earthquake Engineering*, (30): 990–1000.

Bishop, A.W. (1955) The use of the slip circle in the stability analysis of slopes, *Geotechnique*, 5(1): 7-17.

Bray J.D., Rathje E.R. (1998) Earthquake-induced displacements of solid-waste landfills, *Journal of Geotechnical and Geoenvironmental Engineering*, ACE 124(3): 242–253.

Bray, J. D. (2007) Simplified seismic slope displacement procedures, 327-353, *Earthquake Geotechnical Engineering*, Pitilakis, K.D., Springer, Netherlands.

Bray, J.D. et al. (1995) Seismic stability procedures for solid-waste landfills, *Journal of Geotechnical Engineering*, 121(2): 139-151.

Bray, J.D., Travasarou, T., (2007) Simplified procedure for estimating earthquake-induced deviatoric slope displacements, *Journal of Geotechnical and Geoenviromental Engineering* 133 (4): 381–392.

Bray, J.D., Travasarou, T. (2009) Pseudostatic coefficient for use in simplified seismic slope stability evaluation, *Journal of Geotechnical and Geoenvironmental Engineering*, 135(9): 1336-1340.

Chopra, A. K. (1966) The importance of the vertical component of earthquake motions, *Bulletin of the Seismological Society of America*, 56(5): 1163-1175.

Chugh, A.K. (1986) Variable interslice force inclination in slope stability analysis, *Soils and Foundation, Japanese Society of SMFE,* 26(1):115-21.

Clough, R. W. (1960) The finite element method in plane stress analysis, *Proceedings of the 2nd ASCE Conference on Electronic Computation*, Pittsburgh.

Darendeli, M.B. (2001) *Development of a new family of normalized modulus reduction and material damping curves*, Doctor of Philosophy, The University of Texas at Austin, USA, 362.

Fellunius, W. (1936) Calculations of the Stability of Earth Dams, *Proceedings of the Second Congress of Large Dams*, Washington D. C., 4:445-63.

Hardin, B.O., Drnevich, V.P., (1972) Shear modulus and damping in soils:design equations and curves, *Journal of Soil Mechanics and Foundations Divisions, ASCE*, 98 (7): 667-692.

Hynes-Griffin M.E., Franklin A.G. (1984) Rationalizing the seismic coefficient method, *Misc. Paper No. GL-84-13, U.S. Army Engr. WES*, Vicksburg, MS.

Idriss, I. M., Seed, H. B., (1970) Soil moduli and damping factors for dynamic response analyses, *Report No. EERC 70-10*.

Idriss, I. M., et al. (1973) Soil conditions and building damage in 1967 Caracas earthquake, *Journal of Geotechnical and Geoenvironmental Engineering*, 99(sm7).

Idriss, I. M., Lee, K. L. (1975) Static stresses by linear and nonlinear methods, *Journal of Geotechnical and Geoenvironmental Engineering*, ASCE Proceeding, 101: 11542.

Ishibashi, I., Zhang, X. J. (1993) Unified dynamic shear moduli and damping ratios of sand and clay, *Soils Foundations*, 33(1): 182–191.

Janbu, N. (1954a) *Stability analysis of slopes with dimensionless parameters*, Doctor of Science, Harvard University Soil Mechanics Series, No. 46.

Jia, Y.F., Chi, S.C., (2012) Application of rockfill dynamical characteristic statistic curve in mid-small scale concrete face dam dynamic analysis, *15th World Conference on Earthquake Engineering*, 24-28 September, Lisbon.

Jibson, R.W. (1993) Predicting earthquake-induced landslide displacements using Newmark's sliding block analysis, *Transportation Research Record*, 1411:9–17.

Jibson, R. W. (2007) Regression models for estimating coseismic landslide displacement, *Engineering Geology*, 91(2): 209-218.

Jibson, R.W. (2011) Methods for assessing the stability of slopes during earthquakes—A retrospective, *Engineering Geology*, 122(1): 43-50.

Kuhlmeyer, R.L., Lysmer, J. (1973). Finite element method accuracy for wave propagation problems, *Journal of the Soil mechanics and Foundation Division ASCE*, 99(5): 421-427.

Kramer, S.L., Smith, M.W. (1997) Modified Newmark model for seismic displacements of compliant slopes, *Journal of Geotechnical and Geoenvironmental Engineering*, 123(7): 635-644.

Kramer, S. L. (1996) *Geotechnical earthquake engineering*. Prentice-Hall Civil Engineering and Engineering Mechanics Series, Upper Saddle River, NJ: Prentice Hall, 673.

Liu, J. et al. (2014) Large-scale shaking table model tests of aseismic measures for concrete faced rock-fill dams, *Soil Dynamics and Earthquake Engineering*, 61-62: 152–163.

Lin, J.S., Whitman R.V. (1986) Earthquake induced displacements of sliding blocks, *Journal of Geotechnical Engineering*, 112(1): 44–59

Lin, J.S., Whitman R.V. (1983) Decoupling approximation to the evaluation of earthquake-induced plastic slip in earth dams, *Earthquake Engineering and Structural Dynamics*, 11: 667–678.

Makdisi F.I., Seed H.B. (1978) Simplified procedure for estimating dam and embankment earthquake induced deformations, *Journal of Geotechnical Engineering*, 104(7): 849–867.

Melo, C., Sharma, S. (2004) Seismic coefficients for pseudostatic slope analysis. *In 13th World Conference on Earthquake Engineering*, August, Vancouver, BC, Canada, Paper (No. 369).

Meehan, C. L., Vahedifard, F. (2013) Evaluation of simplified methods for predicting earthquake-induced slope displacements in earth dams and embankments, *Engineering Geology*, 152(1): 180-193.

Mononobe, H. (1936) Seismic stability of the earth dam, *Proc. of the Second Congress of Jarge Dams*, IV. Washington DC.

Morgenstern, N. R., Price, V. E. (1965) The analysis of the stability of general slip surfaces, *Geotechniqu*e, 15(1): 77-93.

Newmark, N.M. (1965) Effects of earthquakes on dams and embankments, *Géotechnique*, 15: 139–160.

Özkan, M.Y. et al. (1996) An evaluation of Sürgü dam response during 5 May 1986 earthquake, *Soil Dynamics and Earthquake Engineering*, 15(1): 1-10.

Pathmanathan, R. (2007) *Numerical modelling of seismic behaviour of earth retaining walls*, Master of Science, Rose School, 159.

Pinto, P.S.S. (2001) Dam engineering-earthquake analysis, *International Conferences on Recent Advances in Geotechnical Earthquake Engineering and Soil Dynamics*, March 26, Paper 4.

Rathje, E. M., & Bray, J. D. (2000) Nonlinear coupled seismic sliding analysis of earth structures, *Journal of Geotechnical and Geoenvironmental Engineering*, 126(11): 1002-1014.

Rathje, E. M., & Saygili, G. (2009) Probabilistic assessment of earthquake-induced sliding displacements of natural slopes, *Bulletin of the New Zealand Society for Earthquake Engineering*, 42(1): 18.

Sarma, S.K. (1973) Stability analysis of embankment and slopes, *Geotechnique*, 23 (3):423-33.

Sarma, S. K. (1975) Seismic stability of earth dams and embankments, *Geotechnique*, 25(4): 743-761.

Seed, H.B. (1981) Earthquake-resistant design of earth dams, *International Conferences on Recent Advances in Geotechnical Earthquake Engineering and Soil Dynamics*, April 26, Paper 23.

Seed, H.B., et al., 1986 Moduli and damping factors for dynamic analysis of cohesionless soils, *J. Geotech. Eng.,* ASCE, 112 (11): 1016–1103

Seed, H. B. (1979) Considerations in the earthquake-resistant design of earth and rockfill dams. *Geotechnique*, 29(3): 215-263.

Sherard, J. L., Cooke, J. B. (1987) Concrete-face rockfill dam: I. Assessment. *Journal of Geotechnical Engineering*, 113(10): 1096-1112.

Silva, W.J., et al. (1996), Description and validation of the stochastic ground motion model, *Report Submitted to Brookhaven National Laboratory*, Associated Universities, Inc. Upton, New York.

Spencer, E. (1967) A method of analysis of the stability of embankments, assuming parallel interslice forces, *Geotechnique*, 17: 11-26.

Stewart J.P., et al. (2001) Seismic performance of hillside fills. *Journal of Geotechnical and Geoenvironmental Engineering ASCE*, 127(11): 905–919.

Terzaghi, K. (1950) Mechanisms of landslides, *The Geological Survey of America Engineering Geology*, 83-123.

Vucetic, M., Dobry, R. (1991) Effect of soil plasticity on cyclic response, *Journal of Geotechnical Engineering*, 117(1):89-107.

Yegian, M.K., et al. (1991) Earthquake-induced permanent deformations: probabilistic approach. *Journal of Geotechnical Engineering*, 117(1): 35–50

.

# APPENDIX

## Appendix A. Matlab Code for Permanent Displacement Calculation

```
clc; clear all; close all;
files = dir('*.xls');
for file = files'
   outfile =strcat(file.name,'x');
   % disp(file.name); disp(outfile);
   A = xlsread(file.name);%,'1220200.06.m','A3:P5179');
   % B is average acceleration in m/s^2 for 0.75h;
   B =
(((((A(:,4)+A(:,5))/2)*A(6,11))+(((A(:,5)+A(:,6))/2)*A(5,11))+(((A(:,6)+A(:,7))/2)*
A(4,11))+(((A(:,7)+A(:,8))/2)*A(3,11))+(((A(:,8)+A(:,9))/2)*A(2,11))+(((A(:,9)+A(:
,10))/2)*A(1,11)))/(A(1,11)+A(2,11)+A(3,11)+A(4,11)+A(5,11)+A(6,11)))*9.81;
   % C is average acceleration in m/s^2 for 0.50h;
   C =
(((((A(:,6)+A(:,7))/2)*A(4,12))+(((A(:,7)+A(:,8))/2)*A(3,12))+(((A(:,8)+A(:,9))/2)*
A(2,12))+(((A(:,9)+A(:,10))/2)*A(1,12)))/(A(1,12)+A(2,12)+A(3,12)+A(4,12)))*9.8
1;
   % D is average acceleration in m/s^2 for 0.25h;
   D =
(((((A(:,8)+A(:,9))/2)*A(2,13))+(((A(:,9)+A(:,10))/2)*A(1,13)))/(A(1,13)+A(2,13)))
*9.81;
   Dt=0.005;
   %y75 means yield acceleration in m/s^2 for 0.75h
   y75= A(1,14)*9.81;
   %y50 means yield acceleration in m/s^2 for 0.50h
   y50= A(1,15)*9.81;
   %y25 means yield acceleration in m/s^2 for 0.25h
   y25= A(1,16)*9.81;
      l=length(A);
      %plot(B);
   %hold on
   sum=0;
```

```
B=B;%displacement calculation for positive part of 0.75h
for i=1:l;
if (B(i)<=y75)&&(sum<=0)
vel(i)=0;
t=i;
elseif (B(i)>y75) || (sum>0);
B(i)=B(i)-y75;
y=t+1;
for x=y:i
vel(i)=trapz(B(y:i))*Dt;
sum=vel(i);
end
end
end
for k=1:l
if(vel(k)<0)
vel(k)=0;
end
end
%plot(vel)
%hold on
for z=1:l
disp(z)=trapz(vel(1:z))*Dt;
sum=disp(z);
end
d1=sum;
%figure
%plot(disp)
%hold on
      sum=0;
B=-B;%displacement calculation for negative part 0.75h
%plot(B)
%hold on
for i=1:l;
```

```
if (B(i)<=y75)&&(sum<=0)
vel(i)=0;
t=i;
elseif (B(i)>y75) || (sum>0);
B(i)=B(i)-y75;
y=t+1;
for x=y:i
vel(i)=trapz(B(y:i))*Dt;
sum=vel(i);
end
end
end
for k=1:l
if(vel(k)<0)
vel(k)=0;
end
end
%plot(vel)
%hold on
for z=1:l
disp(z)=trapz(vel(1:z))*Dt;
sum=disp(z);
end
d2=sum;
%figure
%plot(disp)
%hold on
   %plot(C)
%hold on
sum=0;
C=C;%displacement calculation for positive part 0.5h
for i=1:l
if (C(i)<=y50)&&(sum<=0)
vel(i)=0;
```

```
t=i;
elseif (C(i)>y50) || (sum>0);
C(i)=C(i)-y50;
y=t+1;
for x=y:i
vel(i)=trapz(C(y:i))*Dt;
sum=vel(i);
end
end
end
for k=1:l
if(vel(k)<0)
vel(k)=0;
end
end
%plot(vel)
%hold on
for z=1:l
disp(z)=trapz(vel(1:z))*Dt;
sum=disp(z);
end
d3=sum;
%figure
%plot(disp)
%hold on
   sum=0;
C=-C;%displacement calculation for negative part 0.5h
%plot(C)
%hold on
for i=1:l
if (C(i)<=y50)&&(sum<=0)
vel(i)=0;
t=i;
elseif (C(i)>y50) || (sum>0);
```

```
C(i)=C(i)-y50;
y=t+1;
for x=y:i
vel(i)=trapz(C(y:i))*Dt;
sum=vel(i);
end
end
end
for k=1:l
if(vel(k)<0)
vel(k)=0;
end
end
%plot(vel)
%hold on
for z=1:l
disp(z)=trapz(vel(1:z))*Dt;
sum=disp(z);
end
d4=sum;
%figure
%plot(disp)
%hold on
   %plot(D)
%hold on
sum=0;
D=D;%displacement calculation for positive part 0.25h
for i=1:l
if (D(i)<=y25)&&(sum<=0)
vel(i)=0;
t=i;
elseif (D(i)>y25) || (sum>0);
D(i)=D(i)-y25;
y=t+1;
```

```
for x=y:i
vel(i)=trapz(D(y:i))*Dt;
sum=vel(i);
end
end
end
for k=1:l
if(vel(k)<0)
vel(k)=0;
end
end
%plot(vel)
%hold on
for z=1:l
disp(z)=trapz(vel(1:z))*Dt;
sum=disp(z);
end
d5=sum;
%figure
%plot(disp)
%hold on

sum=0;
D=-D;%displacement calculation for negative part 0.25h
%plot(D)
%hold on
for i=1:l
if (D(i)<=y25)&&(sum<=0)
vel(i)=0;
t=i;
elseif (D(i)>y25) || (sum>0);
D(i)=D(i)-y25;
y=t+1;
for x=y:i
```

```
vel(i)=trapz(D(y:i))*Dt;
sum=vel(i);
end
end
end
for k=1:l
if(vel(k)<0)
vel(k)=0;
end
end
%plot(vel)
%hold on
for z=1:l
disp(z)=trapz(vel(1:z))*Dt;
sum=disp(z);
end
d6=sum;
%figure
%plot(disp)
%hold on


E = xlswrite(outfile,A,file.name,'A3:P5179');
Name1 = {'Time','History Point7','History Point8','History Point9','History Point10','History Point11','History Point12','History Point13','History Point14','History Point15','area m^2','area m^2','area m^2','yield acc (g)','yield acc (g)','yield acc (g)','displacements'};
Name2 = {'Second','X-Acceleration (g)','X-Acceleration (g)','X-Acceleration (g)','X-Acceleration (g)','X-Acceleration (g)','X-Acceleration (g)','X-Acceleration (g)','X-Acceleration (g)','0.75h','0.50h','0.25h','0.75h','0.50h','0.25h','(m)'};
Name3 = {'+0.75h';'-0.75h';'+0.50h';'-0.50h';'+0.25h';'-0.25h'};
Name4 = {'Absolute Max.Acc.(g)'};
Name5 = {'Normalized Acc.'};


F1 = xlswrite(outfile,Name1,file.name,'A1:Q1');
F2 = xlswrite(outfile,Name2,file.name,'A2:Q2');
```

```
F3 = xlswrite(outfile,Name3,file.name,'Q3:Q8');
F4 = xlswrite(outfile,Name4,file.name,'A5182');
F5 = xlswrite(outfile,Name5,file.name,'A5183');
F6 = xlswrite(outfile,B,'0.75h avg acc','A1:A5177');
F7 = xlswrite(outfile,C,'0.50h avg acc','A1:A5177');
F8 = xlswrite(outfile,D,'0.25h avg acc','A1:A5177');
% M is used for max
M1 = max(abs(A(:,2)));
M2 = max(abs(A(:,3)));
M3 = max(abs(A(:,4)));
M4 = max(abs(A(:,5)));
M5 = max(abs(A(:,6)));
M6 = max(abs(A(:,7)));
M7 = max(abs(A(:,8)));
M8 = max(abs(A(:,9)));
M9 = max(abs(A(:,10)));
M1W = xlswrite(outfile,M1,file.name,'B5182:B5182');
M2W = xlswrite(outfile,M2,file.name,'C5182:C5182');
M3W = xlswrite(outfile,M3,file.name,'D5182:D5182');
M4W = xlswrite(outfile,M4,file.name,'E5182:E5182');
M5W = xlswrite(outfile,M5,file.name,'F5182:F5182');
M6W = xlswrite(outfile,M6,file.name,'G5182:G5182');
M7W = xlswrite(outfile,M7,file.name,'H5182:H5182');
M8W = xlswrite(outfile,M8,file.name,'I5182:I5182');
M9W = xlswrite(outfile,M9,file.name,'J5182:J5182');
% MA is used for normalized accelerations
MA1 = max(abs(A(:,2)))/max(abs(A(:,2)));
MA2 = max(abs(A(:,3)))/max(abs(A(:,2)));
MA3 = max(abs(A(:,4)))/max(abs(A(:,2)));
MA4 = max(abs(A(:,5)))/max(abs(A(:,2)));
MA5 = max(abs(A(:,6)))/max(abs(A(:,2)));
MA6 = max(abs(A(:,7)))/max(abs(A(:,2)));
MA7 = max(abs(A(:,8)))/max(abs(A(:,2)));
MA8 = max(abs(A(:,9)))/max(abs(A(:,2)));
```

```
    MA9 = max(abs(A(:,10)))/max(abs(A(:,2)));
    MA1W = xlswrite(outfile,MA1,file.name,'B5183:B5183');
    MA2W = xlswrite(outfile,MA2,file.name,'C5183:C5183');
    MA3W = xlswrite(outfile,MA3,file.name,'D5183:D5183');
    MA4W = xlswrite(outfile,MA4,file.name,'E5183:E5183');
    MA5W = xlswrite(outfile,MA5,file.name,'F5183:F5183');
    MA6W = xlswrite(outfile,MA6,file.name,'G5183:G5183');
    MA7W = xlswrite(outfile,MA7,file.name,'H5183:H5183');
    MA8W = xlswrite(outfile,MA8,file.name,'I5183:I5183');
    MA9W = xlswrite(outfile,MA9,file.name,'J5183:J5183');
    % dw is used for displacement writing
    dw1 = xlswrite(outfile,d1,file.name,'R3:R3');
    dw2 = xlswrite(outfile,d2,file.name,'R4:R4');
    dw3 = xlswrite(outfile,d3,file.name,'R5:R5');
    dw4 = xlswrite(outfile,d4,file.name,'R6:R6');
    dw5 = xlswrite(outfile,d5,file.name,'R7:R7');
    dw6 = xlswrite(outfile,d6,file.name,'R8:R8');
end
```

## CURRICULUM VITAE

### PERSONAL INFORMATION


Name Surname :Selda DURMAZ
Date of Birth :22.01.1989
Telephone :+90 506 609 2147
E-mail :seldadurmaz_22@hotmail.com
seldadurmaz@mu.edu.tr


### EDUCATION

2013-2016 Master of Science - Muğla Sıtkı Koçman University, Department of Civil Engineering, Geotechnics Division, Muğla, Turkey

2008-2013 Bachelor's Degree - Muğla Sıtkı Koçman University, Department of Civil Engineering, Muğla, Turkey

2003-2007 High School - Muğla Anatolian High School, Muğla, Turkey

### WORK EXPERIENCES

02/2014-Present Research Assistant, Muğla Sıtkı Koçman University, Department of Civil Engineering, Muğla

07-08/2012 Office Training, DİYA Mimarlık, Tekirdağ

07-08/2011 Site Training, Anıt & Detay Mühendislik, Muğla

### PROJECTS

Ülgen, D., Durmaz, S. (2015-2016) Ön Yüzü Beton Kaplı Kaya Dolgu Barajlarda Sismik Yükleri Altındaki Kalıcı Deformasyonun İncelenmesi, Muğla Sıtkı Koçman University Scientific Research Project (BAP), Project Number: 15-131.

### PUBLICATIONS

National Symposium

Durmaz, S., Ülgen, D. (2015) Ön Yüzü Beton Kaplı Kaya Dolgu Barajların Deprem Yükleri Altındaki İvme Tepkilerinin İncelenmesi, *6. Geoteknik Sempozyumu*, 26-27 November, Adana, Turkey, 12 pages.

### COMPUTER SKILLS

AutoCAD, Matlab, Plaxis, Shake 91, GeoStudio, SoilWorks, Slide.